

Dipl.-Ing. Marc Sens,  
Dr.-Ing. Christoph Danzer, Dipl.-Ing. Carsten von Essen, Dr.-Ing. Maximilian Brauer,  
Dipl.-Ing. Ralf Wascheck, Dr.-Ing. Joern Seebode, Dipl.-Ing. Matthias Kratzsch

## **Hydrogen Powertrains in Competition to Fossil Fuel based Internal Combustion Engines and Battery Electric Powertrains**

### **Wasserstoffantriebe im Wettbewerb mit Verbrennungsmotoren für fossile Kraftstoffe und dem batterieelektrischen Antrieb**

#### **Abstract**

The achievement of future climate goals means an urgent shift towards a CO<sub>2</sub>-neutral society. Alongside renewably generated electricity, hydrogen plays a key role in this. Hydrogen is seen as "the" solution for a post-fossil but still flexible energy supply, particularly because of its storage and transport capability.

Even if hydrogen is currently more being discussed as a basic material for industrial applications or their CO<sub>2</sub>-neutral energy supply and is already being widely used in some cases, it also represents a highly interesting energy carrier for mobility. On the one hand side, it can be used in conventional combustion engines, but also in fuel cells for electric powertrains.

However, this article presents how hydrogen-based powertrains compare to purely battery-electric powertrain and diesel engine powertrains powered by fossil fuel in three different vehicle classes. The three vehicle classes are in detail a heavy passenger car, a light commercial vehicle and finally the heavy commercial vehicle. To classify the potential of the powertrains in terms of TtW, WtW and also CtG CO<sub>2</sub> intensities as well as manufacturing costs and the TCO (Total Cost of Ownership), a techno-economic study was carried out, the results of which are discussed in detail in this paper.

The study comes to the following main conclusions:

1. In passenger cars, hydrogen powertrain may well be an alternative to battery electric powertrains, at least in the medium term, until a sufficient amount of nationally generated fully renewable electricity is available.
2. For the fuel cell, it is even possible to speak of a long-term alternative in the passenger car sector. In this case, however, blue and turquoise hydrogen or imported green hydrogen must be available and used.
3. Hybridized H<sub>2</sub> ICE powertrains represent a real alternative to battery-electric mobility and the fuel cell for light commercial vehicles in the medium and long term, both from a CO<sub>2</sub> equivalent and TCO point of view.
4. In heavy-duty commercial vehicles for long-haul application, hydrogen powertrains represent a rapid measure for achieving a CO<sub>2</sub>-free mobility, especially in the short and medium term. From a TCO point of view, the H<sub>2</sub>-ICE can be seen as a short-term solution with an advantage over the FC. This will change from 2030, when the FC will also have an advantage in terms of TCO. In the regional delivery sector, the BEV will prevail. For special applications with increased power density requirements, highly efficient diesel (e-fuel) or H<sub>2</sub>-ICE powertrains will also play a role in the long term.
5. If the focus is purely on the TtW efficiency of the powertrain, the FC is basically at an advantage over the H<sub>2</sub> ICE in all applications.

## **Kurzfassung**

Die Erreichung zukünftiger Klimaziele bedeutet zwingend den Schwenk hin zu einer CO<sub>2</sub>-neutralen Gesellschaft. Neben regenerativ erzeugtem Strom kommt dem Wasserstoff dabei eine Schlüsselrolle zu. Insbesondere aufgrund seiner Speicher- und Transportfähigkeit wird Wasserstoff als „die“ Lösung für eine post-fossile aber weiterhin flexible Energieversorgung angesehen.

Auch wenn Wasserstoff aktuell eher als Grundstoff für industrielle Anwendungen oder deren CO<sub>2</sub>-neutrale Energieversorgung diskutiert wird und bereits teilweise breite Anwendung findet, so stellt er auch für die Mobilität einen hoch interessanten Energieträger dar. Einerseits kann er in konventionellen Verbrennungsmotoren zum Einsatz kommen, andererseits aber auch in Brennstoffzellen für elektrische Antriebsstränge. Wie sich die wasserstoffbasierten Antriebe im Vergleich zu rein batterieelektrischen Antrieben und den mit fossilem Kraftstoff betriebenen dieselmotorischen Antrieben in drei verschiedenen Fahrzeugklassen einordnen lassen, wird in diesem Beitrag erörtert. Bei den drei Fahrzeugklassen handelt es sich im Einzelnen um einen schweren PKW, ein leichtes Nutzfahrzeug und schließlich ein schweres Nutzfahrzeug. Zur Einordnung der Potenziale der Antriebe in Bezug auf die TtW-, WtW- und auch CtG-CO<sub>2</sub>-Intensitäten sowie die Herstellkosten und die Total Cost of Ownership wurde eine techno-ökonomische Studie durchgeführt, deren Ergebnisse in der vorliegenden Arbeit detailliert diskutiert werden.

Zu folgenden Schlussfolgerungen kommt die Studie:

1. Im PKW Fahrzeug können Wasserstoffantriebe wenigstens mittelfristig, bis eine ausreichende Menge an national erzeugtem regenerativem Strom zur Verfügung steht, durchaus eine Alternative zu batterieelektrischen Antrieben darstellen.
2. Für die Brennstoffzelle kann im PKW-Bereich sogar von einer langfristigen Alternative gesprochen werden. Hierbei muss aber eben auch blauer und türkiser Wasserstoff bzw. importierter grüner Wasserstoff zur Verfügung stehen und genutzt werden.
3. Hybridisierte H<sub>2</sub> VKM-Antriebe stellen für das leichte Nutzfahrzeug mittel- und auch langfristig sowohl aus CO<sub>2</sub>-Äquivalente als auch TCO-Sicht eine echte Alternative zur batterieelektrischen Mobilität und der Brennstoffzelle dar.
4. Im schweren Nutzfahrzeug stellen die Wasserstoffantriebe vor allem kurz- und mittelfristig eine schnelle Maßnahme zur Erzielung CO<sub>2</sub>-freier Mobilität im Schwerlastverkehr dar. Hierbei kann aus TCO-Sicht als kurzfristige Lösung die H<sub>2</sub> VKM gegenüber der BZ im Vorteil gesehen werden. Dies ändert sich ab 2030, dann ist die BZ auch bezüglich TCO im Vorteil.
5. Wird rein auf den TtW-Wirkungsgrad des Antriebs fokussiert, so ist die BZ grundsätzlich im Vorteil zur H<sub>2</sub> VKM.

## **Table of contents**

Abstract.....	1
Kurzfassung.....	2
Introduction.....	5
Comparative study of hydrogen-based powertrain systems for passenger cars and commercial vehicles in their ecosystems.....	6
Approach and aim of the comparative study.....	6
Vehicle overview, powertrain systems and H <sub>2</sub> production paths.....	6
Powertrain optimization.....	7
Results for passenger car.....	8
Powertrain parameters and optimization.....	8
System specification, consumptions and CO <sub>2</sub> footprints.....	9
TCO and manufacturing costs.....	11
Summary Passenger Car.....	11
Results for light commercial vehicle.....	12
System specification, consumptions and CO <sub>2</sub> footprints.....	12
TCO and manufacturing costs.....	14
Summary light commercial vehicle.....	15
Results for heavy-duty commercial vehicles.....	15
System specification, consumptions and CO <sub>2</sub> footprints.....	15
TCO and manufacturing costs.....	19
Summary of heavy-duty commercial vehicles.....	20
Overall comparison and conclusion.....	20
Powertrain-specific challenges and possible technical solutions.....	21
Efficiency of fuel cell and H <sub>2</sub> -ICE in comparison.....	21
Technological Challenges and Potentials in the Development of PEM Fuel Cell Systems	22
System efficiency and power density.....	23
Cost reduction of fuel cell systems.....	26
Lifetime and durability.....	27
Technological challenges and potentials in the development of H <sub>2</sub> -ICE.....	29
Objective.....	29
Methodology.....	29
Challenges of an H <sub>2</sub> ICE.....	32
Summary and development priorities H <sub>2</sub> -ICE.....	45
Exhaust gas aftertreatment concepts to achieve future emission regulations for H <sub>2</sub> -ICEs.	47
Passenger cars and light commercial vehicles.....	47
Heavy-duty vehicles.....	51

Hydrogen storage systems .....	55
Overview hydrogen storage systems.....	55
CGH <sub>2</sub> (Compressed Gaseous Hydrogen).....	56
LH <sub>2</sub> (Liquid Hydrogen) .....	57
CcH <sub>2</sub> (Cryo Compressed Hydrogen).....	57
Selection of the most advantageous storage system .....	57
Potential analysis of hybridized H <sub>2</sub> -ICE powertrains .....	58
Demand analysis and development of the necessary H <sub>2</sub> infrastructure.....	63
Status of H <sub>2</sub> infrastructure 2021 .....	64
H <sub>2</sub> infrastructure in 2030: requirements and vision .....	64
H <sub>2</sub> demand for road transport .....	64
Production and supply .....	64
Type and density of the service station network .....	66
Techno-economic comparison of H <sub>2</sub> supply pathways.....	67
Summary of the study findings.....	70
Appendix A .....	74
Acknowledgements.....	74
List of abbreviations .....	74
Bibliography .....	76

## **Introduction**

What does the optimal mobility scenario look like? This question is currently being addressed not only by automotive manufacturers, their suppliers and development partners, but also by policymakers. The battery-electric drive concept is expected to play a key role here. Because it is emission-free at local level, has a high degree of drive efficiency and is compatible with the direct use of electricity generated from renewable sources, it is also an appealing idea to convert road traffic from internal combustion engine-based drives to a completely battery-electric fleet. If only there were not the currently known and present weak points of electromobility:

1. Low storage densities of batteries compared to liquid energy sources and thus considerably reduced ranges per "energy filling."
2. Limited availability of raw materials for electric machines, power electronics and batteries.
3. Energy-intensive battery production and associated high CO<sub>2</sub> emissions.
4. Higher vehicle costs due to high battery costs.
5. Foreseeable lack of CO<sub>2</sub>-free electricity for battery charging and also in the long term not enough to cover the energy demand in all sectors.

All of the above points repeatedly lead to controversial discussions, especially on the question of whether pure battery electric e-mobility is the drive concept to strive for in all use cases. The current political framework in the form of EU regulations and additionally, at least in Germany, the high monetary incentives are currently leading to a rapidly increasing market share of battery electric e-drives in the passenger car segment. Furthermore, regulations have already been passed for commercial vehicles as well, which will lead to shifts in the type of drive over the next few years. Particularly when it comes to long-distance applications, there is controversy about the "right" drive. But where does long-distance mobility begin and do statements then always apply to all vehicle segments? In this context, hydrogen is repeatedly discussed as an energy carrier for mobile applications. It plays a key role in the energy transition, and its storage and transport capabilities are decisive factors. However, its use in road traffic is controversial: which vehicle segment should use batteries and which hydrogen as an energy storage medium?

In order to obtain a largely objective view of the potential of hydrogen in comparison with battery-electric electric mobility and to understand the respective influencing factors, a techno-economic study was carried out, the results of which are reported in this paper. The following framework covers the study, which has the year 2030 in view:

1. techno-economic comparison of 4 drive concepts in 3 vehicles:
  - Diesel VKM drive vs. E-drive vs. fuel cell vs. H<sub>2</sub>-VKM
  - Each of the above powertrains is evaluated in a heavy passenger vehicle, a light commercial vehicle, and a heavy commercial vehicle
2. evaluation criteria for each combination:
  - CO<sub>2</sub> intensity according to TtW, WtW, and CtG evaluation, with the hydrogen evaluated coming from different production sources (gray, turquoise, blue, and green hydrogen from national production are considered, as well as 100% renewable green hydrogen imported from the MENA region).
  - Cost of propulsion including energy storage
  - TCO costs for adjusted lifetime and mileage per vehicle class.

In order to take into account the then prevailing boundary conditions for the various drive systems in 2030, the study also examines the further technical development possibilities for fuel cell drives and combustion engine drives with hydrogen as fuel. Finally, aspects of the infrastructure required to establish hydrogen mobility are also addressed.

The following topics are presented and discussed in this paper:

1. Techno-economic study
2. Further development potential of the fuel cell system with a time horizon of 2030
3. Further development potential of the hydrogen combustion engine with a time horizon of 2030
4. Exhaust gas aftertreatment system considerations for compliance with the strictest emission limits with H<sub>2</sub> VKM drives in all 3 vehicle classes
5. Expectation for the development of H<sub>2</sub> storage systems
6. Evaluation of the necessary infrastructural requirements for the realization of a nationwide H<sub>2</sub> mobility scenario
7. Techno-economic evaluation of hydrogen production/provision pathways.

## **Comparative study of hydrogen-based powertrain systems for passenger cars and commercial vehicles in their ecosystems**

### **Approach and aim of the comparative study**

The objective of the comparative study is the universal evaluation of hydrogen-based powertrain systems, including hydrogen production, and their comparison with powertrains using fossil fuels and battery-electric powertrains. The objective comparison includes the powertrain and the storage systems as well as the generation paths for hydrogen with different processes and the provision of electrical energy. This Well-to-Wheel (WtW) consideration is additionally extended by the analysis of the complete vehicle life cycle (LCA), which enables the environmental impact of the production and recycling of the vehicles and powertrains from Cradle to Grave (CtG). Furthermore, the economic aspects of hydrogen production and propulsion system deployment are considered, leading to the specification of manufacturing costs and total cost of ownership (TCO). The manufacturing cost calculation is based on physical component models and includes material, production, assembly and overhead costs assuming individual unit quantities.

The study was prepared with particular attention to objective comparability between the powertrain concepts and the manufacturing paths for all vehicles and types of use. Thus, all powertrain systems in all vehicle classes were individually optimized in their main parameters and examined under the same operating boundary conditions. Since the technical, ecological and economic aspects are the main focus of this study, fiscal control elements and usability aspects (e.g. charging times und influence of ambient conditions) were largely excluded, particularly for hydrogen and electricity generation and vehicle operation. The result makes it possible to compare different powertrain concepts in different vehicle classes, taking into account the generation paths of hydrogen and electrical energy, with regard to technical, ecological and economic aspects.

### **Vehicle overview, powertrain systems and H<sub>2</sub> production paths**

**Figure 1** schematically shows the considered H<sub>2</sub> generation paths, the vehicle segments and the powertrain types. For the production of hydrogen, the processes steam methane reforming (SMR) - grey hydrogen, SMR with carbon capture and storage (CCS) - blue

hydrogen, methane pyrolysis - turquoise hydrogen and water electrolysis with different electricity mixes are considered. In addition, the import of renewable hydrogen from MENA (Middle East North Africa) countries is considered. In addition to the feedstocks, the required electrical energy is considered in a differentiated manner, either from the electricity mix anticipated for 2030 [1] or exclusively from renewable generation. This differentiation is also applied to the charging processes of the BEV's and partly to the production of the vehicles and powertrain components.

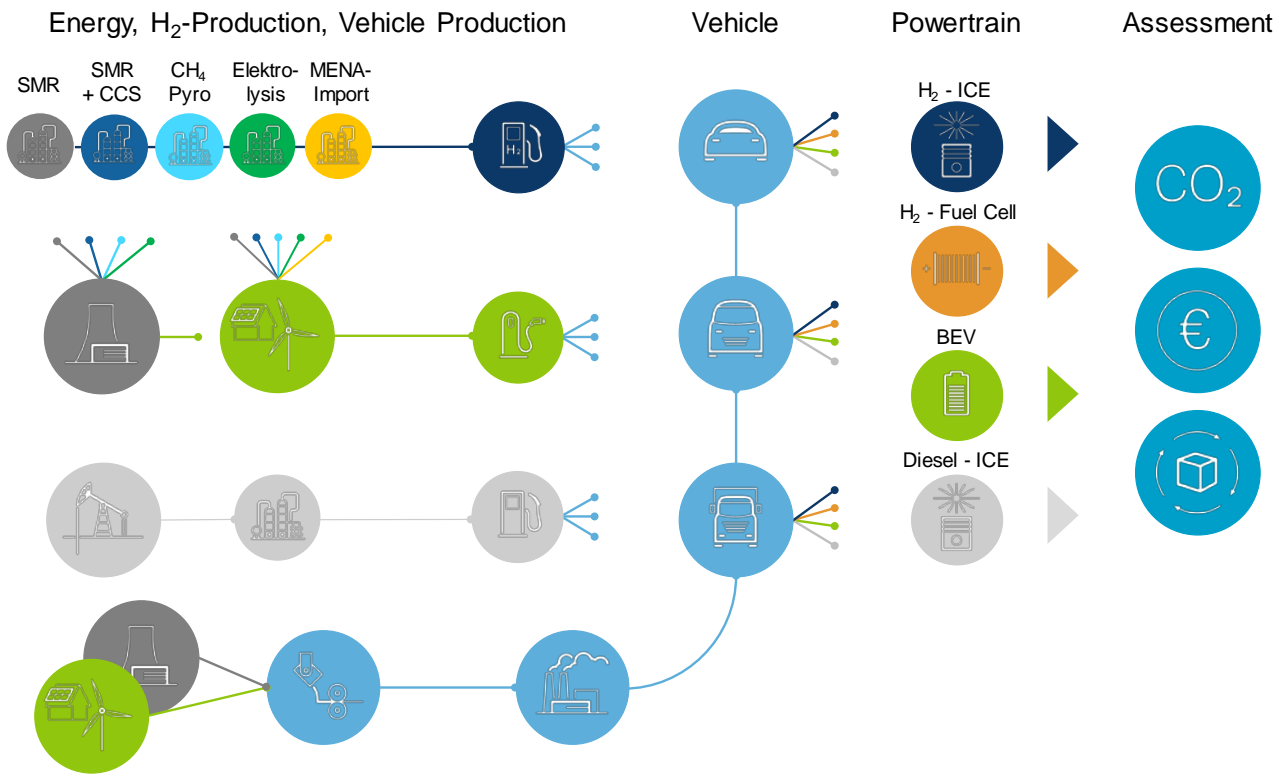


**Figure 1:** Overview of H<sub>2</sub>-Production paths, energy supply, vehicle segments and powertrain types

On the vehicle side, this study differentiate in passenger cars (SUV-segment) and commercial vehicles (light and heavy). Each vehicle segment is considered with H<sub>2</sub> combustion engine powertrain (H<sub>2</sub>-ICE), H<sub>2</sub> fuel cell powertrain (H<sub>2</sub>-FCEV) and pure battery powertrain (BEV). In addition, diesel combustion engines (Diesel-ICE) are used as fossil reference systems for evaluation. For each combination of energy supply, H<sub>2</sub> generation pathway, vehicle and powertrain, fuel and energy consumptions, equivalent CO<sub>2</sub> emissions for WtW and CtG balancing, manufacturing costs of the powertrains and TCO trajectories are calculated. The focus is on Germany in 2030. All other assumptions and detailed information are included in Appendix A.

### Powertrain optimization

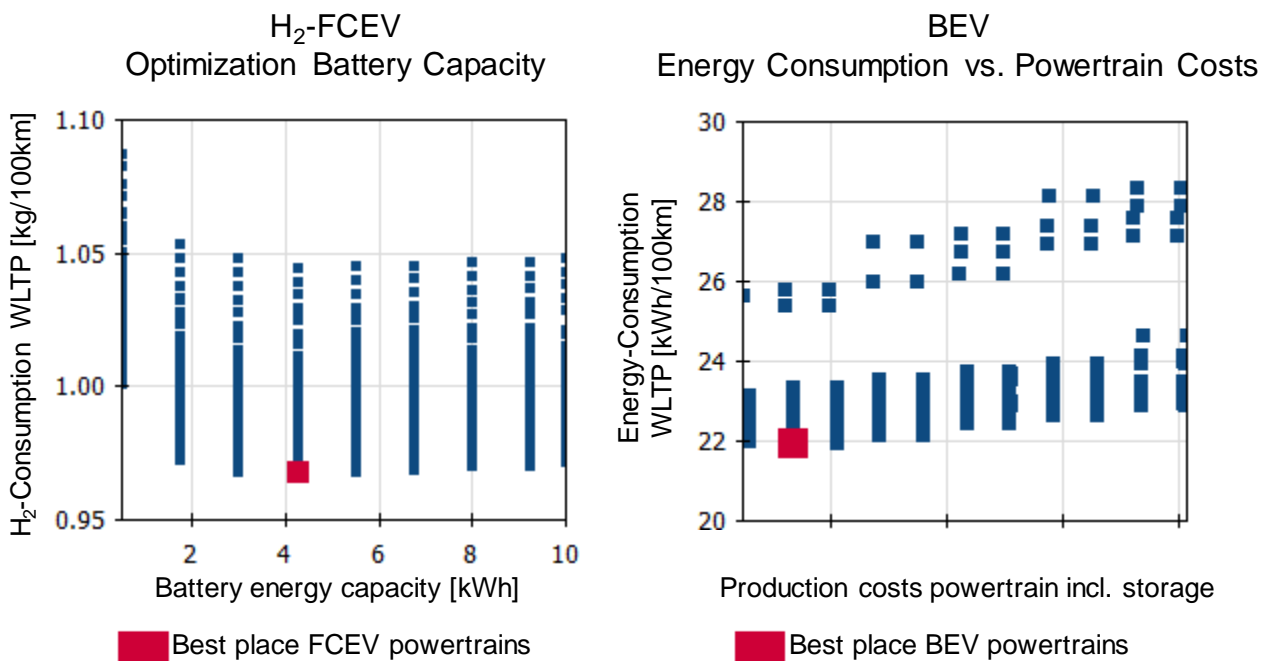
To ensure comparability between the powertrain systems, systematic variation studies of the powertrain parameters were carried out for each vehicle segment. This is based on IAV's unique Powertrain Synthesis methodology [2], [3] with coupled life cycle and cost assessment. This methodology enables fully combinatorial optimization of all key powertrain parameters. Thus, depending on the type of powertrain, the transmission ratios, the power characteristics of the electric drives and the energy capacities of the batteries are varied

completely systematically. In compliance with typical requirement profiles, consumption optimizations are then carried out to ensure the highest possible overall efficiency of the primary converter and powertrain components. The sizing of the H<sub>2</sub> tank systems (H<sub>2</sub>-ICE, H<sub>2</sub>-FCEV) and the traction battery (BEV) are always range-scaled, whereby the system efficiency directly influences the storage size and thus the cost and life cycle footprint. This constraint enables a focused optimization on the fuel or energy consumption of the powertrain variants. Furthermore, the vehicle-specific requirements are applied to the complete amount of variants, allowing the optimization of the various powertrain types with parity in performance characteristics.

## Results for passenger car

### Powertrain parameters and optimization

For the passenger car segment, a compact-class SUV with a range of 500 km was assumed. For the 90 kW H<sub>2</sub>-ICE, a transmission optimization for a 6-speed dual clutch transmission was performed. The fuel cell propulsion system was optimized in terms of HV battery energy capacity and key axle drive parameters (EM power, EM torque, number of speeds, and transmission ratios). The axle drive parameters were also varied for the BEV. Both hydrogen-powered systems, as well as the battery electric powertrain, were designed to always have the same target range. The number of powertrain concepts considered in the passenger car thereby comprises approximately 68,300 variants. Detailed value ranges can be found in Appendix A. **Figure 2** shows two exemplary sensitivity diagrams for the FCEV and BEV powertrains. The left figure shows the dependence of the minimum achievable hydrogen consumption over the battery energy content, after which the value of 4.25 kWh was optimized as optimal in the system context. The right figure shows the typical BEV relationship between energy consumption and powertrain costs (incl. battery), according to which particularly efficient powertrain systems also enable more cost- storage systems for the same range.

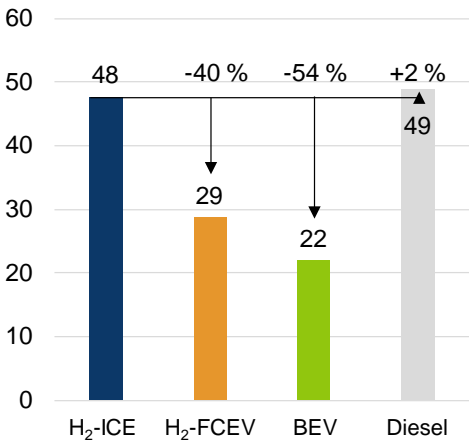


**Figure 2:** Optimization of the powertrain parameters for FCEV and BEV

## System specification, consumptions and CO<sub>2</sub> footprints

The powertrain optimization results in optimum system specifications for each powertrain type, which are shown in the **Table 1**. In addition to the powertrain components, this also includes the scaled storage sizes and the tank-to-wheel (TtW) consumption for the WLTP.

**Table 1:** Optimized system specifications for passenger cars in 2030

Vehicle, Range, Cycle	 <b>Passenger Car</b> 1.600 kg basic curb weight, FWD 500 km range, WLTP	2030
Powertrain	Optimal System Specification	Consumption energy for WLTP, TtW [kWh/100km]*
<b>H<sub>2</sub> ICE</b>	<b>ICE:</b> H <sub>2</sub> -DI, 2.0l 90 kW, 280 Nm, 2-Stage VTG, Max. Efficiency = 45 % <b>Transmission:</b> 6-Speed DCT 15.50 / 10.43 / 7.02 / 4.72 / 3.18 / 2.14 <b>Storage System:</b> 700 bar CGH <sub>2</sub> / 7.1 kg H <sub>2</sub>	
<b>H<sub>2</sub> FCEV</b>	<b>Fuel Cell System:</b> PEM 90 kW, Single Stack Max. FC-System Efficiency = 65 % <b>E-Motor:</b> 170 kW Peak, 400 Nm Peak <b>Transmission:</b> 2-Speed, 15.0 / 7.5 <b>Battery:</b> NMC, 400 V, 4.25 kWh <b>Storage System:</b> 700 bar CGH <sub>2</sub> / 4.3 kg H <sub>2</sub>	
<b>BEV</b>	<b>E-Motor:</b> 120 kW Peak, 300 Nm Peak <b>Transmission:</b> 2-Speed, 16.5 / 8.25 <b>Battery:</b> NMC, 400 V, 120 kWh	
<b>Diesel</b>	<b>ICE:</b> DI, 2.0l, 110 kW, 350 Nm <b>Transmission:</b> 6-Speed DCT	

\*Consumption values consider powertrain-individual factors for All-Seasons-Operation

The FCEV system with an optimized operating strategy achieves a consumption advantage in the WLTP of approx. 40 % compared to the optimal H<sub>2</sub>-ICE system. Here, the fuel cell is often operated in low power operating points with highest efficiencies. Compared to the BEV, the energy consumption of the H<sub>2</sub>-ICE is more than twice as high. The additional consumption potential due to hybridization for the ICE-variant is discussed separately in the corresponding chapter. The results are based on an assumed maximum speed for the FCEV- and ICE-systems of 180 km/h. At lower speeds of e.g. 160 km/h, depending on the vehicle, further consumption potentials can be enabled for the FCEV [4]. By modifying the combination of battery capacity and fuel cell power, full range extender operation can be realized, which means operation at a few specified operating points.

Based on the results of the powertrain optimization and the H<sub>2</sub> as well as electricity production paths considered, the respective CO<sub>2</sub> emissions (WtW) were determined and compared with those of the battery- and diesel-powered vehicles. From the UBA-RESCUE study [1] the shares of the energy production paths for the GreenEe1 scenario were used to calculate the CO<sub>2</sub> emissions of the future electric energy mix. From this, a CO<sub>2</sub> burden of 220 g CO<sub>2e</sub>/kWh is derived for the 2030 electricity mix in Germany.

For a production in Germany with 2030 electricity mix, blue hydrogen represents the lowest CO<sub>2</sub> pathway according to well-to-wheel balances, as shown in **Figure 3**. With low-CO<sub>2</sub> hydrogen from the MENA region, CO<sub>2</sub> emissions in both hydrogen-powertrains systems could even be reduced to about half compared to blue hydrogen from Germany. With blue hydrogen generated with German 2030 electricity mix, a fuel cell vehicle would then be about 10 g CO<sub>2e</sub>/km better than a battery vehicle charged with the same electricity mix and

33 g/km worse if it would be possible to charge the BEV with renewably generated electricity. A vehicle with an H<sub>2</sub> combustion engine would result in a CO<sub>2</sub> reduction (WtW) of about 54 % with blue hydrogen compared to a diesel engine. **Figure 3** also shows that hydrogen production by electrolysis in Germany with ordinary electricity mix would cause CO<sub>2</sub> emissions about a factor of two to three higher than production by methane pyrolysis or steam reformation with CCS.

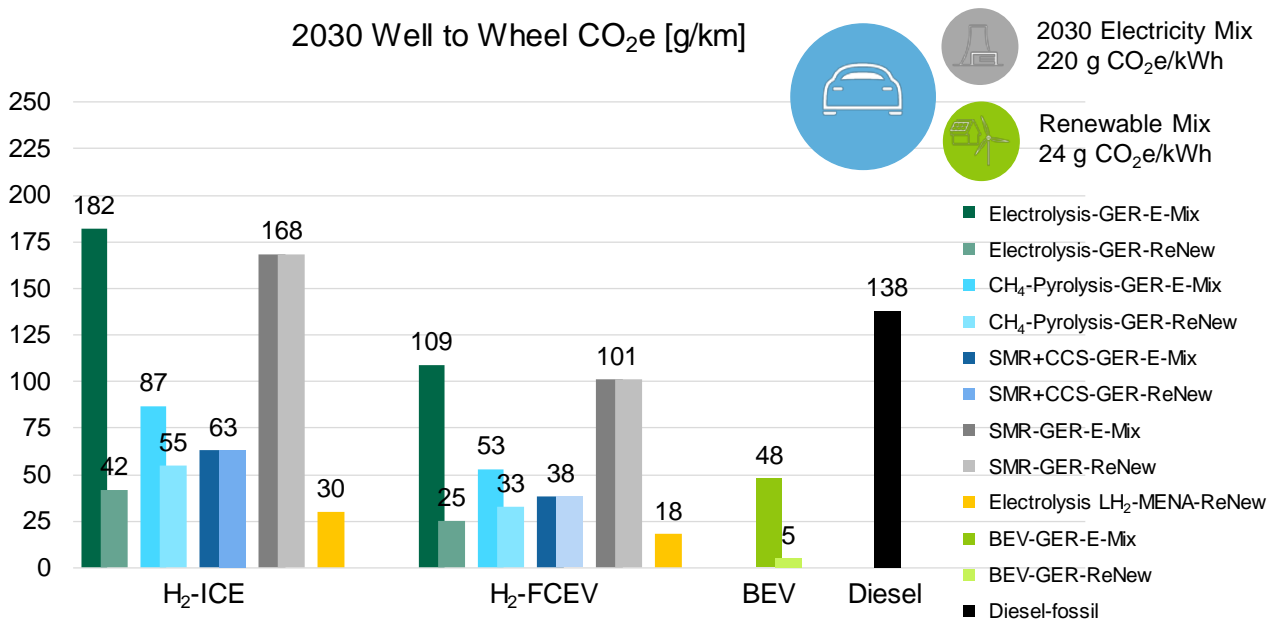


**Figure 3:** CO<sub>2</sub> emissions WtW for general and renewable electricity mix in 2030

Only if 100 % renewable electricity (assumption: 25 %-solar / 75 %-wind) can be used for hydrogen production, electrolysis in Germany represents a considerable CO<sub>2</sub> potential. If the complete amount of hydrogen required for the mobility-transformation is produced in Germany, this results in emissions that are only 7 or 12 g CO<sub>2</sub>e/km higher than if the hydrogen is produced in MENA regions using renewable electricity.

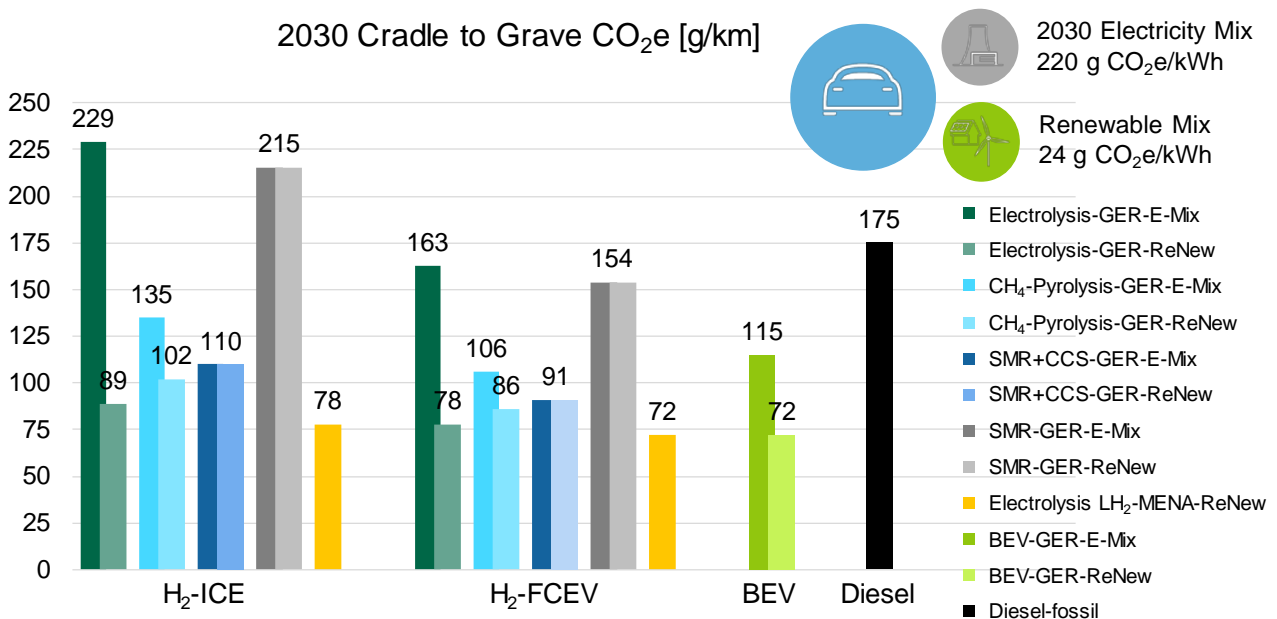


**Figure 4:** CO<sub>2</sub> emissions CtG for general and renewable electricity mix in 2030

Looking at the entire vehicle life cycle, **Figure 4** shows that with imported MENA-H<sub>2</sub>, both hydrogen powertrains reach almost the same CO<sub>2</sub> level as the battery vehicle, even if this is charged with 100 % renewable energy. It is highly likely that hydrogen can be produced in larger quantities with renewable energy in 2030. Assuming this is the case, the considered hydrogen powertrains would even emit about 40 g CO<sub>2</sub> per kilometer less than a battery vehicle, which is charged in average with ordinary electricity mix. In total, the comparison shows that in case of using renewable electricity for the passenger cars segment, the CO<sub>2</sub> backpack of the battery vehicles almost balances out with the additional emissions of H<sub>2</sub> generation over the vehicle life cycle.

### TCO and manufacturing costs

**Figure 5** shows the production costs of the entire powertrain including exhaust gas aftertreatment and storage system and the TCO values for 2030.

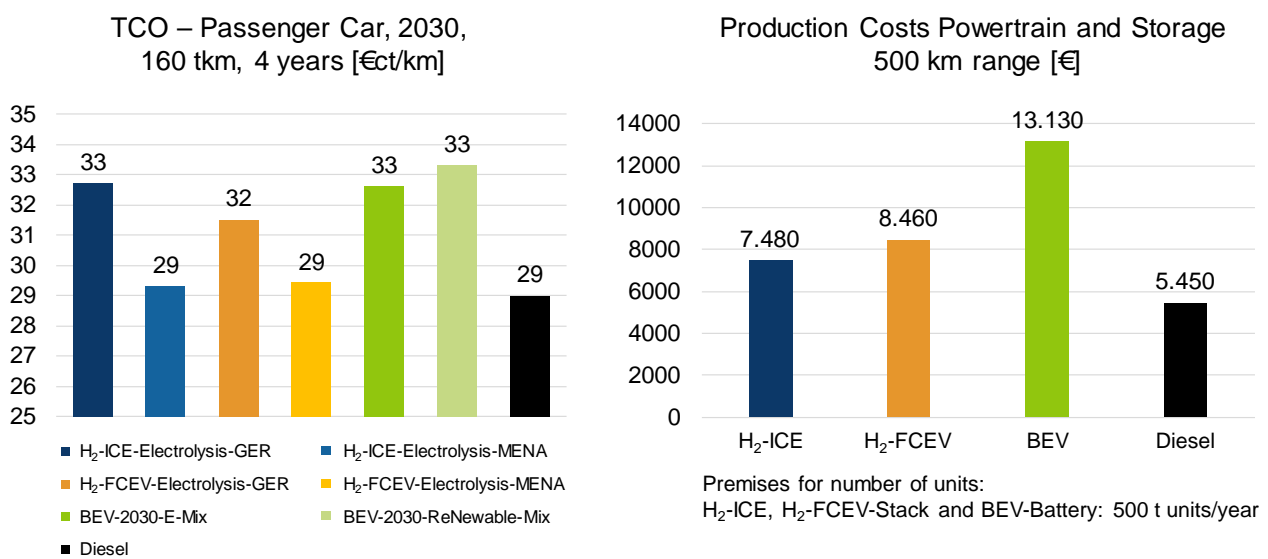


**Figure 5:** TCO and production costs for passenger cars

An annual number of 500,000 units was assumed for all powertrain systems in 2030. Despite the larger storage volume of the H<sub>2</sub>-ICE system due to consumption, the component costs of the FCEV systems are around 1,000 € higher. Due to the tank technology, both hydrogen powertrains are in total about 2,000 € to 3,000 € more expensive than the diesel reference. Looking at the TCO values for 2030, it is noticeable that when using MENA hydrogen, the total costs are at the same level as diesel and even 3 to 4 €ct/km cheaper than with a battery vehicle. In terms of TCO, no clear trend can be identified for either of the two hydrogen propulsion systems.

### Summary Passenger Car

The well-to-wheel CO<sub>2</sub> potential of the examined passenger cars with hydrogen powertrains is significant with 54 % compared to a corresponding diesel vehicle, even if the hydrogen is produced in Germany in 2030 with ordinary electricity mix. In the considered passenger car SUV segment, both the H<sub>2</sub>-ICE and the FCEV powertrains with blue hydrogen are on a similar level in terms of CO<sub>2</sub> as the battery powertrains. With MENA imported hydrogen and fuel cell propulsion system, CO<sub>2</sub>-emissions can be reduced to only 18 g CO<sub>2</sub>e/km (WtW, WLTP). Considering the whole vehicle life cycle, it is clear that with imported MENA-H<sub>2</sub>, both hydrogen powertrains can reach almost the same CO<sub>2</sub> level of a battery vehicle, even if this

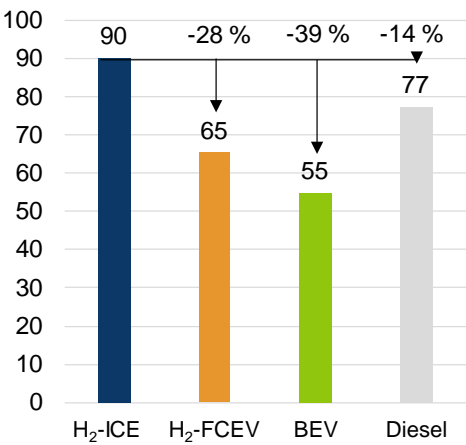
would be charged with 100 % renewable energy. In terms of overall costs, the hydrogen propulsion systems are even cheaper than a comparable battery vehicle. Overall, for the passenger car segment, the fuel cell system shows the greatest potential in terms of efficiency, cost and sustainability. The approximately 40 % higher fuel consumption of the non-hybridized H<sub>2</sub>-ICE leads to larger tank systems, which significantly affects both the production costs and the CO<sub>2</sub> footprints of the vehicle and the hydrogen. The improvement potential of hybridization concepts is therefore considered in more detail in the chapter: Potential analysis of hybridized H<sub>2</sub>-ICE powertrains.

## Results for light commercial vehicle

### System specification, consumptions and CO<sub>2</sub> footprints

The powertrain systems in the light commercial vehicle segment were also optimized in the same way as for passenger cars. From the total concept amount of approx. 192,000 variants, the consumption-optimized systems were selected in relation to a 500 km range. The **Table 2** shows the optimal system specifications and energy consumption. According to this, the consumption advantage of the fuel cell powertrain system is reduced to about 28 % compared to the H<sub>2</sub>-ICE. This is mainly due to the specific higher utilization of the LCV-ICE compared to the passenger car application. In terms of consumption, a diesel powertrain also exhibits about 14 % lower fuel consumption compared to the H<sub>2</sub>-ICE. The optimization resulted in a capacity of 9.25 kWh as the most fuel-efficient battery size for the FCEV systems. The predictive operating strategy (dynamic programming) assumed for the year 2030 keeps the fuel cell in the loss-favorable range for long periods at low power levels around 11 kW. Only at higher driving power requirements does the primary converter follow the requested DC link power, while otherwise the cycle dynamics are balanced by the HV battery.

**Table 2:** Optimized system specifications LDCV in 2030

Vehicle, Range, Cycle		<b>Light Commercial Vehicle</b> 2.250 kg basic curb weight, RWD 500 km range, WLTP	2030
Powertrain	<b>Optimal System Specification</b>		<b>Consumption energy for WLTP, TtW [kWh/100km]*</b>
<b>H<sub>2</sub> ICE</b>	<b>ICE:</b> H <sub>2</sub> -DI, 2.0l 130 kW, 350 Nm, 2-Stage VTG, Max. Efficiency = 45 % <b>Transmission:</b> 7-Speed AT 16.50 / 11.93 / 8.63 / 6.24 / 4.51 / 3.26 / 2.36 <b>Storage System:</b> 700 bar CGH <sub>2</sub> / 13.5 kg H <sub>2</sub>		
<b>H<sub>2</sub> FCEV</b>	<b>Fuel Cell System:</b> PEM 2x65 kW, Double Stack Max. FC-System Efficiency = 65 % <b>E-Motor:</b> 240 kW Peak, 500 Nm Peak <b>Transmission:</b> 2-Speed, 21.0 / 10.5 <b>Battery:</b> NMC, 400 V, 9.25 kWh <b>Storage System:</b> 700 bar CGH <sub>2</sub> / 9.8 kg H <sub>2</sub>		
<b>BEV</b>	<b>E-Motor:</b> 170 kW Peak, 450 Nm Peak <b>Transmission:</b> 2-Speed, 23.0 / 14.4 <b>Battery:</b> NMC, 400 V, 302 kWh		
<b>Diesel</b>	<b>ICE:</b> DI, 2.0l, 150 kW, 400 Nm <b>Transmission:</b> 7-Speed AT		

\*Consumption values consider powertrain-individual factors for All-Seasons-Operation

The consideration of the WtW-CO<sub>2</sub> balances in **Figure 6** shows that in the light commercial vehicle, the combustion engine with blue hydrogen from Germany can achieve slightly lower WtW-CO<sub>2</sub> emissions than an equivalent battery vehicle with 2030 electricity mix.

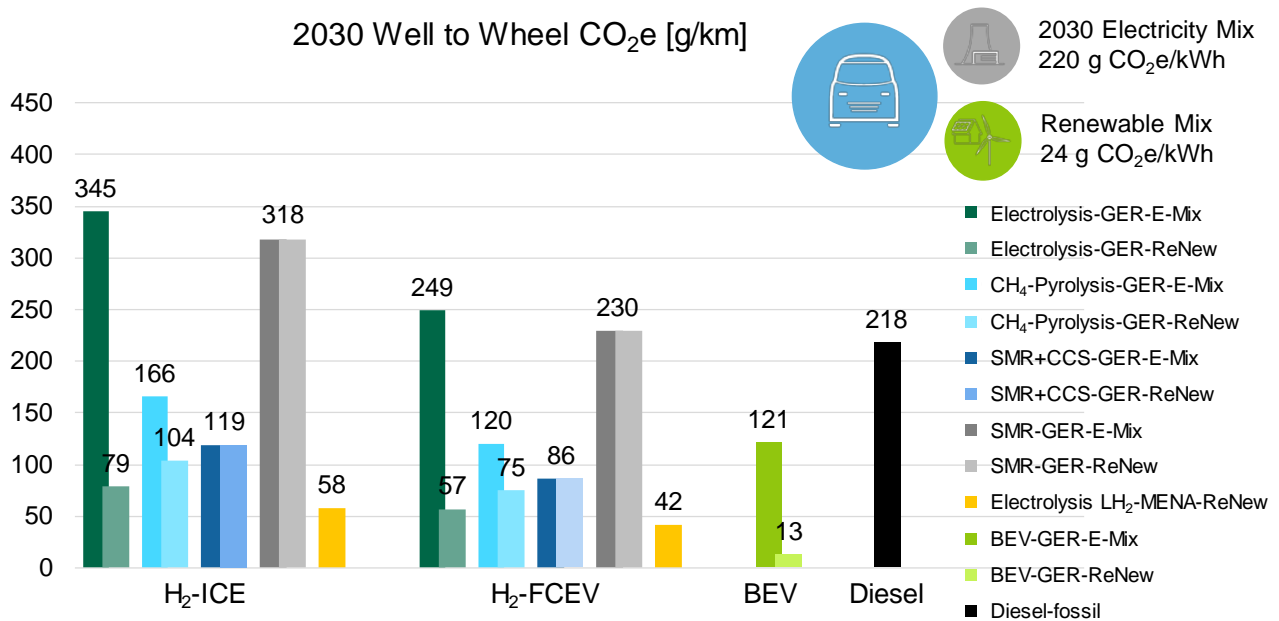


**Figure 6:** CO<sub>2</sub> emissions WtW for general and renewable electricity mix in 2030

Furthermore, it can be seen that with imported MENA hydrogen, the equivalent CO<sub>2</sub> emissions are between a factor of two to three lower than with a battery vehicle charged with 2030 electricity mix. A H<sub>2</sub>-ICE vehicle with blue hydrogen would be approximately 50 % lower in CO<sub>2</sub> (WtW) than a diesel-powered vehicle.

With 100 % renewable electricity, the resulting WtW-emissions for the electrolysis and methane pyrolysis pathways can be lowered below the level of blue hydrogen. Assuming an all-seasons target range of 500 km, the BEV systems have a battery energy content of more than 300 kWh, which has a significant impact on the CO<sub>2</sub> footprint of the powertrain. **Figure 7** shows the CtG-CO<sub>2</sub> values, which include both the electrical energy and the vehicle production. Here, the hydrogen powertrains show a very similar level compared to the BEV variants almost regardless of the generation path. It can be deduced from this that in case of using renewable energy the operating emissions of the various powertrain systems and the CO<sub>2</sub> footprints of the components almost balance each other out in terms of the entire life cycle. If the battery vehicle is charged with ordinary electricity mix, blue and turquoise hydrogen result in significant CO<sub>2</sub> potentials for the hydrogen powertrain of up to 86 g CO<sub>2</sub>e/km assuming the predicted electricity mix for 2030.

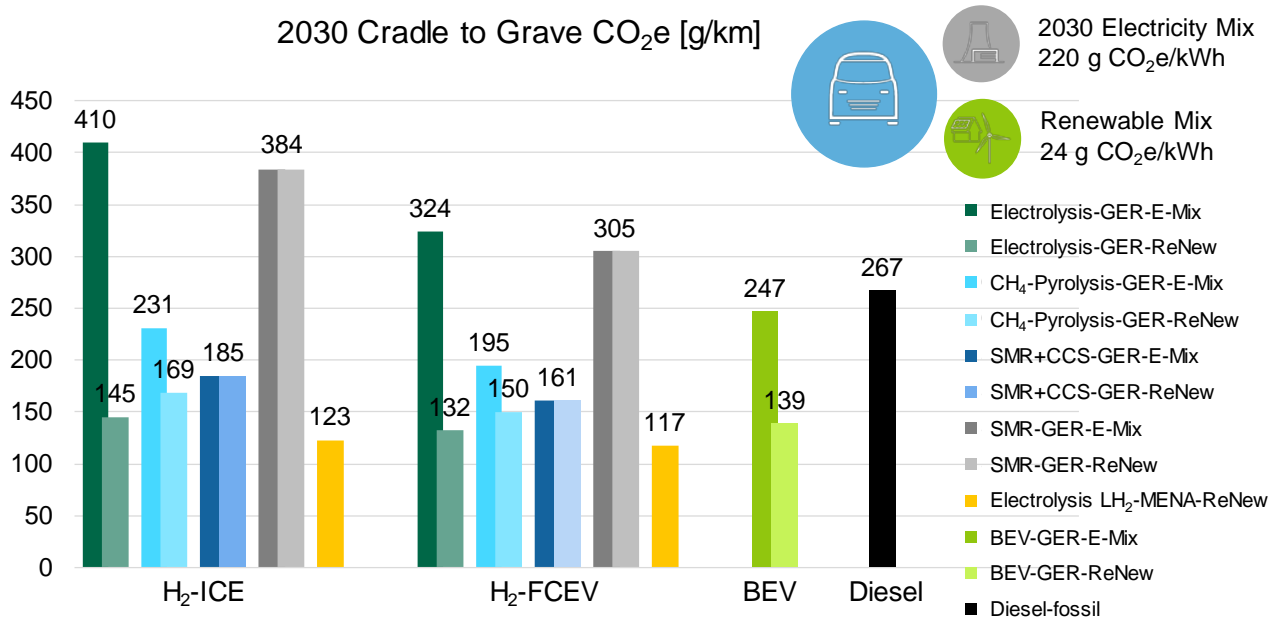


Figure 7: CO<sub>2</sub> emissions CtG for general and renewable electricity mix in 2030

### TCO and manufacturing costs

The high energy content of the EV battery systems is reflected not only in a high impact on the CO<sub>2</sub> footprint, but also in increased production costs, which is illustrated in **Figure 8**. Even assuming full carry over use of passenger car cell modules, the total cost of the powertrain system in the LCV rises to over 30,000 €. The more powerful fuel cell, battery and e-drive unit (EDU) compared to the passenger car increases the production costs of the FC-powertrain by about 3,000 € compared to the H<sub>2</sub>-ICE powertrain, despite the smaller tank system. Looking at the TCO values for 2030, it is noticeable that with MENA hydrogen the total cost per kilometer can be reduced to below 34 €/t/km. According to **Figure 8**, the scenarios with ICE propulsion are even cheaper overall than the FC-systems, despite the additional hydrogen consumption.

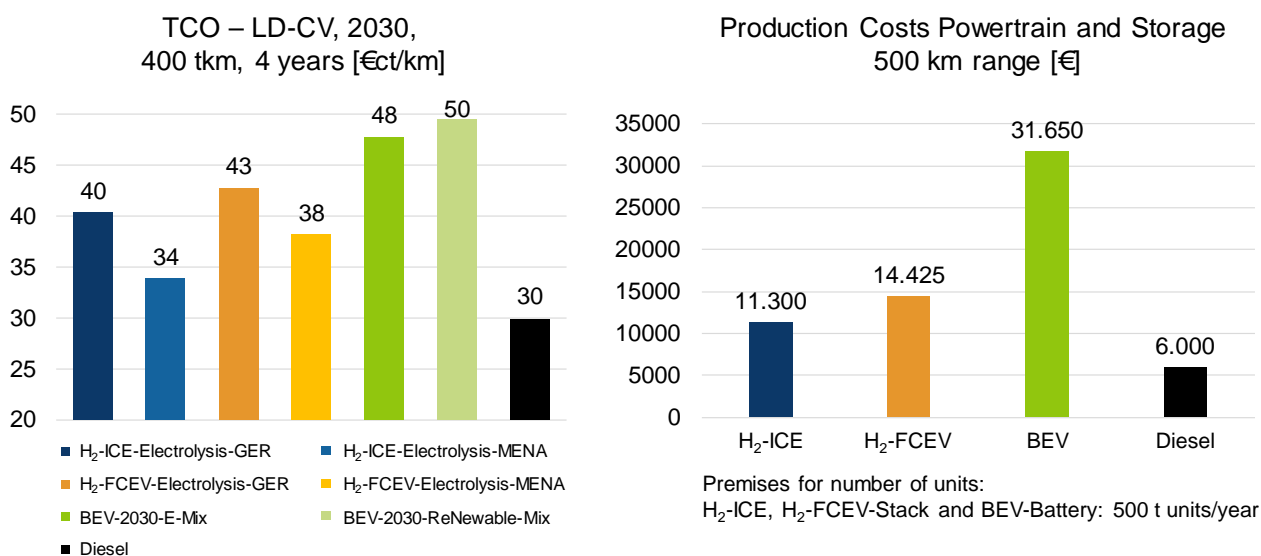


Figure 8: TCO and manufacturing costs for LDCV in 2030

The higher H<sub>2</sub> consumption of the ICE powertrain is also liable for the fact that those systems benefit more from the assumed decreasing of the hydrogen production costs until 2030, which is especially true for hydrogen from the MENA region. Nevertheless, in terms of cost, diesel is the cheapest propulsion system at 30 €/ct/km. Assuming that the high production costs of the battery systems are passed on to the sales prices in the same way as for the other powertrains, the BEV systems represent the most expensive mobility scenario for this vehicle segment at around 48 to 50 €/ct/km.

### **Summary light commercial vehicle**

For the light commercial vehicle, there is particular potential for the H<sub>2</sub>-ICE powertrain. Compared to passenger cars, the combustion engine has a higher specific load, which means that the consumption gap to the FCEV powertrains are smaller in this vehicle segment. This results in a relatively compact and cost-efficient system settings. Both the FC- and ICE-powertrain offer lower WtW-CO<sub>2</sub> emissions per kilometer in 2030 using blue hydrogen compared with a BEV using German electricity mix. Another CO<sub>2</sub> and cost potential is possible by using renewable MENA hydrogen, where in terms of TCO the H<sub>2</sub>-ICE is even the cheapest scenario among the low-CO<sub>2</sub> systems. Only fossil diesel is still expected to be about 4 €/ct/km cheaper in 2030 without any fiscal intervention. Accordingly, the FC-powertrain and the H<sub>2</sub>-ICE are interesting alternatives to fossil and battery electric powertrains under all evaluation criteria. Based on the premises made, there are slight advantages for the H<sub>2</sub>-ICE powertrain type in the LCV segment.

## **Results for heavy-duty commercial vehicles**

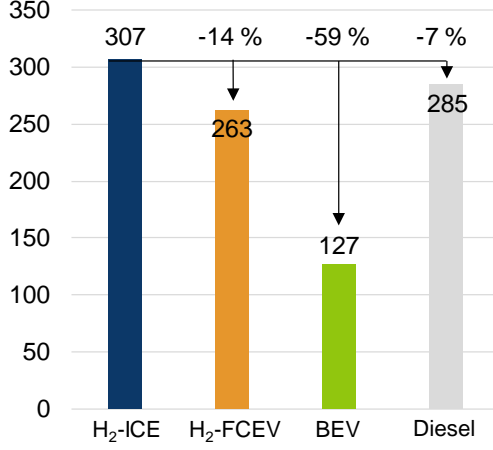
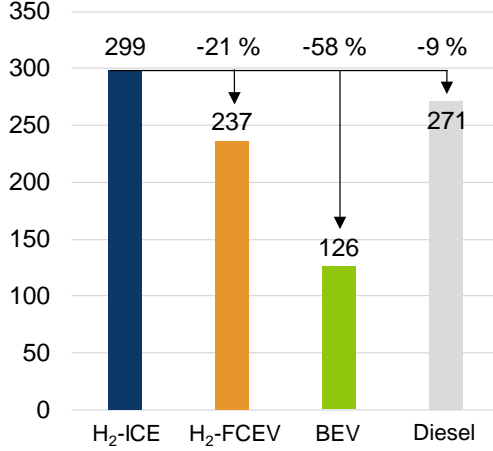
### **System specification, consumptions and CO<sub>2</sub> footprints**

Due to the variance of application scenarios, the heavy-duty commercial vehicles segment is characterized by a high degree of diversification in the requirements placed on the powertrain system. In addition, legal requirements, in particular exhaust emission and CO<sub>2</sub> legislation, determine the powertrain layout. The CO<sub>2</sub> legislation of the European Union (EU), which stipulates a CO<sub>2</sub> reduction in the heavy on-highway sector of 15 % by 2025 and 30 % by 2030 compared to 2019, is particularly noteworthy here. In addition, entry bans for inner cities with internal combustion engines are to be expected, which means that electric drives will come into focus, especially in the heavy regional delivery sector. Furthermore, attractive total cost of ownership (TCO) forms the basis for the marketability of a technological solution. This is currently given above all for zero-emission powertrains by the current incentives. The reasons listed above result in widely differing solutions for application-specific optimum powertrain layout.

In this study, the focus is on the application in heavy-duty long-haul commercial vehicles. Heavy delivery trucks are discussed comparatively. The optimum system layout in each case was determined using IAV's own optimization tools and subjected to a complete vehicle simulation. The resulting optimum powertrain system configurations are shown separately for the years 2025 and 2030 in the **Table 3**.

For the long-haul application, the BEV has the lowest energy consumption, followed by H<sub>2</sub>-FCEV, Diesel and H<sub>2</sub>-ICE. This basic picture does not change in 2030. However, the percentage improvements in consumption between 2025 and 2030 differ between the powertrain types. For Diesel, an efficiency increase of about 10 % is possible with the help of a high-efficiency concept. This includes waste heat recovery, phase change cooling, friction optimization, an optimized injection system and intelligent thermal management.

**Table 3:** Optimized system specifications HDCV in 2025 and 2030

Vehicle, Range, Cycle	 <b>Heavy Duty Commercial Vehicle</b> Tractor vehicle, 35 t Simulation mass, 800 km range, Vecto Long-haul cycle	2025															
Powertrain	<b>Optimal System Specification</b>	<b>Consumption energy for Vecto LH, TtW, 2025 [kWh/100km]</b>															
<b>H<sub>2</sub> ICE</b>	<b>ICE:</b> H <sub>2</sub> -LPDI, 12.5l, 310 kW Max. Efficiency = 44 % <b>Transmission:</b> 12-Speed AMT 14.93 / 11.64 / 9.02 / 7.04 / 5.64 / 4.40 / 3.39 / 2.65 / 2.05 / 1.60 / 1.28 / 1.00 <b>Storage System:</b> 700 bar CGH <sub>2</sub> / 81 kg H <sub>2</sub>	 <table border="1"> <caption>Consumption energy for Vecto LH, TtW, 2025 [kWh/100km]</caption> <thead> <tr> <th>Powertrain</th> <th>Consumption [kWh/100km]</th> <th>% Change vs H<sub>2</sub>-ICE</th> </tr> </thead> <tbody> <tr> <td>H<sub>2</sub>-ICE</td> <td>307</td> <td>-</td> </tr> <tr> <td>H<sub>2</sub>-FCEV</td> <td>263</td> <td>-14 %</td> </tr> <tr> <td>BEV</td> <td>127</td> <td>-59 %</td> </tr> <tr> <td>Diesel</td> <td>285</td> <td>-7 %</td> </tr> </tbody> </table>	Powertrain	Consumption [kWh/100km]	% Change vs H <sub>2</sub> -ICE	H <sub>2</sub> -ICE	307	-	H <sub>2</sub> -FCEV	263	-14 %	BEV	127	-59 %	Diesel	285	-7 %
Powertrain	Consumption [kWh/100km]		% Change vs H <sub>2</sub> -ICE														
H <sub>2</sub> -ICE	307		-														
H <sub>2</sub> -FCEV	263		-14 %														
BEV	127		-59 %														
Diesel	285	-7 %															
<b>H<sub>2</sub> FCEV</b>	<b>Fuel Cell System:</b> PEM 2x110 kW Max. FC-System Efficiency = 62 % <b>E-Motor:</b> 600 kW Peak, 700 Nm Peak <b>Transmission:</b> 4-Speed, 65.0 / 39.4 / 23.8 / 14.4 <b>Battery:</b> NMC, 400 V, 70 kWh <b>Storage System:</b> 700 bar CGH <sub>2</sub> / 69 kg H <sub>2</sub>																
<b>BEV</b>	<b>E-Motor:</b> 650 kW Peak, 700 Nm Peak <b>Transmission:</b> 4-Speed, 75.0 / 45.4 / 27.5 / 16.7 <b>Battery:</b> NMC, 800 V, 1,120 kWh																
<b>Diesel</b>	<b>ICE:</b> DI, 12.5l, 320 kW, 2,400Nm <b>Transmission:</b> 12-Speed AMT																
<b>2030</b>																	
<b>H<sub>2</sub> ICE</b>	<b>ICE:</b> H <sub>2</sub> -LPDI, 12.5l, 310 kW Max. Efficiency = 46 % <b>Transmission:</b> 12-Speed DCT 13.40 / 10.33 / 8.02 / 6.19 / 4.77 / 3.68 / 2.81 / 2.16 / 1.68 / 1.30 / 1.00 / 0.77 <b>Storage System:</b> 700 bar CGH <sub>2</sub> / 79 kg H <sub>2</sub>	 <table border="1"> <caption>Consumption energy for Vecto LH, TtW, 2030 [kWh/100km]</caption> <thead> <tr> <th>Powertrain</th> <th>Consumption [kWh/100km]</th> <th>% Change vs H<sub>2</sub>-ICE</th> </tr> </thead> <tbody> <tr> <td>H<sub>2</sub>-ICE</td> <td>299</td> <td>-</td> </tr> <tr> <td>H<sub>2</sub>-FCEV</td> <td>237</td> <td>-21 %</td> </tr> <tr> <td>BEV</td> <td>126</td> <td>-58 %</td> </tr> <tr> <td>Diesel</td> <td>271</td> <td>-9 %</td> </tr> </tbody> </table>	Powertrain	Consumption [kWh/100km]	% Change vs H <sub>2</sub> -ICE	H <sub>2</sub> -ICE	299	-	H <sub>2</sub> -FCEV	237	-21 %	BEV	126	-58 %	Diesel	271	-9 %
Powertrain	Consumption [kWh/100km]		% Change vs H <sub>2</sub> -ICE														
H <sub>2</sub> -ICE	299		-														
H <sub>2</sub> -FCEV	237		-21 %														
BEV	126		-58 %														
Diesel	271	-9 %															
<b>H<sub>2</sub> FCEV</b>	<b>Fuel Cell System:</b> PEM 2x110 kW Max. FC-System Efficiency = 65 % <b>E-Motor:</b> 600 kW Peak, 700 Nm Peak <b>Transmission:</b> 4-Speed, 65.0 / 39.4 / 23.8 / 14.4 <b>Battery:</b> NMC, 400 V, 70 kWh <b>Storage System:</b> 700 bar CGH <sub>2</sub> / 63 kg H <sub>2</sub>																
<b>BEV</b>	<b>E-Motor:</b> 650 kW Peak, 700 Nm Peak <b>Transmission:</b> 4-Speed, 75.0 / 45.4 / 27.5 / 16.7 <b>Battery:</b> NMC, 800 V, 1,110 kWh																
<b>Diesel</b>	<b>ICE:</b> DI, 12.5l, 320 kW, 2,400Nm <b>Transmission:</b> 12-Speed DCT																

The hydrogen variants also improve significantly towards 2030, the FCEV benefiting more than the H<sub>2</sub>-ICE truck, thanks to the application of an intelligent and predictive operating strategy and the resulting higher recuperation potential. One way to leverage further efficiency potential of the H<sub>2</sub>-ICE is a corresponding hybridization. This was not considered because it is not currently taken into account in VECTO.

In addition to efficiency, technological maturity is crucial for market penetration. It is expected that the H<sub>2</sub>-ICE can go into series production as early as 2024, thus offering a short term CO<sub>2</sub> reduction potential. In this way, the H<sub>2</sub>-ICE powertrain will become a pioneer of establishing a suitable hydrogen infrastructure for the transportation sector. Fuel cell technology currently does not yet meet all the robustness requirements of a long-haul application and must be operated with high-purity hydrogen. In the long term, however, the

H<sub>2</sub>-FCEV offers the optimal long-haul propulsion system. A highly efficient Diesel is attractive to leverage CO<sub>2</sub> potential in the short term in combination with zero emission vehicles in the fleet, and only offers full potential in the long term if e-fuels are approved as zero emission fuels by future legislation. A long-haul BEV should be seen as a solution for selected and appropriate use cases. Even with further development of the battery technology, the geometric integration of the cell modules, as well as charging infrastructure and reduction of the payload remain as challenges.

The Heavy Regional Delivery sector presents a differentiated picture. As described at the beginning, however, the application profiles of the applications and the needs of the fleet operators differ. Due to political and public pressure, the BEV is coming to the fore here. It enables locally emission-free, CO<sub>2</sub>-free and low-noise operation, combined with the lowest energy consumption of all compared powertrains.

Despite the high energy efficiencies of the BEV and H<sub>2</sub>-FCEV, they are not suitable for all applications. This is especially true for vehicles with multiple auxiliary power outputs or applications that do not have access to high-purity hydrogen or corresponding charging infrastructure. For these applications, the robust H<sub>2</sub>-ICE powertrain or, if necessary, a highly efficient Diesel drive is the optimal CO<sub>2</sub>-free or low-CO<sub>2</sub> solution.

The analysis of the WtW-CO<sub>2</sub> balances in **Figure 9** shows that the blue hydrogen pathway is CO<sub>2</sub> favorable in the heavy-duty vehicle as well, if the H<sub>2</sub> generation in Germany with ordinary electricity mix is assumed. Furthermore, a vehicle with H<sub>2</sub> combustion engine with blue hydrogen would offer about 45 % lower CO<sub>2</sub> emissions (WtW) than a diesel powertrain.

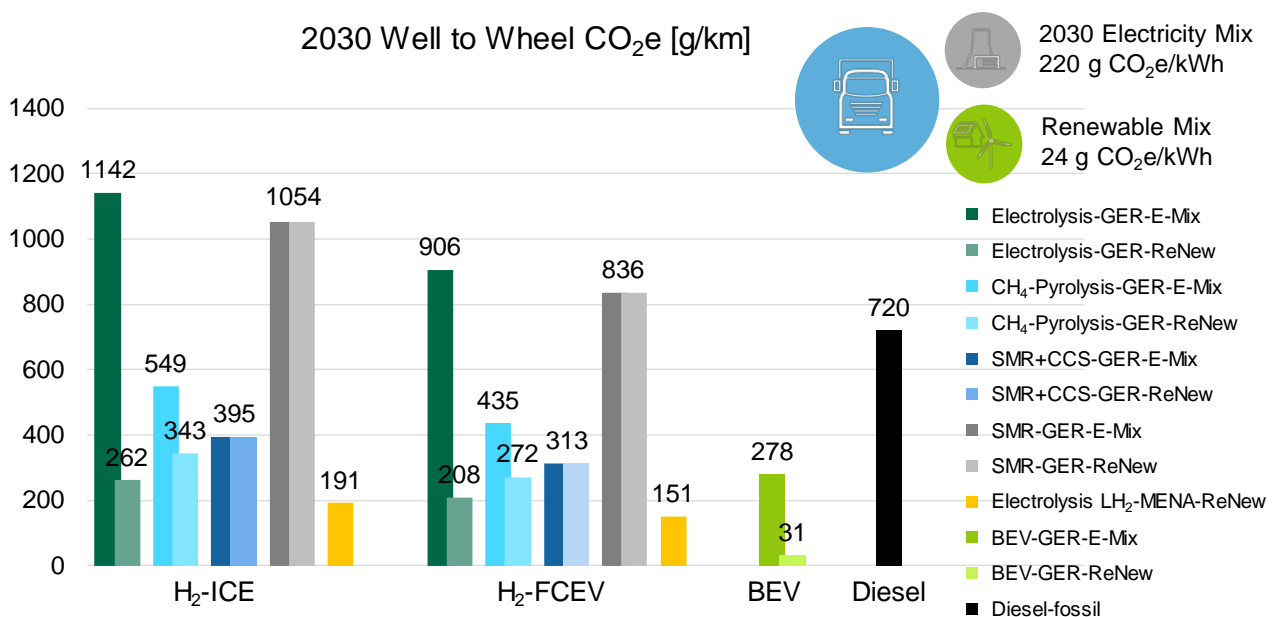


**Figure 9:** CO<sub>2</sub> emissions WtW for general and renewable electricity mix in 2030

For 2030, centralized generation of hydrogen with renewable electricity mix is foreseeable, which significantly reduces equivalent emissions for the electrolysis and methane pyrolysis processes. With blue hydrogen, the two hydrogen powertrains produce an additional CO<sub>2</sub>e-consumption of 35 to 117 g/km compared to a battery vehicle charged with German 2030 electricity mix. Furthermore, it can be seen in **Figure 9** that with renewably produced MENA hydrogen, the equivalent WtW-CO<sub>2</sub> emissions can be between 87 and 127 g/km lower than

for a battery vehicle charged with ordinary electricity mix, depending on the powertrain system. Only if the BEV is also charged locally with real renewable electricity the WtW-CO<sub>2</sub> emissions be reduced to values of about 30 g/km, which is unattainable for any hydrogen application. It can also be stated, that already in TtW the H<sub>2</sub>-FCEV has an advantage in comparison to the H<sub>2</sub>-ICE.

The **Figure 10** shows the CtG-CO<sub>2</sub> values for the entire life cycle, which include the emissions for hydrogen production as well as for the production of the vehicle and powertrain system and their operation. The basic influences from the WtW-analysis remain also for the CtG view.

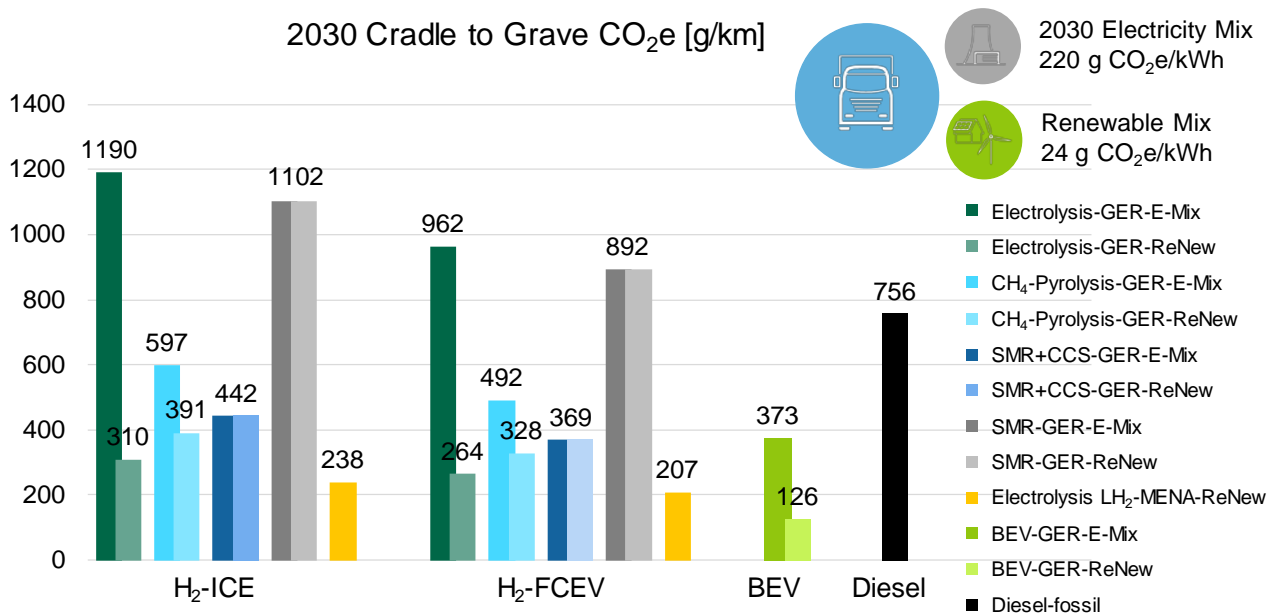


**Figure 10:** CO<sub>2</sub> emissions CtG for general and renewable electricity mix in 2030

Thus, the use of grey hydrogen without CCS is still to be avoided from a CO<sub>2</sub> point of view. The combination of those fuels with any hydrogen powertrain is neither with WtW nor CtG balancing better than a fossil-fueled diesel, which is due to the fossil base and the occurrence of CO<sub>2</sub> in electricity generation. Assuming a target range of 800 km, the BEV systems have a required battery capacity of over 1,100 kWh, which has a significant impact on the CO<sub>2</sub> footprint. However, since the heavy-duty vehicles have much higher mileage compared to the LCV and passenger cars, the CO<sub>2</sub> impact from the large battery systems is relativized over the lifetime. Depending on the electricity mix used to charge the BEV, the hydrogen powertrains may have higher or lower CO<sub>2</sub> emissions. If the battery vehicles are charged with ordinary electricity mix, CtG-emissions increase to 373 g CO<sub>2</sub>e/km. Only with domestically produced blue hydrogen and FC-propulsion this CO<sub>2</sub> level can be undercut for the same electricity mix. In contrast, MENA hydrogen can reach significantly reduced CtG-CO<sub>2</sub> emissions compared to BEV's. Only if the battery vehicles are charged with renewable electricity, these propulsion systems would be the best option in terms of CO<sub>2</sub> according to both WtW and CtG balancing. Looking at the H<sub>2</sub>-FCEV it can be seen, that also in CtG there is an advantage to the H<sub>2</sub>-ICE.

## TCO and manufacturing costs

For the TCO calculation the vehicle retail prices were used as well as for the other vehicles. The pure manufacturing costs of the powertrains are also shown in the **Figure 11**. Another input condition relates to energy and fuel consumption, which was calculated on a tank-to-wheel basis. Additional charging and refueling losses were not taken into account in the TCO due to the technology improvements assumed up to 2030.

Due to the ongoing increase in efficiency, the expected additional costs for exhaust aftertreatment systems, and rising fuel prices (CO<sub>2</sub> tax in Germany from 2021), a reduction in costs for Diesel vehicles cannot be expected. Nevertheless, Diesel powertrains will remain the most attractive mobility solution from a TCO perspective at least until 2030. Only purchase incentives, toll reductions and further increasing prices, which were not considered in this study, can cause a cost advantage for long-haul trucks with hydrogen or battery powertrain.

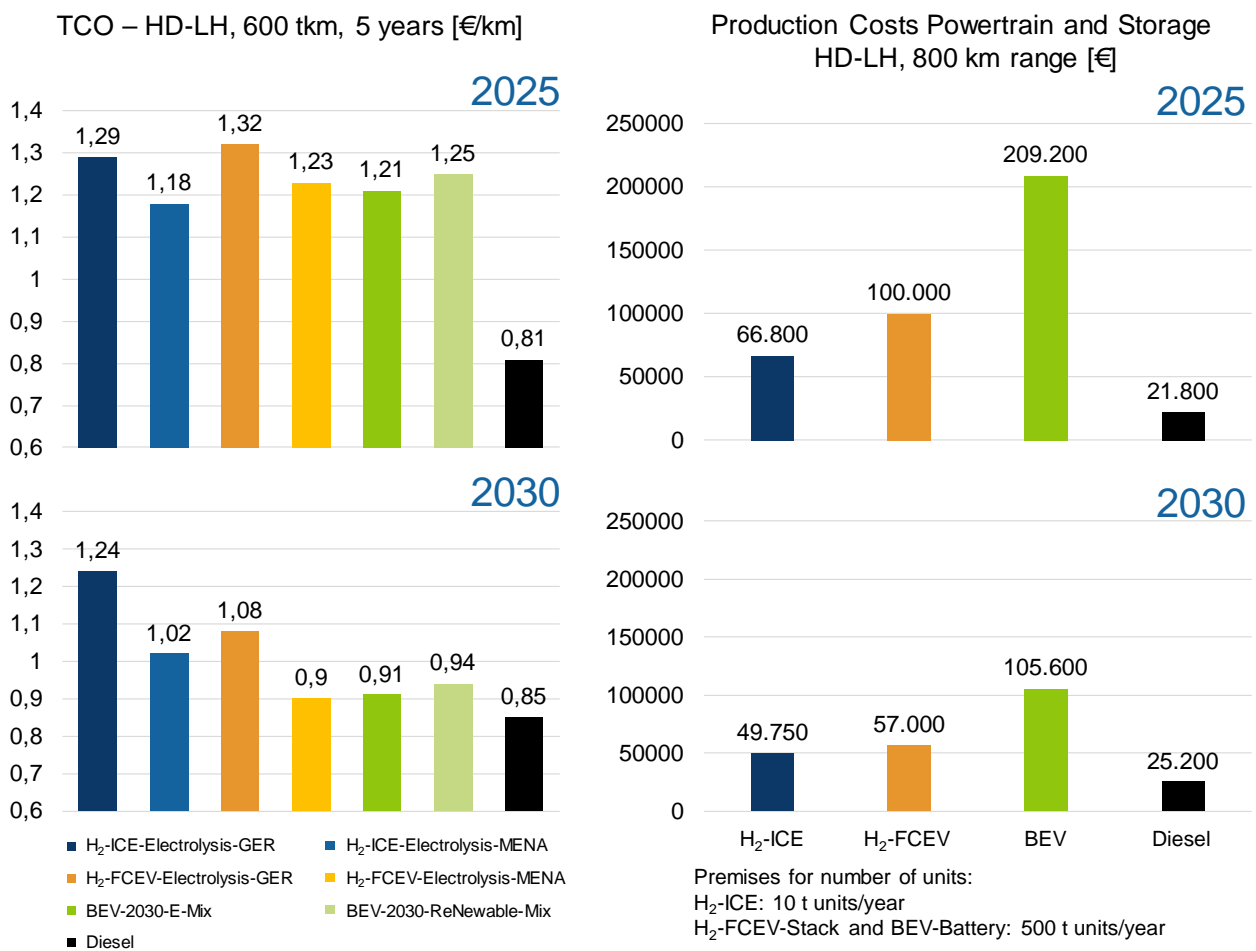


**Figure 11:** TCO and manufacturing costs for HDCV in 2025 and 2030

The additional price of the H<sub>2</sub>-ICE compared to the Diesel powertrain comes in particular from the costs of the 700 bar CGH<sub>2</sub> storage system. Here, an LH<sub>2</sub> tank from 2025 onwards could possibly reduce the cost difference. The FCEV system is the most expensive, but its purchase price will fall sharply by 2030. The main reason for this are the scaling effects that will then set in due to the use of passenger car fuel cells in a modular concept. In BEV systems, the powertrain costs are mainly driven by the battery size. Due to the range-scaled 1,110 kWh battery, the vehicle price is correspondingly high.

The TCO curve of H<sub>2</sub>-ICE and H<sub>2</sub>-FCEV over time in 2025 shows an advantage of 3-5 €ct per km for the H<sub>2</sub>-ICE. This advantage for the H<sub>2</sub>-ICE is expected to reverse into a TCO advantage for the H<sub>2</sub>-FCEV, depending on the rate of decrease of the prices for the FC-systems. The timing of this reversal will also be partly determined by the price of hydrogen over the period 2025-2035. In total, H<sub>2</sub>-FCEV and BEV are on a similar TCO level in the period 2025-2030. Cheap electricity (< 20 €ct/kWh) and a hydrogen price > 6 €/kg could give the BEV a benefit in TCO.

### **Summary of heavy-duty commercial vehicles**

In the long-haul sector, the H<sub>2</sub>-ICE powertrain must go into series production as early as possible in order to be able to leverage a high CO<sub>2</sub> reduction potential in the short term at acceptable additional costs compared to Diesel systems. The presumably rapidly decreasing price of the FC powertrains, as well as the further consumption potential, will lead to a widening of the TCO gap between H<sub>2</sub>-ICE and H<sub>2</sub>-FC powertrain after 2025. The main focus here is on tank technology, the LH<sub>2</sub> technology will offer a significant cost potential. An H<sub>2</sub>-ICE with mild hybrid and waste heat recovery could close the efficiency gap to the H<sub>2</sub>-FC powertrain to some extent. The CO<sub>2</sub> analysis for WtW and full life cycle shows that hydrogen powertrains can undercut fossil powertrains by a factor of three to four. The hydrogen powertrains are also competitive with the BEV. In terms of CO<sub>2</sub>, and depending on the electricity mix, both the H<sub>2</sub>-ICE and the H<sub>2</sub>-FC even offer a significant potential compared to the BEV powertrains. The TCO balance of this constellation in the period 2025-2035 will depend on how fast the prices for the FC-systems will fall and how expensive hydrogen can be produced in large scale. For heavy-duty regional delivery tasks, the BEV systems will become more prevalent. Special applications also will benefit in the long term from the largely infrastructural independence of a highly efficient Diesel powertrain and the robustness of ICE's in general (H<sub>2</sub> and Diesel).

### **Overall comparison and conclusion**

Hydrogen powertrains offer a huge potential to contribute economically and ecologically to a sustainable mobility sector. In 2030 blue hydrogen produced with ordinary electricity mix in Germany has a WtW-CO<sub>2</sub> potential of 54 % (H<sub>2</sub>-ICE) and 72 % (H<sub>2</sub>-FC) compared to diesel powertrains in the passenger car segment. Analyzing the WtW and full life cycle CO<sub>2</sub> emissions, it can be seen that in the passenger car segment, both H<sub>2</sub>-ICE and H<sub>2</sub>-FC powertrains can achieve similar levels as BEV's. With green hydrogen imported from MENA countries, WtW-CO<sub>2</sub> emissions can even be reduced to 18 g CO<sub>2e</sub>/km for the FC system and 30 g CO<sub>2e</sub>/km for the H<sub>2</sub>-ICE powertrain. This corresponds to approximately one and two thirds less emissions, compared to a BEV charged with German 2030 electricity mix. Also in terms of TCO, both H<sub>2</sub> propulsion systems are 2030 likely even cheaper compared to the battery electric system and almost at the same level as a diesel powertrain. In total, for passenger cars the fuel cell powertrain is the more balanced system, as it can convince with a significantly lower consumption and a smaller tank system both in terms of equivalent CO<sub>2</sub> emissions of hydrogen production, as well as with a comparatively low component footprint. Under consideration of the total life cycle emissions, hydrogen powertrains can reach the same CO<sub>2</sub> level as an equivalent BEV already in 2030, even if the BEV would be charged with 100 % renewable energy. The advantage of the battery powertrains becomes clear for small and medium vehicle sizes, where excellent life cycle emissions can be achieved with competitive total costs. The challenges are the provision of local renewable charging energy and to improve the environmental impact of the battery system.

For the light commercial vehicle, there is a particular potential for the H<sub>2</sub>-ICE powertrain, which reduces the efficiency-related consumption gap to the FC powertrain by means of a high specific utilization. Moreover, the power scaling between passenger cars and light commercial vehicles can be achieved more costily with a combustion engine than this is possible with the more complex FC powertrain system. In 2030, the H<sub>2</sub>-ICE powertrain operated with blue hydrogen produced with German electricity mix causes nearly the same WtW-CO<sub>2</sub> emissions compared to a BEV with the same range and the same electricity mix. A further CO<sub>2</sub> and cost potential is possible with imported MENA hydrogen, where in terms of TCO the H<sub>2</sub>-ICE is even the best hydrogen powertrain. Altogether, both the FC and the H<sub>2</sub>-ICE powertrains are interesting alternatives to fossil and battery electric powertrains under all evaluation criteria. Based on the premises made, there is a slight advantage of the H<sub>2</sub>-ICE compared to the FC systems. Especially the high costs and the CO<sub>2</sub> footprint of the BEV systems show that for LCV's a range of about 250 km should not be exceeded in order to achieve a balance between costs, payload and CO<sub>2</sub> footprint.

The heavy-duty truck sector is characterized by a high diversity of use cases and must contribute a significant share to the CO<sub>2</sub> reduction of the transportation sector. In the long-haul truck sector, vehicles with H<sub>2</sub>-ICE can become the pioneers of a hydrogen infrastructure. Already in 2024, this technology will be ready for series production and thus contribute to a significant CO<sub>2</sub> reduction in the fleet mix. After solving technical challenges, especially regarding robustness, H<sub>2</sub>-FC trucks can be seen as the preferred hydrogen technology in the long term. A highly efficient Diesel is attractive to leverage CO<sub>2</sub> potentials in combination with zero emission vehicles in the fleet in the short term and offers potential in the long term only if legislation considers e-fuels as zero emission fuels. Battery electric trucks will become widely accepted especially in the regional delivery sector, for long-haul applications the technological disadvantages and limitations of use (range, payload, charging infrastructure) will lead to a breakthrough of hydrogen technologies. Special applications also will benefit in the long term from the largely infrastructural independence of a highly efficient Diesel powertrain and the robustness of ICE's in general (H<sub>2</sub> and diesel). The heavy-duty vehicle sector can play a key role in the establishment of the hydrogen infrastructure: due to the plannable routes and refueling processes in central hubs, fleet operators have the opportunity to build their own hydrogen infrastructure. This speeds up the infrastructure extension and allows the regenerative hydrogen production at favorable prices.

## **Powertrain-specific challenges and possible technical solutions**

### **Efficiency of fuel cell and H<sub>2</sub>-ICE in comparison**

In the efficiency comparison of a current H<sub>2</sub>-ICE, technology status 2020, for the passenger car sector with a fuel cell system of a similar power class, a clear superiority of the fuel cell system over the H<sub>2</sub>-ICE in the entire operating range is shown, **Figure 12**. The steady-state electrical efficiency of a current fuel cell system is shown, which already includes the losses for the media supply (air compressor, hydrogen recirculation, coolant pump) as well as the electrical energy conversion at the DCDC converter between fuel cell and HV intermediate circuit. For the H<sub>2</sub>-ICE, the steady-state efficiency of approx. 42.2 % in the peak of the LNFZ engine with 130 kW is considered.

Particularly in the low load range, the fuel cell system shows significantly higher efficiencies than the H<sub>2</sub>-ICE, which leads to consumption advantages in driving profiles with low power

requirements. In the higher load range, the efficiencies between the H<sub>2</sub>-ICE and the fuel cell system converge.

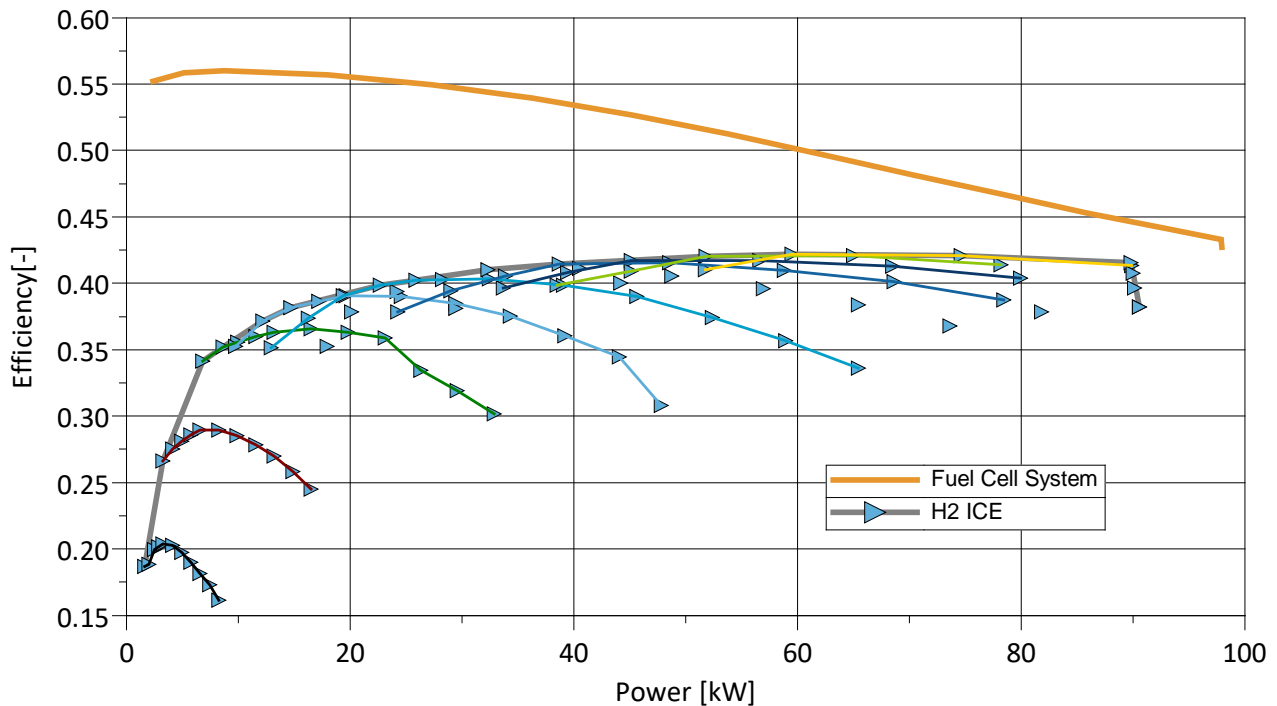


**Figure 12:** Typical system efficiency of a fuel cell system and H<sub>2</sub>-ICE in comparison for a technology status 2020

On this basis, the following chapter discusses further technological development options for both hydrogen-based drive concepts and evaluates the maximum efficiency increases that can be expected by 2030. Technical solutions for tank systems and hydrogen are also discussed.

## Technological Challenges and Potentials in the Development of PEM Fuel Cell Systems

In competition with conventional propulsion concepts, there are technological challenges for PEM fuel cell systems that need to be overcome for a broad market acceptance of the technology. Some of the major challenges can be summarized as follows, see as well **Figure 13**:

1. Package, in particular of the hydrogen storage system
2. Increasing the efficiency and power density of the fuel cell system
3. Cost reduction
4. Increase durability and service life
5. Reduction of the mass of the drive system

IAV offers solutions and development tools for all of the above challenges, which are discussed in detail below.

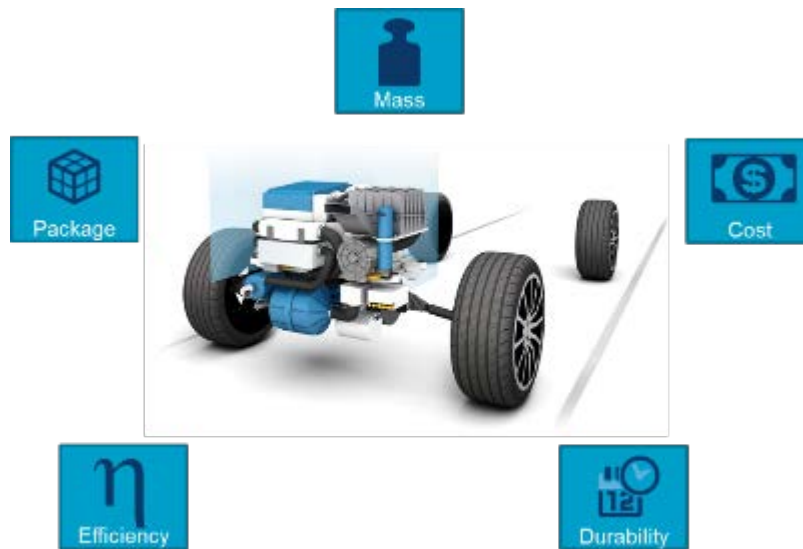


**Figure 13:** Technological challenges for PEM fuel cell systems

**System efficiency and power density**

In order to be able to evaluate the potential of individual technological optimization options for increasing the efficiency of fuel cell systems, IAV uses detailed simulation tools for the fuel cell system components and their interaction in the vehicle [5].

**Figure 14** shows the efficiency losses of a typical PEM fuel cell system (as of 2020) for automotive applications in WLTP. The fuel cell stack achieves an average cycle efficiency of 60 %, 3.6 % of the chemical energy used is lost unused via purge and membrane losses and leakage, another 36.4 % of the chemical energy is converted into heat. Within the fuel cell system, about 5 % of the original energy input (12 % in relation to the electrical power) is required to drive the auxiliary units. By far the largest share of the energy demand of the auxiliary units is accounted for by the air compressor, slightly more than 1 % of the total energy is required to drive the hydrogen recirculation fan and for the coolant pump. Over the entire cycle, the fuel cell system achieves an average electrical cycle efficiency (before conversion losses at the DC/DC converter) of 54.9 %.

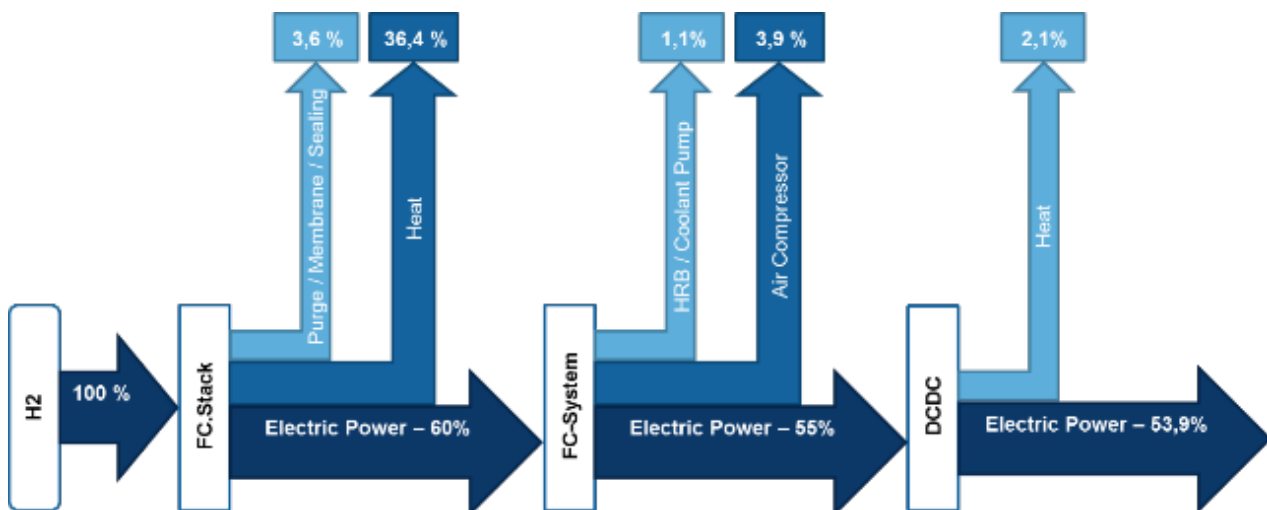


**Figure 14: Fuel Cell system efficiency losses in WLTP**

Current technological developments enable further optimization potential through

1. Reduction of electrochemical losses within the fuel cell stack,
2. Oversizing of the system,
3. Reduction of electrical power consumption of system components,

A reduction in the electrochemical losses of the fuel cell stack can be achieved in the future, for example, by an optimized and coordinated design of the bipolar plates (BPP) and gas diffusion layers (GDL) within the cell, in order to improve the mass transport of oxygen in the last part of the channel in particular. Further optimization potentials concern the ion conductivity of membrane and electrodes (especially at high current densities) and general improvements of the cathode catalyst (in the whole power range). All these measures improve the polarization characteristic of the cells in such a way that the current density increases for a given lower voltage limit or the cell voltage is increased for a constant upper current limit.

Since current density and stack efficiency are coupled via the individual voltage, the improvements achieved can either be used to reduce installation space and costs ("downsizing" by reducing the number of cells and/or active area at constant rated power) or they lead to improved stack efficiency. In the latter case, at constant geometrical boundary conditions/costs, the nominal power increases and the stack is - for a given power requirement - oversized. This leads to lower relative load points (relative to nominal power) and thus to higher cell voltages with higher stack efficiencies.

For the latter case, electrical stack efficiencies in the cycle between 65 % and 70 % are foreseeable in the future. The U.S. Department of Energy even mentions 70 % as the target value for FC systems (for 80 kW, [6]), which implies even higher stack efficiencies. However, for a further increase in stack efficiency, progress must also be made in service life (see below), since the resulting high single-cell stresses lead to various aging phenomena.

However, because of the challenges in terms of service life, the very flat polarization characteristic in the high-load range and the tendency for costs to be too high, the decision is currently usually made in favor of "downsizing".

A similar approach is the oversizing of the system: Here, too, stacks and possibly also system components are designed for higher nominal powers than actually required. On the one hand, this leads to an increase in stack efficiency (see above) and, on the other hand, often to lower parasitic losses in the fuel cell system, because lower stack load points tend to be accompanied by lower charging pressures and mass flows. Accordingly, the challenges with regard to thermal management (see below) can also be mitigated by such oversizing. Moreover, this is possible - given sufficient installation space - without any technological advances. Only a suitable modularization and series strategy appears necessary in order to be able to absorb the cost increases associated with oversizing through increased unit numbers (such as by using systems across different vehicle classes). A special case of this approach arises in the case of the heavy commercial vehicle. Here, not only the stack and/or the system itself can be scaled, but also their number [7]. For example, in the case investigated above a powertrain consisting of three instead of two FC systems (100 kW each) and a smaller battery - assuming the necessary installation space for the stacks themselves and their cooling - achieves a further consumption saving of approx. 9 %. This in turn is reflected in a smaller storage system. Due to the high cost sensitivity of the tanks, the higher acquisition costs of the third FC system are offset to an appreciable extent, so that the additional FC system results in a significantly lower TCO overall. However, it should be emphasized that this is not a blanket statement, but must always be based on a holistic optimization of the powertrain in the context of the requirements, especially package restrictions.

For a given system size, reducing the electrical power consumption of the system components offers a further opportunity to increase efficiency. This mainly refers to the active components of the subsystems - H<sub>2</sub> recirculation fan, electric air compressor and coolant pump - with the air compressor consuming by far the most power.

One approach to this is to suitably coordinate all components as well as the operating parameters of the stack in an early phase of the system design. If, for example, the stack can be made suitable for low volume flows and/or pressures (especially on the cathode side) by advantageous design of the BPP and membrane electrode unit, the system efficiency can be increased, especially in the medium and upper power range. However, such a stack usually does not achieve very high current densities, so that a balance must be struck here between "downsizing" the stack and (system) efficiency optimization. The former is mainly relevant for passenger car systems, while the latter is more likely for high-load applications such as certain commercial vehicles and especially for aerospace systems. [8]. Here, too, a global optimum requires a holistic approach.

Furthermore, there is potential at the component level. For example, the active recirculation blower can be replaced by a passive recirculation unit that uses the pressure difference between the pressure applied to the supply at the system inlet and the lower operating pressure at the stack inlet. The challenge in designing the passive recirculation unit is to ensure sufficient hydrogen recirculation over the entire operating range as well as during dynamic load changes. This makes the use of passive recirculation particularly suitable today for fuel cell systems that operate with low dynamics and limited start-stop cycles, such as those encountered in range extender concepts. [4].

The parasitic losses in the cooling system can be reduced mainly by reducing the pressure losses in the cooling circuit. In addition, raising the operating temperature of the fuel cell is advantageous, which can reduce the coolant flow rate and thus the power requirement of the coolant pump. In this context, water management or humidification of the membrane must be taken into account to ensure sufficient proton conductivity and service life.

The air compressor offers the greatest potential for increasing system efficiency. It is possible to use different charging units in the fuel cell system; for example, centrifugal or Roots compressors are used in current vehicles. Due to their characteristic maps, different compressor types offer various possibilities for optimizing the operating parameters of the stack, such as cathode stoichiometry and cathode pressure, with a view to maximum system efficiency (see above). Furthermore, the charging units can be optimized, for example, by using a turbine to utilize the exhaust gas enthalpy (relevant above all for high-load applications and in aviation) or by variable compressor geometry (Variable Trim Compressor - VTC). As shown in [5] the power consumption in the cycle can be drastically reduced by up to 50 % by optimizing the operating parameters of the fuel cell and using a variable compressor geometry, resulting in a reduction in consumption of 3 - 4 % in the WLTP cycle.

In summary, there are specific routes in fuel cell vehicle development to improve system efficiency, shown in **Figure 15**. All these routes have to be addressed by a holistic approach and based on the requirement of the specific application as well as production scaling effects.

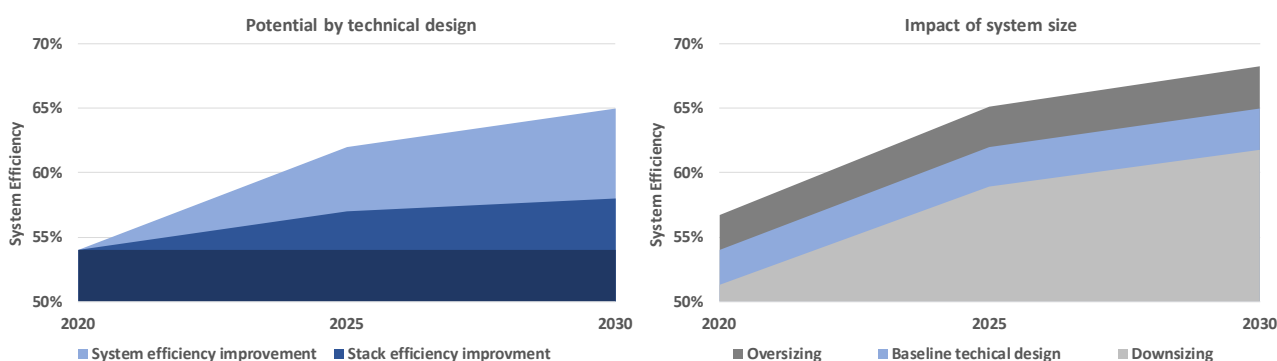


**Figure 15:** Fuel Cell system efficiency potential in WLTP

### Cost reduction of fuel cell systems

The cost of the fuel cell system consists of the cost of the fuel cell stack and the fuel cell system components. Nearly two-thirds of the total cost is for the fuel cell stack, and one-third is for the fuel cell system components, **Figure 16**. The main cost drivers within the fuel cell stack include the BPP, membranes, and catalyst materials. Within the next decade, fuel cell costs are expected to decrease significantly.

The greatest potential for cost reduction lies in economies of scale in the course of mass production and in the optimization of manufacturing processes. In large-scale production, metallic BPPs are increasingly being used instead of graphite BPPs, which are cheaper to produce. At the system level, components such as valves, throttle valves, sensors, etc. that are already available in large-scale production can be qualified for fuel cell applications with little effort. Furthermore, the systems can be optimized in terms of lower complexity. For example, it is possible to dispense with the humidifier as a component, as Toyota has demonstrated in the first Mirai. [9].

It is expected that the current production volumes of a few 1,000 fuel cell systems per year will be increased to several 100,000 units in the next few years (assumption 500,000 units per year in 2030). As production volumes increase, automotive fuel cell systems will also be

used in other applications. Modularization and scalability of the individual components are therefore urgently required for the widespread use of fuel cell systems.

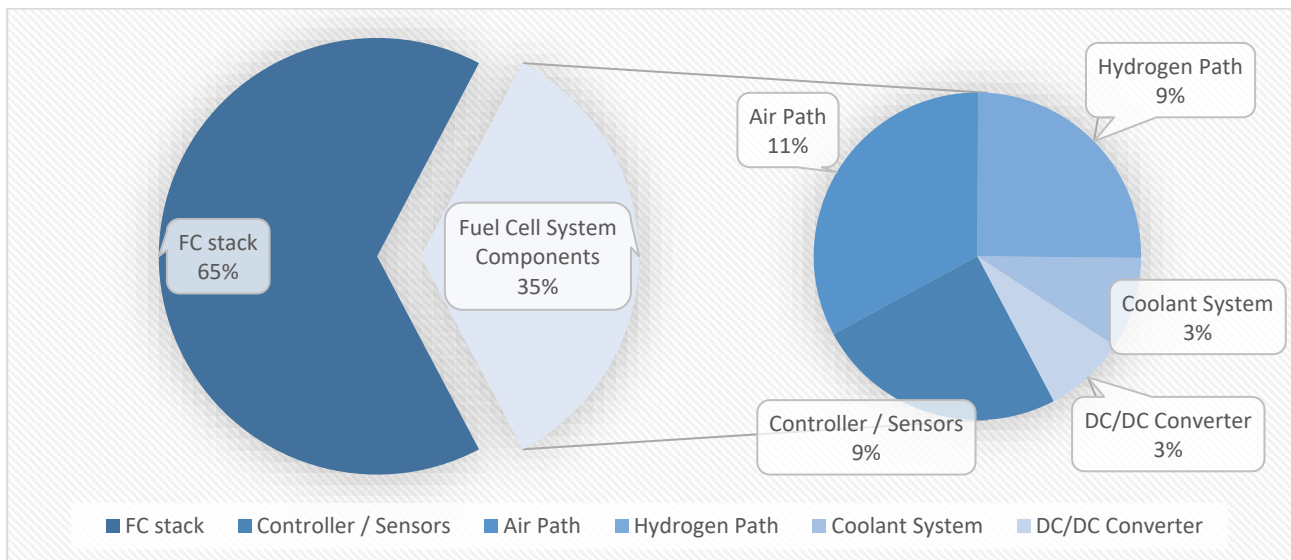


**Figure 16:** Cost analysis of a fuel cell system

### Lifetime and durability

The lifetime of a fuel cell propulsion system depends mainly on the design of the stack, the system and powertrain dimensioning (see above) as well as the operation management of the system and the hybrid strategy. Because of the importance of lifetime in the cost trade-off, accurate knowledge of aging mechanisms is critical. Basically, PEM fuel cells are subject to aging mechanisms during operation, which lead to a continuous cell voltage loss and consequently to a loss of performance. This loss of performance can be largely attributed to a reduction in the electrochemically active surface area (ECSA) of the cathode catalyst. The reduction in ECSA is referred to as degradation. For a realistic determination of ECSA, IAV has developed and validated a dynamic physicochemical model of platinum degradation within PEM fuel cells. [10]. Within the physicochemical model, effects of platinum oxide formation, platinum dissolution, platinum deposition and platinum diffusion as well as carbon corrosion are considered.

**Figure 17** shows the validation results of the model at cyclic load changes. A good agreement between simulation results and measured data can be seen, even with high temporal duration of the measurements. In principle, increasing the operating temperature, increasing the load cycling frequency, and operating the cell at high cell voltages leads to a greater reduction in ECSA. This loss of ECSA results in a higher performance loss over the operating lifetime of the fuel cell.

**Figure 18** shows the influence of the ECSA on the cell voltage and thus on the performance of the fuel cell. A reduction of the ECSA leads to a reduction of the cell voltage and thus to a collapse of the fuel cell efficiency. A reduction of the ECSA by 90 % compared to the reference curve causes a drop in the cell voltage between 8 % at low loads up to 12 % at full load point.

With this model, it is possible to predict the lifetime of fuel cells up to a defined criterion, e.g. a loss of cell voltage of 10 % compared to the reference voltage. Furthermore, the operating

strategy and operating parameters of the fuel cell can be adapted to enable operation at low degradation. And it is possible to integrate the model within the Fuel Cell Control Unit in order to implement an online remaining lifetime prognosis (State-of-Health Monitoring).

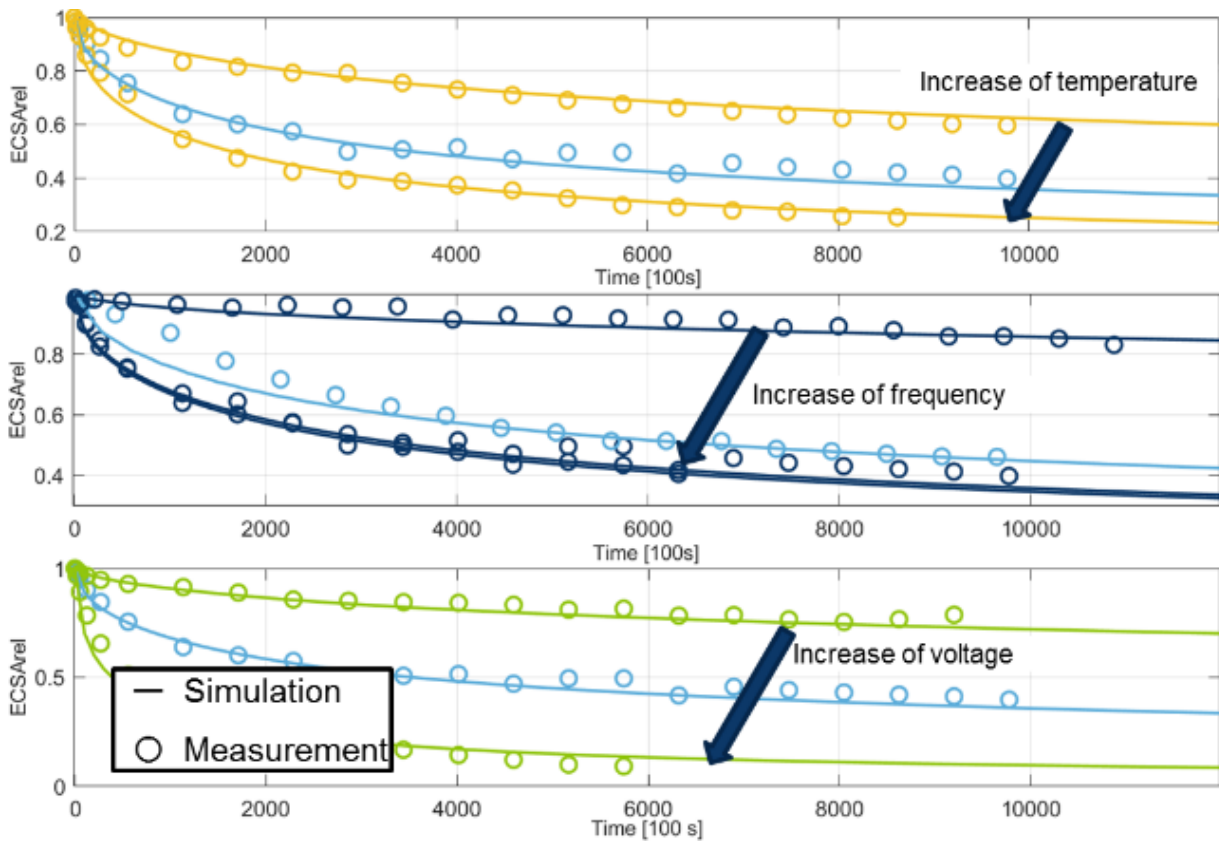


**Figure 17:** Validation of ECSA decrease by variation of impact parameters

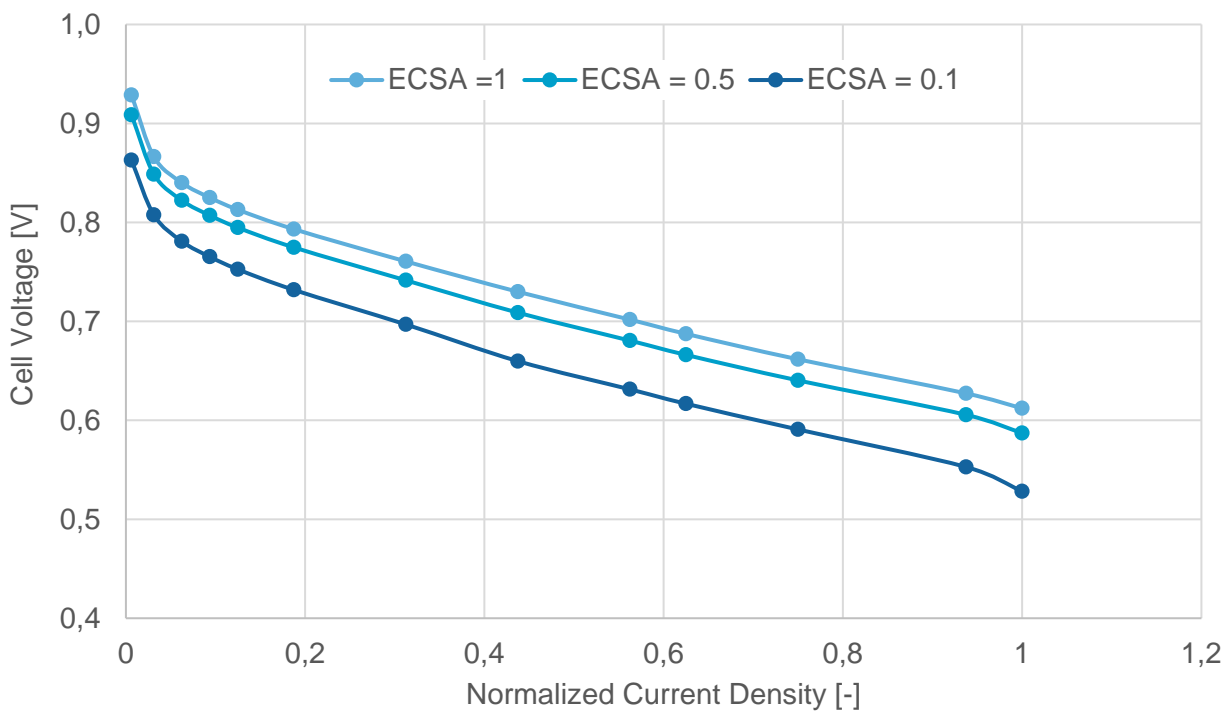


**Figure 18:** Polarization curve and impact of ECSA on cell voltage

## Technological challenges and potentials in the development of H<sub>2</sub>-ICE

### Objective

In the context of this thesis, the potential of a hydrogen combustion engine is discussed in the area of conflict between efficiency and the generation of raw emissions while the CO<sub>2</sub> potential of the ICE in turn is compared with the BSZ and a diesel VKM-based powertrain.. In this chapter, a virtual twin of an engine for an application in the passenger car segment and in the light commercial vehicle segment are presented respectively. The single-cylinder tests and model-based development of heavy-duty commercial vehicles with holistic optimization of engine and exhaust gas aftertreatment have been described in previous publications [11], [12], [13] in detail and are not presented here in detail..

**Figure 19** shows the requirements of the two vehicle concepts for the non-electrified H<sub>2</sub>-ICE in terms of torque and rated power as well as some defined design parameters for the virtual development.

Vehicle Type		Vehicle Application	
		Passenger car	Light duty
Power	kW	90 @ 3000 rpm	130 @ 4000 rpm
Compression Ratio		12	11.2
Stroke / Bore Ratio	mm	1.13	
Displacement of 4 cyl engine	l	2	
Max. Engine Speed	rpm	5000	5500
Max. Torque (LET @ rpm)	Nm	280 (@ 1500 rpm)	350 (@ 1500 rpm)
H <sub>2</sub> Injection		DI (3.82 g/s at 30bar)	
Ignition		Spark Plug	
Cam Phasing	°CA	40°CA on Intake / Exhaust	
2 Step Charging System incl. 2 Intercooler			
	High Pressure	Series production Gasoline VTG	
	Low Pressure	Series production Diesel VTG	

**Figure 19:** Specification of the passenger car and light commercial vehicles

The boundary conditions set for the development are derived from the request for a realistic implementation, so that the technology modules used here are either series-produced components (e.g. with regard to the charging group) or - with regard to H<sub>2</sub>-specific parts - are under development. The latter applies to the selected H<sub>2</sub> mixture preparation components. Here, the low-pressure direct injection of hydrogen was considered most promising, since the advantage of the higher mixture heating value and the associated lower boost pressure requirement directly contributes to the achievable specific power. This is particularly necessary since the parameters of maximum efficiency and lowest possible raw NO<sub>x</sub> emissions are defined as equivalent development goals for the engine design, and thus the aim is to achieve map-wide lean-burn operation.

### Methodology

Hydrogen exhibits highly advantageous properties, essentially resulting in significantly improved lean-burn capability compared with gasoline engines running on conventional fuels. A disadvantage, however, is the tendency to abnormal combustion, which typically manifests itself in a reduced compression ratio and thus limits drastically the efficiency increase potential. The cost-effective virtual design of high-efficiency hydrogen engines

hence requires approaches to predict these fuel-related phenomena. IAV has developed and validated a phenomenological combustion model for spark-ignited hydrogen combustion processes based on measurements on a 1-cylinder engine. Key components of this 0D/1D model developed by IAV are approaches for the calculation of the laminar flame speed and the prediction of auto-ignition in the unburned mass as a prerequisite for the occurrence of knocking phenomena.

To establish a broad measurement database for model development and validation, extensive experimental investigations have been carried out on a modified single-cylinder commercial vehicle Diesel engine with a displacement of two liters, **Figure 20**. Here, hydrogen was injected into the intake manifold at an injection pressure of 9 bar. The additional installation of a flame protection filter has minimized the effects of any backfiring that might occur. The hydrogen combustion measurements were performed under steady-state conditions, systematically varying several engine operation parameters such as engine speed and load, MFB50-point, EGR and air-fuel ratio. Further results of the single-cylinder measurements are presented and discussed in detail in [14] and [15].

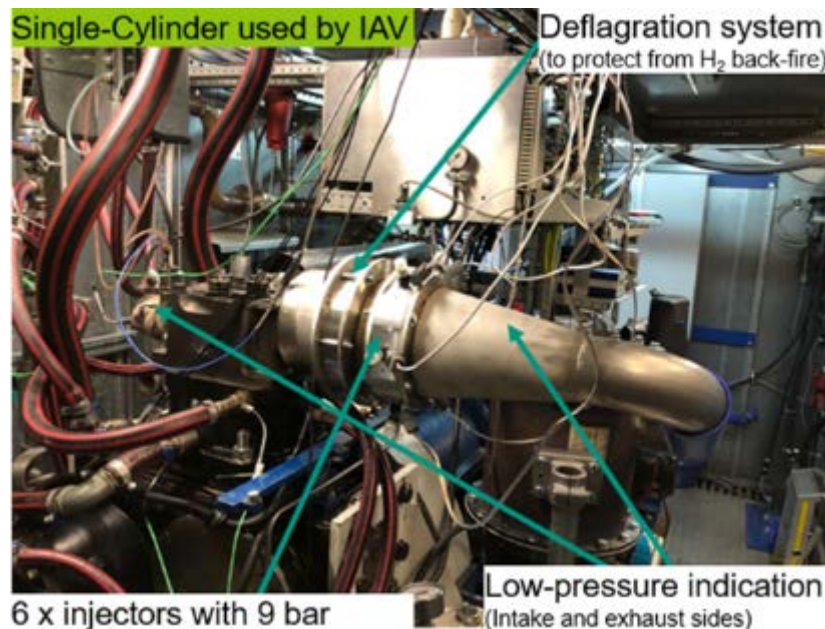


**Figure 20:** Hydrogen heavy duty 2L single-cylinder engine test bench

The subsequent analysis of the experimental results and evaluation of existing phenomenological approaches revealed the need for new simulation models for the prediction of hydrogen combustion. In particular, the inadequate quality of the approaches available in the literature for calculating the laminar flame speed in the relevant parameter range (temperature, pressure, EGR rate, air-fuel ratio) was identified. At this point, a Gaussian process model developed at IAV was used as a basis for calculating the laminar flame speed in the well-established two-zone Entrainment model. Furthermore, an approach based on the Livengood-Wu integral for the prediction of auto-ignition in the unburned mass preceding the occurrence of knocking was developed and verified. A detailed presentation of the new models developed by IAV as well as the development methodology can be found in [12]. The combustion model reproduces with high accuracy the main burn rate characteristics and thus pressure curves estimated from the experimental data **Figure 21**, and can be incorporated into commercial simulation programs.

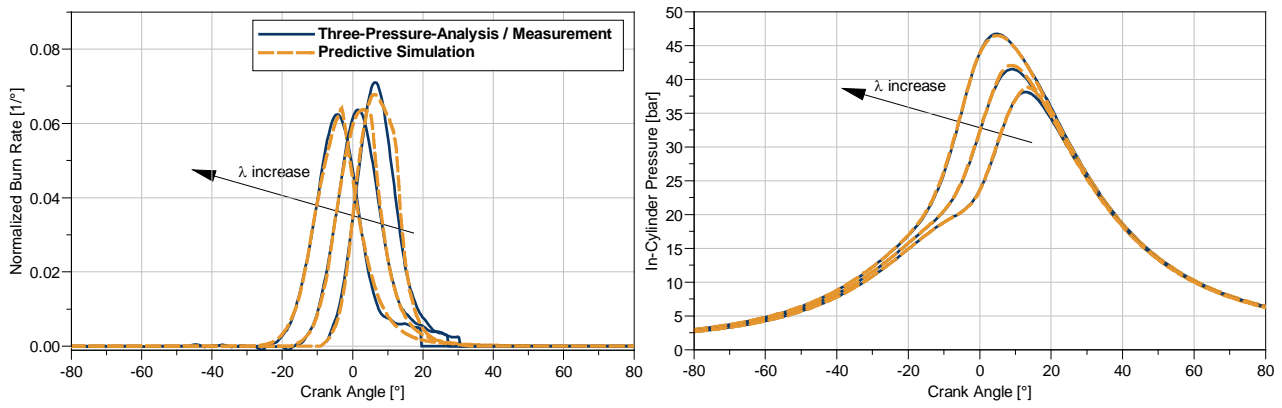


**Figure 21:** Comparison of measured and predicted burn-rates and resulting in-cylinder pressure traces

The fully predictive phenomenological model chain for hydrogen combustion calculation was then validated at over 150 engine operating points. The prediction error for all relevant engine operation parameters is less than 5 % **Figure 22**. High accuracy of the predicted combustion characteristics with a maximum burn time deviation of 3°CA was achieved as well.

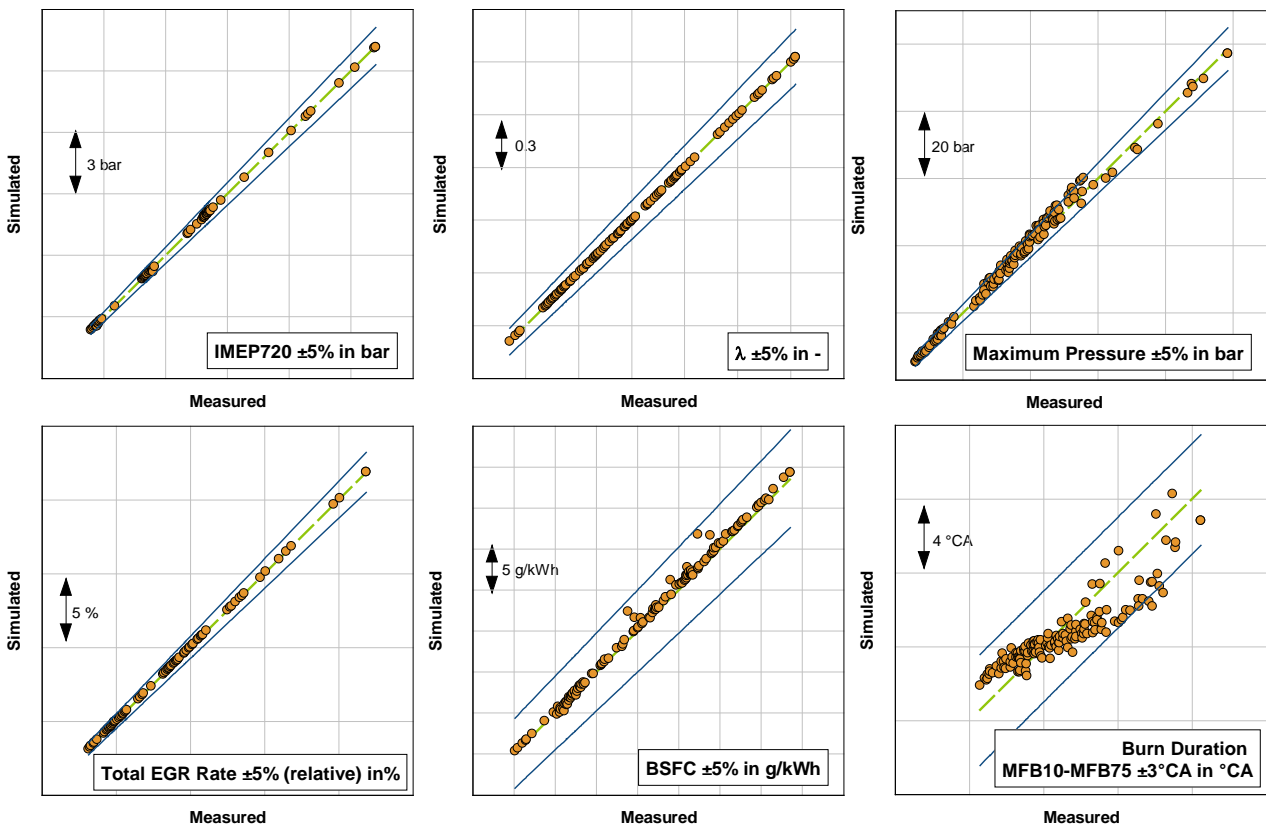


**Figure 22:** Measured and predicted engine operation parameters with IAV's hydrogen combustion model

The extensively validated combustion model was then used to design a high-efficiency hydrogen combustion process, which is presented in the following sections.

## Challenges of an H<sub>2</sub> ICE

According to the properties of hydrogen, there are significant advantages but also new challenges compared to the conventional gasoline internal combustion engine. **Figure 23** schematically illustrates the central design parameters presented in the core: *Compression ratio, turbocharging and injection system* as well as the possible means or operating strategies of *lean combustion, EGR strategy and mixture preparation* in order to resolve the conflicting objectives of *efficiency, performance and emissions* as optimally as possible. In addition, combustion anomalies that are not presented in the graphic are also part of this multidimensional field of trade-offs. For example, the compression ratio is a mean of increasing efficiency with the consequence of an increased knock tendency as well as an increased risk of pre-ignition. For the diffusive H<sub>2</sub> combustion process, with high-pressure direct injection into the combustion, a further efficiency-enhancing increase in compression ratio is achievable. However, this combustion process approach is reserved for heavy-duty commercial vehicle applications. For both combustion processes, increased compression results in an even higher mechanical stress on the engine. Higher peak pressures and pressure gradients as a result of the almost 6-fold greater laminar combustion velocity compared with liquid gasoline result in a greater mechanical stress and higher friction losses. The significantly shorter combustion duration leads to an expected advantage in thermal efficiency due to the closer proximity to the ideal constant volume cycle. However, increasing wall heat losses due to higher combustion temperatures somewhat limit the potential in turn.

A significant advantage of the H<sub>2</sub> properties for use in an ICE are the wide ignition limits, which, based on the aforementioned test bench measurements, allow premixed homogeneous combustion up to an air/fuel ratio of  $\lambda = 4$  with corresponding efficiency benefits. Along with the more than doubled stoichiometric air requirement of  $L_{st} = 34.3$ , the large lean combustion potential poses a major challenge for the turbocharging system: with a low exhaust gas enthalpy level (low exhaust gas temperature because of fast combustion). A high air requirement needs to be ensured in order to optimize efficiency, performance and emissions with low gas exchange losses. As an alternative to lean combustion, a cooled, low-pressure EGR system poses equal challenges for turbocharging, which in principle can be designed as a high-performance "high" e.g. multi-stage VTG system or, at reduced cost, as a simple "low" wastegate-TC with reduced potential.

The low ignition energy requirement (1/14<sup>th</sup> of gasoline) and a self-ignition temperature more than twice as high (585°C in air at atmospheric pressure) are in contrast to each other in terms of knock tendency and pre-ignition. The very low ignition energy requirement, even at high air conditions, also entails a high risk of backfire in the case of port fuel injection (PFI). A decisive parameter for controlling combustion anomalies is the form of mixture formation. Direct injection (DI) after intake closure can eliminate backfire phenomena. The disadvantage here is the shorter time for homogenization of the mixture, so that locally rich zones can form potential knock spots and NO<sub>x</sub> sources.



**Figure 23:** Schematic trade-off for engine layout

The comparison of the mixture preparation PFI vs. DI based on a lambda variation at the naturally aspirated full load (WOT) shown in the **Figure 24** illustrates essential challenges of the H<sub>2</sub>-ICE. The volumetric energy content of gaseous H<sub>2</sub>, which is lower by a factor of 10, results in load losses of 28 % for port fuel injection compared to DI-H<sub>2</sub>-injection at stoichiometric operation due to the high displacement effect. The direct-injection H<sub>2</sub> variant after inlet closure (IVC), on the other hand, shows a load gain in the naturally aspirated full load compared with the two gasoline variants DI and PFI due to the higher mixture heating value. However, the potential of the approximately 18.6 % higher mixture heating value of the H<sub>2</sub>-DI variant compared to gasoline DI (for  $\lambda = 1$  and atmospheric conditions) is not fully exploited in this engine. This is due to an approximately 1.2 % worse high-pressure efficiency due to the higher process temperature of hydrogen combustion, which leads to higher wall heat losses and a lower gamma in the expansion phase. Further losses are due to the higher peak pressures of hydrogen combustion and increase friction losses by 12 %. With port fuel injection, liquid fuel benefits in the volumetric efficiency from the high volumetric energy content (low displacement effect) but also from the cooling effect due to the evaporation of the liquid fuel.

In an ideal, hydrocarbon-free hydrogen combustion, only water forms in the chemical reaction, which would theoretically allow pollutant-free H<sub>2</sub> ICE operation. In fact, in real engine operation, due to the necessity of lubrication (hydrocarbon-based oil) hydrocarbon emissions are recorded in very low concentrations at the detection limit. The only remaining emissions are therefore unburned hydrogen and nitrogen oxides, which are formed at excess air and high combustion temperatures. A NO<sub>x</sub> maximum is recorded at the air ratio of approx.  $\lambda = 1.2$ ; with leaner mixture, the combustion temperature is lowered, so that the decisive, thermal NO<sub>x</sub> formation process is strongly inhibited. In steady-state operation, from an air ratio of approx.  $\lambda = 2$ , NO<sub>x</sub> emission is thus reduced to low two-digit ppm values. An appropriate lean-combustion design with good lambda control quality, e.g. electrically assisted turbocharging or intermittent water injection, can enable a further drastic reduction in raw NO<sub>x</sub> emissions for transient operation and thus reduce system expenditure considering the exhaust gas aftertreatment.

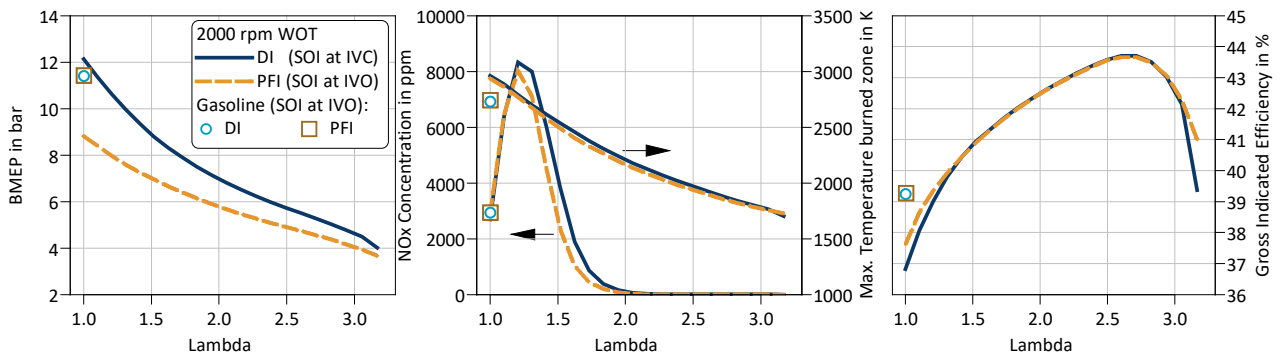


**Figure 24:** Influence of the injection type (DI vs. PFI) on naturally aspirated engine performance

In principle, the load loss due to leaner mixture (= lowering the mixture heating value) discussed above can be compensated by means of supercharging. In addition to the compensation of the load losses to the mean pressure of 12 bar, a significant efficiency gain is achieved by leaning the mixture compared with the stoichiometric operation (34.5 % with CR = 11.2), as shown in **Figure 25**. The brake efficiency essentially follows the gross indicated efficiency, which here finds its maximum at  $\lambda = 2.5$  with a constant MFB<sub>50</sub> of 8°CAaFTDC. Up to this air ratio, the advantages from reduced wall heat losses and improved calorics predominate. At even higher air ratios, these advantages are overcompensated by longer combustion duration and rising incomplete combustion, and the high-pressure efficiency drops significantly. In this context, the turbocharging system, a two-stage VTG system, is also decisive. Due to the low exhaust gas temperatures of the very fast and lean hydrogen combustion, the turbocharging unit has to meet an increasing boost pressure requirement with a steadily lower exhaust gas enthalpy supply. Ultimately, exhaust back pressure, the gas exchange work and the internal residual gas content are increased significantly to the detriment of the gross indicated and brake efficiency. Thus, the turbocharging system forms a key to resolve the conflicting goals: high power density with high efficiency at low NO<sub>x</sub> emissions.

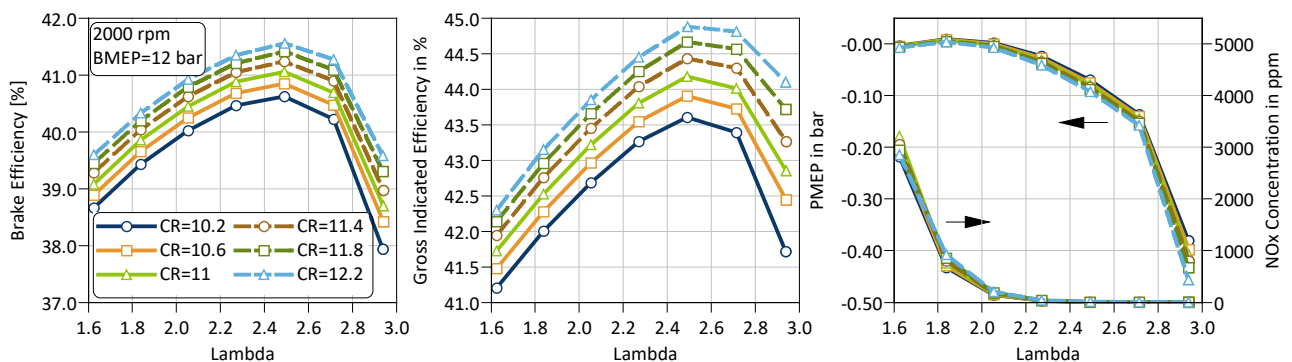


**Figure 25:** Efficiency potential by means of lean mixture and compression ratio (CR) rise

#### Potential analysis of different charging concepts

Using the best-performing and most efficient of the here investigated turbocharging concepts, a two-stage VTG system, the main potentials and limitations of turbocharging are discussed in **Figure 26** by means of a lambda and boost pressure variation at 2000 rpm. The two-stage VTG system has one by-pass each on the turbine side and one by-pass each on the compressor side, as well as two charge air coolers to ensure efficient charge air compression, especially at high-load operating points. The switching of the by-pass valves

has been optimized in terms of load requirement and efficiency and can be divided into a LET range in which only the "small" high-pressure VTG (from gasoline engine applications) is active, a medium speed range from 2000 to 3000 rpm where both VTGs are actively controlled, and a rated power range starting at 3000 rpm in which only the "large" low-pressure VTG (from diesel engine applications) provides the required boost pressure. In the center of the diagrams the gross indicated efficiency is shown, which increases successively with rising boost pressure up to approx. 2.5 bar (reduction of relative wall heat losses) and leaner mixture up to approx.  $\lambda = 2.4 \dots 2.6$  (improvement of calorics) and reaches a maximum value at 45 %, which is limited by the knock limit, increase in combustion duration and incomplete combustion with further enleanment. In the brake efficiency, this pattern can be found again and is additionally reduced by pressure- and speed-dependent friction losses and mainly by the gas exchange work. Particularly relevant here is the throttled region to represent small loads with a sharp drop in efficiency down to  $\eta_{\text{eff}} = 20 \%$  and the region of high lambda and boost pressure values, which represents the limitation of the turbocharger unit and leads to significant charge exchange losses at correspondingly high exhaust backpressures. The isoload curves now illustrate the maximum achievable efficiency at the given  $\text{NO}_x$  level in the respective load. For example, at a BMEP of 22 bar, the two-stage VTG system enables a brake efficiency of 42 % and  $\text{NO}_x$  emission below 100 ppm.

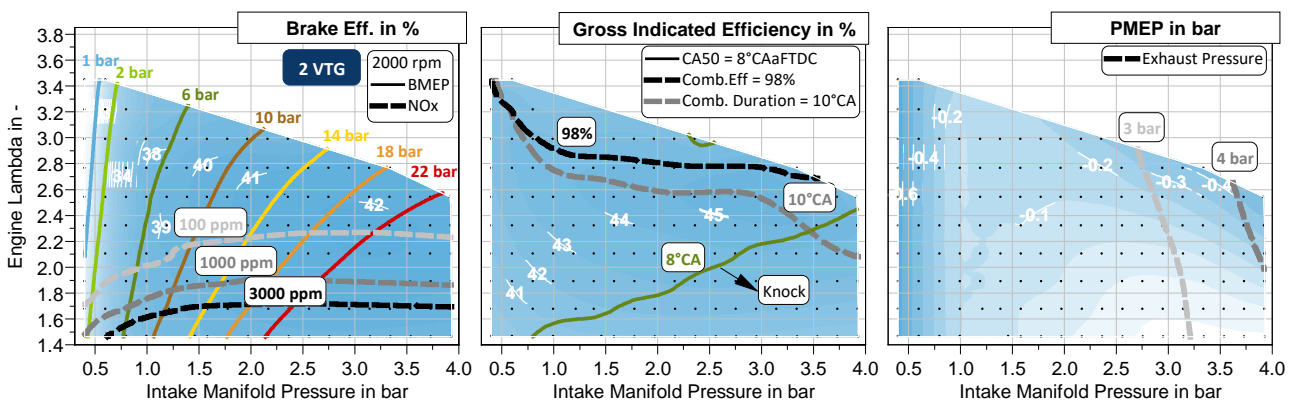


**Figure 26:**  $\text{NO}_x$ -Emission and efficiency at 2000 rpm depending on lambda and load pressure

**Figure 27** shows the LET potentials of three investigated turbocharging concepts: a cost-oriented variant with one wastegate-TC, a mixed variant with "small" high-pressure VTG and low-pressure TC with wastegate control, and the high-performance variant with two VTGs already discussed. The maps shown in blue are the results at the LET target speed of 1500 rpm. The variant with WG-TC does not reach the target load of 22 bar by far, so that 2000 rpm are additionally shown here, where the target load can only be reached with a lambda of 1.8 and correspondingly high  $\text{NO}_x$  emissions of over 1000 ppm. Only with the two active VTGs it is possible to gain an air/fuel ratio of  $\lambda > 2$  in the LET with correspondingly low nitrogen oxide emissions.

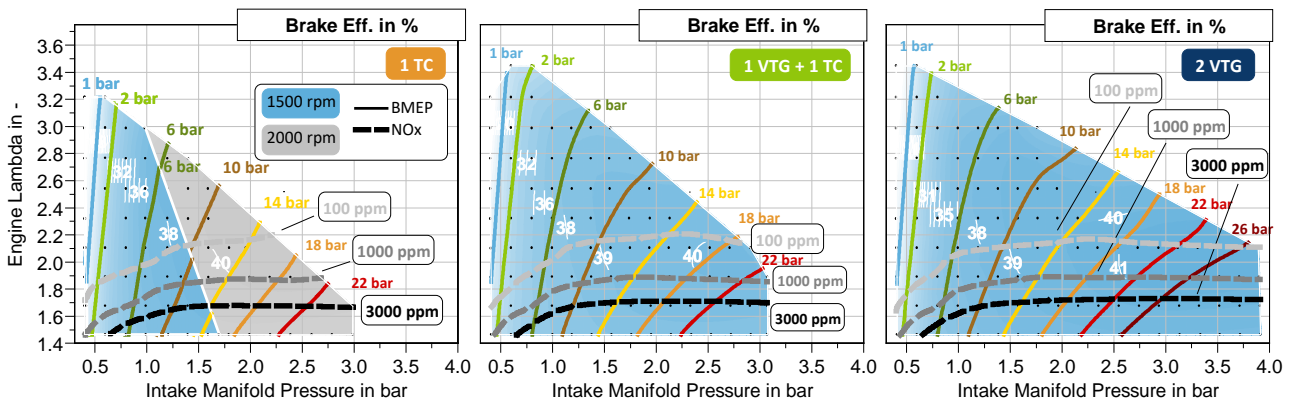


**Figure 27:** Comparison of emission, efficiency and load potentials of different charging concepts in the LET.

The comparison at the rated power range at 4000 rpm in **Figure 28** illustrates the achievable power densities of the units. With the wastegate TC, 14 bar mean pressure with NO<sub>x</sub> emissions well below 100 ppm and thus a power density of 45 kW/l can be achieved. A BMEP of 19.6 bar (dark blue isoline) and thus the target power density of 65 kW/l for the light commercial vehicle can be achieved with the two two-stage variants with similar efficiency and nitrogen oxide levels.

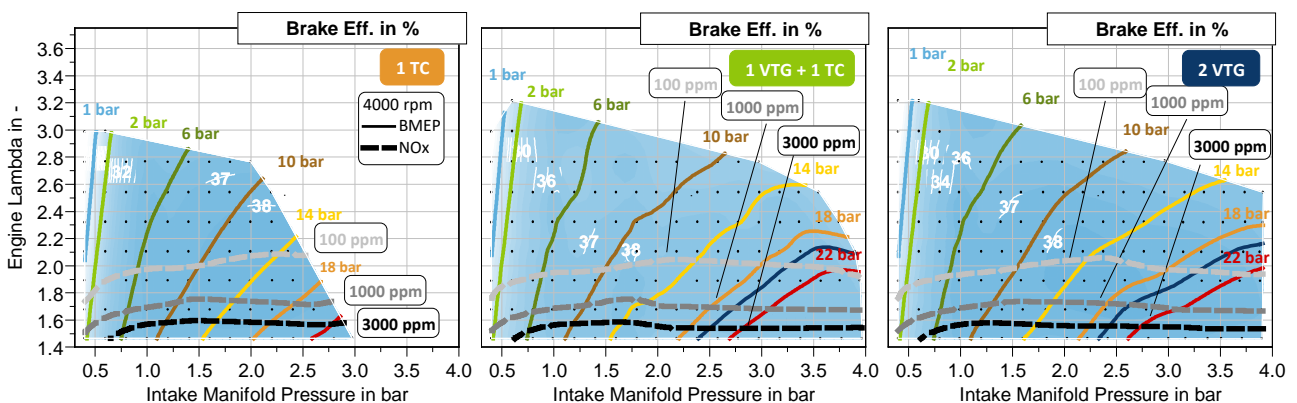


**Figure 28:** Comparison of emission, efficiency and load potential of different charging concepts at the rated power area

From the potentials at the LET and at the rated power range, the possible applications of the different charging concepts can be derived, which are shown in **Figure 29**. Single-stage TC charging offers a cost-oriented solution for an application in combination with an electrified system, which can compensate for the weakness at the LET. Thus, efficient lean operation with low NO<sub>x</sub> emissions can be implemented throughout the map without sacrificing vehicle performance. With the objective of maximizing efficiency, the two-stage VTG variant is selected for the passenger car and the LCV. For the LCV, a slightly lower compression ratio of 11.2 is selected to reduce the knock tendency due to the higher loads required (specific power of 65 kW/l) compared to the passenger car ICE (specific power of 45 kW/l). Both maps exhibit a high brake efficiency greater than 40 % over a wide range, with a maximum value of 42.2 % at low NO<sub>x</sub> emissions below 100 ppm.

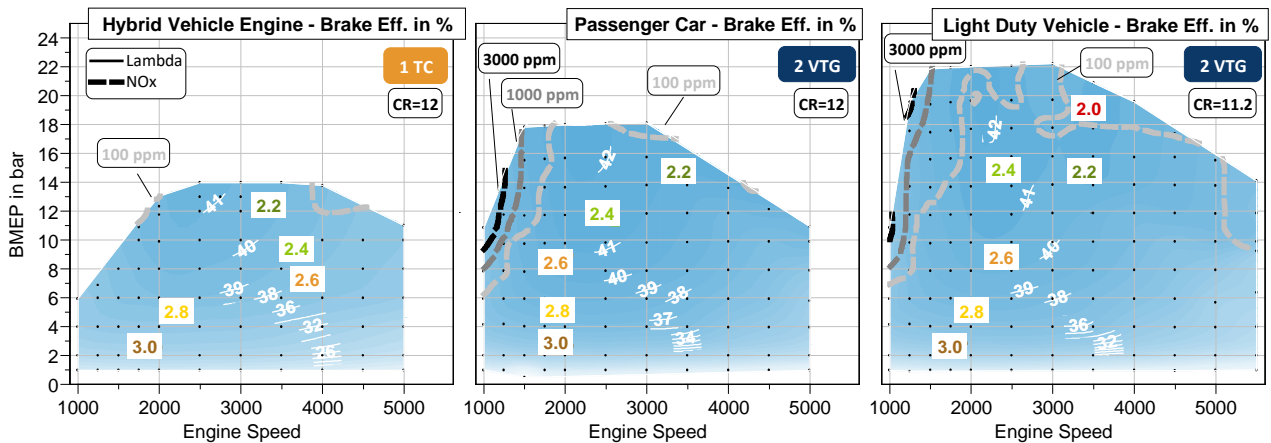


**Figure 29:** Comparison of the H<sub>2</sub>-ICE brake efficiency maps of hybrid, passenger car and LCV

### Investigations of external and internal mixture formation

The external, cylinder-individual port fuel injection in front of the intake valves is synchronized with the intake cycle at the time of intake opening (IVO) and thus has the advantage of a longer period for homogenization of the mixture. In addition, lower injection pressures can be realized, which simplifies the injection system and increases the driving range of the vehicle. In this case, the internal direct injection takes place immediately after the intake closure. The advantage is that anomalous combustion phenomena such as backfire can be completely prevented, while pre-ignition can only be mitigated with even later injection. A disadvantage is the reduced time required for mixture preparation for the homogeneous combustion. However, direct injection enables the implementation of other combustion processes, such as stratified combustion. Multiple injection at different times is also possible. The injection pressures must be higher for DI systems compared to PFI systems. The design is based on the maximum load (filling), compression and the resulting maximum cylinder pressure at the end of injection (EOI). In order to always ensure a supercritical pressure ratio at EOI for a pressure-independent injection rate, the injection pressure must be twice as high as the cylinder pressure at the time of EOI. The test was carried out with an injection rate of 3.8 g/s for DI and PFI. In order to also investigate efficiency influences of very late SOI, the injection pressure was not limited in the 1D simulation. Based on a lambda variation at part load at a BMEP of 12 bar and 2000 rpm, the two injection systems in combination with the two turbocharging systems a wastegate TC and a two-stage VTG system are compared in **Figure 30**. A significantly higher intake manifold pressure clearly illustrates the displacement effect of the hydrogen (low volumetric energy density of 3 MJ/dm<sup>3</sup>) with external mixture formation, which can be completely avoided with direct injection after IVC. Already at an air ratio of  $\lambda = 1.6$ , the PFI system in combination with the wastegate TC reaches its lean- or boost pressure limit. Direct injection, on the other hand, with the TC enables lean mixture up to  $\lambda = 2.3$  with corresponding advantages in the gross indicated and brake efficiency. The efficient, two-stage VTG system can also ensure lean combustion up to  $\lambda = 2.6$  with external mixture formation. Compared to the DI-VTG combination, a significantly more efficient operating point in the VTG follows as a consequence of higher boost pressure requirement (smaller VTG adjustment) along with a VTG efficiency advantage of up to 18 % at  $\lambda = 1.5$ . This enables a more favorable gas exchange loop despite the higher exhaust and boost pressure levels, with corresponding advantages in gas exchange work, which are reflected in brake efficiency benefits up to  $\lambda = 2.4$ .

Despite the displacement effect, the performant two-stage VTG system thus achieves a maximum brake efficiency of 41.2 % at the external mixture formation PFI in the medium part load, which is comparable to that of the DI. However, the compensation of the disadvantageous displacement effect with the advantages in the charge change depends on the operating point and, in particular, fundamentally on the design of the charging unit. As the boost pressure requirement rises, i.e. with increasing load and speed, this effect is limited, so that direct injection offers greater leaning potential with the corresponding advantages in efficiency and NO<sub>x</sub> emissions.

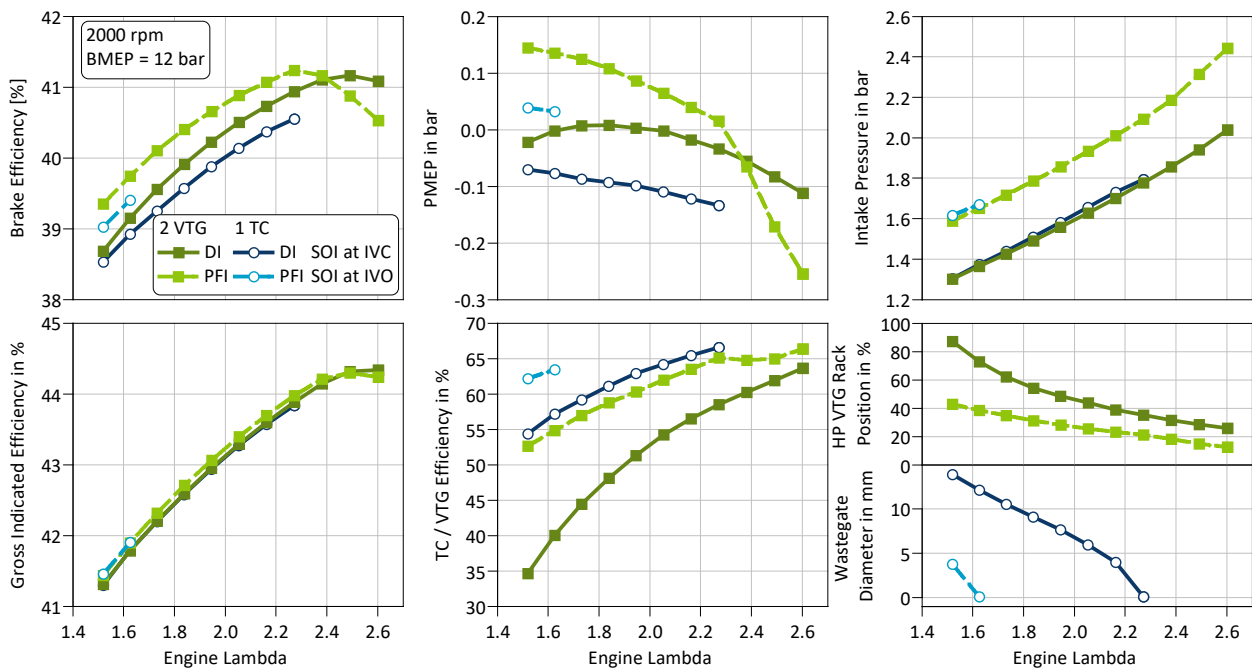


**Figure 30:** Influence of external (PFI) vs. internal (DI) mixture preparation on efficiency at 2000 rpm and 12 bar BMEP

The conditions with the highest brake efficiency from the lambda variation were used to investigate the influence of the injection timing of the two systems in **Figure 31** and to exploit maximum potentials with the two-stage VTG charging. It should be noted, that in the 1D simulation the influence of the homogenization is not considered. The latter is assumed to be optimal, thus the maximum potentials are reported here. The sudden increase in the boost pressure requirement as well as the charge exchange work can be clearly seen if the SOI is brought forward significantly before the inlet closing time (IVC) during direct injection. In the case of injection during the opened intake valve, the reduction in the degree of delivery that would otherwise result (effect of the displacement effect) must be compensated for by the higher boost pressure. A late adjustment of the intake, on the other hand, increases the indicated high-pressure efficiency due to thermodynamic advantages. The reason for the increase is to be found in the different properties of the substances air and hydrogen and the timing of the composition of the two. The later the injection, the longer only air is compressed, thus a smaller amount of substance in the cylinder, which is why the compression curve flattens out with increasingly late injection. The high-pressure loop is enlarged while the expansion curve remains approximately constant. This effect can also be seen in the falling final compression pressure and final compression temperature, which significantly reduce the starting conditions for the combustion process.

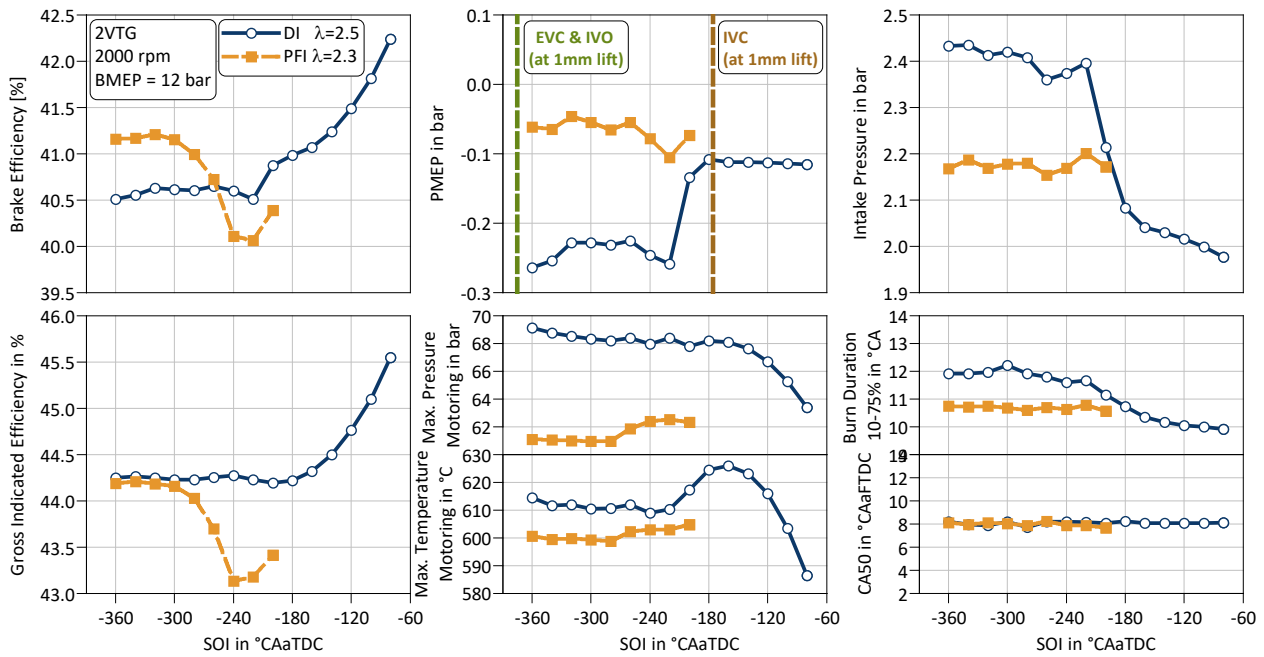


**Figure 31:** Influence of injection timing for external (PFI) and internal (DI) mixture formation at 2000 rpm and 12 bar BMEP

Especially at operating points with knocking combustion, the effect of late injection can be used to reduce knocking, as shown in the **Figure 32** in the LET. Due to the more efficiency-favorable MFB50, a significantly larger efficiency gain of more than 2 % (DI,  $\lambda = 1.9$ ) can be observed compared to injection after IVC. To exploit this potential, the major challenge of mixture homogenization in the short time must be solved, e.g., by injection injectors with targeted injection jet dispersion. The injection pressure must also be designed to be correspondingly high or the injection rate must be increased in order to implement such a late injection. In principle, direct injection offers more freedom in terms of combustion design. Very lean but ignitable mixtures in the low load could replace throttling with its efficiency losses. Stratified combustion with late injection, but also multiple injection, including during combustion for combustion control, are conceivable if appropriate injectors and injection pressure make this possible. A system with variable injection pressure and correspondingly adapted valve opening duration could also tap the maximum efficiency potential depending on the operating point.

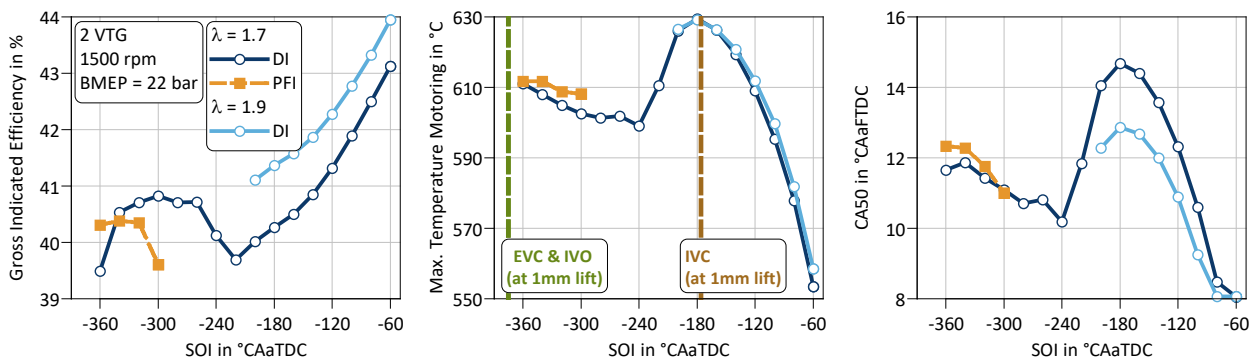


**Figure 32:** Influence of injection timing on knock tendency for external (PFI) and internal (DI) mixture formation at 1500 rpm and 22 bar BMEP

### Nitrogen oxide reduction measures: low-pressure EGR, high-pressure EGR and Miller valve lifts incl. low-pressure EGR

To reduce peak combustion temperatures, cooled exhaust gas recirculation is a possible alternative to lean burn to positively influence emissions and efficiency. Basically, there is the possibility of high-pressure and low-pressure EGR. In the case of low-pressure EGR (LP-EGR), the extraction here takes place downstream of the low-pressure VTG and is fed back after the EGR cooler (conventional diesel EGR cooler) via an EGR valve upstream of the low-pressure compressor. Due to the low exhaust gas temperature level of the H<sub>2</sub>-ICE and the flow through the supercharger unit, the extracted exhaust gas already has relatively low temperatures even at full load points, so that EGR outlet temperatures of 60-75 °C could be achieved with the EGR cooler shown, depending on the operating point. The EGR cooler was also used in the high-pressure EGR variant (HP-EGR), where the extraction point is upstream of the high-pressure VTG. Consequently, the supercharger unit lacks exhaust gas enthalpy, which it in turn does not need, since the EGR mass flow taken replaces the fresh air mass requirement and, in accordance with the exhaust gas pressure to boost pressure gradient, delivery is possible without additional compression. The EGR feed takes place downstream of the high-pressure compressor and upstream of the LLK using an EGR valve with non-return function, which is necessary to prevent backflow of fresh air into the exhaust tract, which would occur due to temporary negative pressure gradients corresponding to the exhaust gas pressure pulsation depending on the operating point. The comparison of the two EGR variants and a Miller valve lift profile in combination with low-pressure EGR is shown in **Figure 33** at the full-load operating point at 3000 rpm. The maximum achievable dilution is different due to the system and the x-axis is scaled differently for better representation. Marked in the blue frame is the base point without EGR and in the green frames the respective efficiency-optimal points of the three variants investigated. With the low-pressure EGR, an efficiency increase of 1 % to 40.8 % can be achieved with 20 % EGR and  $\lambda = 1.6$ , with comparably low NO<sub>x</sub> emission values. The advantage is attributable to a lower boost pressure requirement, lower charge exchange work and an efficiency-optimal combustion center. The highest efficiency of 42.3 % is achieved by the high-pressure EGR system with an EGR of 24 % and an air ratio of  $\lambda = 1.6$ . In particular, the charge exchange work can be greatly reduced here, since the exhaust gas pressure is not relieved via the VTG but is fed directly to the intake side, resulting in a small pressure difference between the exhaust and intake sides with a correspondingly small charge exchange loop. The approximately twice as high heat capacity of the water vapor lowers the process and peak temperature and, concomitantly, NO<sub>x</sub> emissions and knock tendency. The short Miller opening time also allows efficiency to increase to 41.1 % with an air ratio of  $\lambda = 1.4$  and EGR of 19 %. However, as a result of the higher boost pressure requirement, the process and peak temperatures are significantly higher than for the other variants, with a corresponding sharp increase in NO<sub>x</sub> emissions. EGR thus offers a further option for optimizing the H<sub>2</sub>-ICE in terms of efficiency and emission behavior. However, it is critical in terms of dynamic behavior, especially the high-pressure variant with check valve, and therefore requires further investigation.

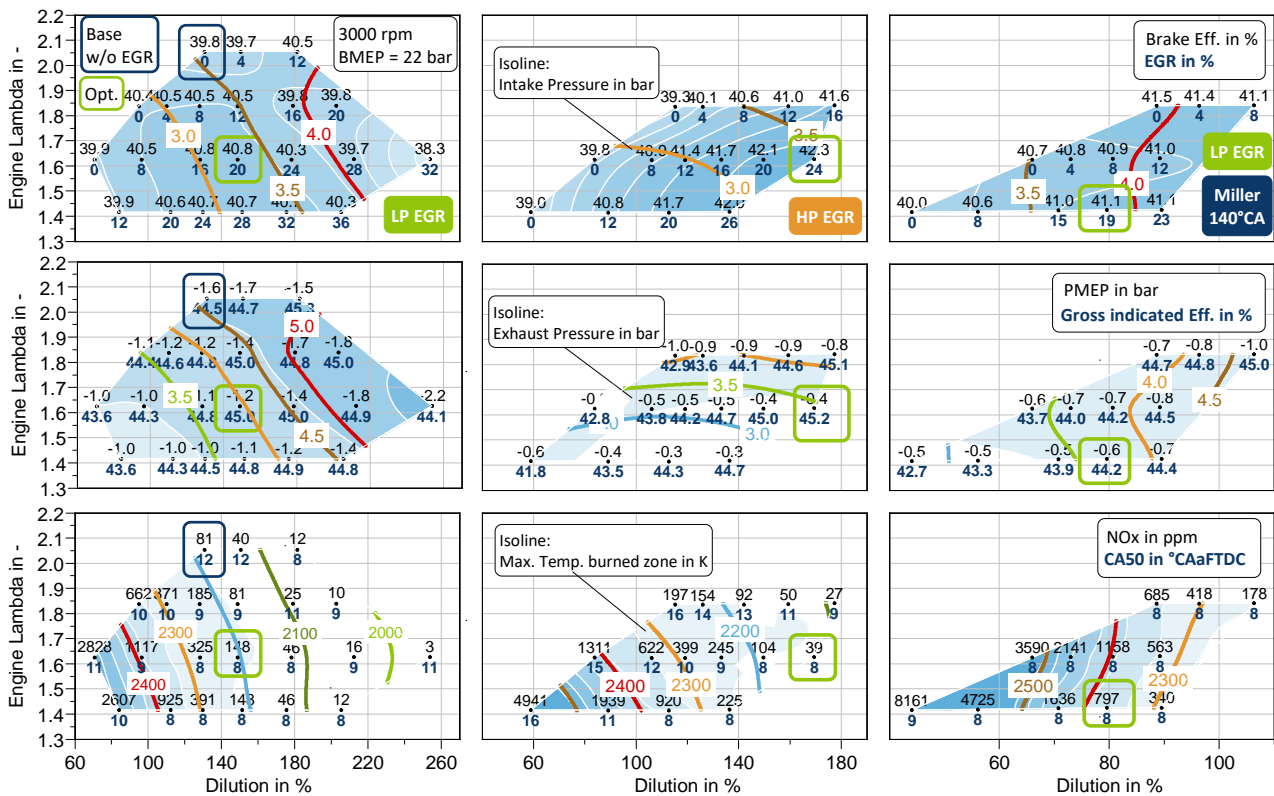


**Figure 33:** Comparison of low-pressure, high-pressure EGR and Miller with EGR at 3000 rpm and 22 bar BMEP

### H<sub>2</sub>-DI low-pressure mixture formation and its challenges

A meaningful application of low-pressure H<sub>2</sub> injection is only possible if the gas-in-gas mixture formation results in a homogenization of the hydrogen-air mixture that does not lead to excessive lambda gradients during combustion. An insufficient homogenization of the mixture would ultimately have the effect of negatively influencing both the auto-ignition behavior and the generation of nitrogen oxide emissions.

For this reason, accompanying the investigations and the design of the two engine concepts for passenger cars and light commercial vehicles, simulations were carried out in 3D CFD with the applied phenomenological models in the 1D world. The main objective of these simulations was to investigate the influence of various boundary conditions (injection pressure, SOI, injector position, injector layout, ...) on the homogenization of the directly injected hydrogen.

The CFD simulations were carried out using the operating point 2000min<sup>-1</sup> / 12bar BMEP and the "LCV" engine concept as examples. The injection behavior of the modeled injector was validated with regard to penetration behavior using pressure chamber measurements and the schlieren measurement principle. The H<sub>2</sub>-DI injector used for this purpose is a solenoid-valve-actuated, outward-opening nozzle with a conical seat and 300um needle stroke, which was not specifically designed for hydrogen operation, but was judged to be sufficient for the methodological investigations at this point.

The injector delivers an H<sub>2</sub> mass flow of 3.8 g/s at a set injection pressure of 30bar and a supercritical pressure ratio. The nozzle is part of the CFD mesh, so that the inflow behavior is physically modeled and thus has a realistic "spray image" as a result. On the other hand, this type of modeling leads to an extremely high-resolution mesh in the area of the nozzle and thus to long computation times. However, according to current knowledge, simplifications of the modeling of H<sub>2</sub>-DI injection (e.g. specification of massflow boundaries

at the nozzle outlet) lead to inadmissible results, so that all simulations were performed with complete meshing of combustion chamber and injector. The calculations were performed with the commercial CFD code Converge and using the following sub-models: k-e RNG turbulence model, multispecies diffusion model, Redlich-Kwong real gas equation, transient temperature and pressure conditions from high-fidelity 1D model, overall cell count ~1.5 million, simulation start at 135°C.

**Figure 34** presents with variants V1...V4 some of the combinations of SOI, injector position and injector layout investigated in this work.

130kW engine setup / $\varepsilon$ 11.2 / 2000min <sup>-1</sup> / 12 bar BMEP / $p_{INJ} = 30\text{bar}$ (3.8g/s) / $\lambda_{\text{mean}} = 2.5$ / IVC <sub>1mm</sub> = 544°C / EVC <sub>1mm</sub> = 347°C
V1: A-Nozzle / SOI 562°C / single injection / lateral injector position
V2: A-Nozzle / SOI 562°C / single injection / <u>central injector position</u>
V3: A-Nozzle / <u>SOI 380°C</u> / single injection / lateral injector position
V4: <u>A-Nozzle + multihole cap</u> / SOI 562°C / single injection / lateral injector position

**Figure 34:** Overview of the simulations performed in 3D CFD for mixture formation

The "base SOI" of 562°KW was chosen so that H<sub>2</sub> injection starts at a time when the intake valve is almost closed (valve lift < 0.1mm). The variation of SOI to an earliest value of 380°C (Variation 3) represents a reasonable time at which the exhaust valve is already closed and a cooling effect has been established on the combustion chamber by the incoming fresh air due to the already open inlet valve. An interesting question with this variation is how much the longer mixture formation time influences homogenization.

It can be assumed that the best homogenization is achieved with configuration V3. In this respect, variant 1 serves as a preliminary benchmark for the homogenization to be achieved with the further variant investigations or optimization steps.

With the V2 configuration, a new geometric variant was created that is characterized by the fact that the injector, which is otherwise positioned laterally, i.e. between the intake valves, has been moved to a central position. The injector finds its position here in place of the spark plug, which was replaced by the injector in the sense of an initial sensitivity study and was not repositioned in the combustion chamber.

The next optimization step is represented by configuration V4. Here, too, a new geometric variant has been created whose characteristic feature is a modified nozzle layout. While all variants 1...3 were calculated with the basic layout of the real injector, i.e. the nozzle opening outwards, the nozzle in V4 is characterized by a cap with 6 individual holes arranged on the injector tip, which are aligned for the lateral injector position in such a way that both the intake port-induced tumble flow and the penetration and combustion chamber capture of the "spray" are improved compared to the A nozzle with hollow cone spray. Again, this experiment is for the purpose of estimating the effect on homogenization and was not developed or tested for real-world feasibility, nor was it validated by pressure chamber measurements. **Figure 35** shows the injector layout with multi-hole cap for the lateral injector position.

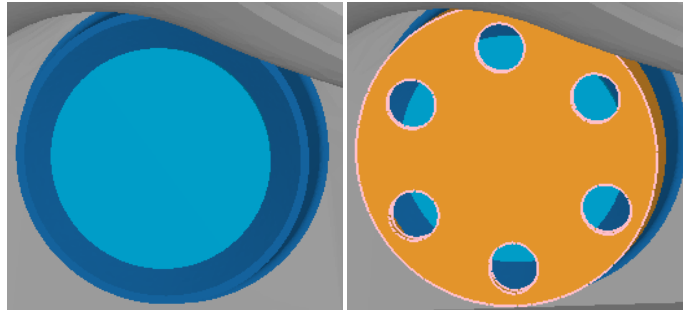


**Figure 35:** Comparison of original injector layout and A nozzle with multi-hole cap for lateral injector position

**Figure 36** shows the  $H_2$  mass fractions in the combustion chamber in an iso view for the 4 simulated variants for selected times after the end of injection. At  $600^\circ KW$ , the advantage of the longer mixture formation time for variant 3 is clearly evident, so that at approx.  $60^\circ KW$  after the charge change UT, mixing is already significantly advanced compared to the variants with late SOI. In principle, this advantage is maintained over the entire compression stroke, so that the best homogenization is also achieved in purely qualitative terms at the ignition OT.

Even though variants 1, 2 and 4 differ very clearly in purely geometrical terms, only minor differences are evident in the qualitative comparison of mixture formation during the compression stroke. Obviously, the central injector position at the late start of injection offers the longest free path length, which, however, does not massively improve homogenization. Only at the times  $680$  and  $720^\circ KW$  is there a slight improvement in mixture formation compared to the lateral injector position with variant 1.

Variant 4 with the multi-hole cap basically shows similar behavior to variant 1. Slight advantages in combustion chamber detection are apparent, but the deflection of the jets into the lower part of the combustion chamber seems to function well only to a limited extent. The latter is apparently due to an unfavorable ratio of hole length to hole diameter of the multi-hole cap, so that an improved perforated plate geometry is already under development. Despite the limited functionality of the perforated plate and the only limited effect of combustion chamber detection, a small improvement in homogenization at late times can nevertheless be seen compared with variant V1 but also compared with variant 2.

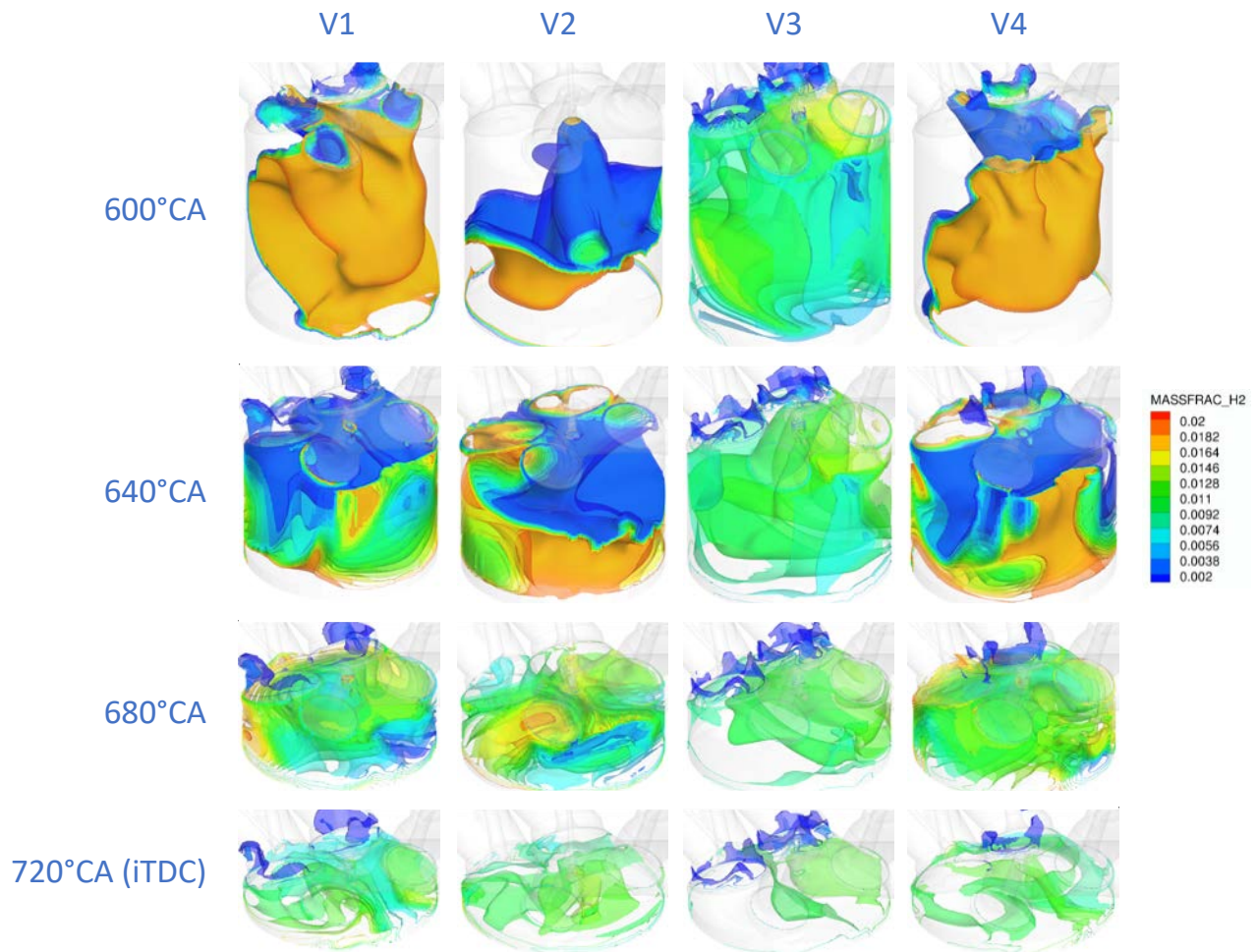


**Figure 36:** Qualitative comparison of mixture homogenization for different timings after end of injection

In addition to the purely optical evaluation of the homogenization from the representation of the H<sub>2</sub> mass fractions, **Figure 37** shows a representation which also allows a quantitative evaluation of the homogenization achieved for the 4 configurations investigated. Shown here is the standard deviation from the mean lambda determined from all cells at the time of ignition OT (720°C).

The interpretation of the results from the optical analysis of the H<sub>2</sub> mass fractions in the combustion chamber is also confirmed by the plot in the figure below. Variant V1 with late SOI shows by far the worst homogenization value, i.e. the highest standard deviation. The early shift of the SOI into the charge change offers - as suspected - the highest potential for improving the homogenization and thus represents the benchmark.

Both the relocation of the A-nozzle to the center of the combustion chamber and the optimization of the laterally arranged injector by means of the multi-hole cap significantly improve the mixture formation compared with the basic variant V1, but do not achieve the good value of variant 3.

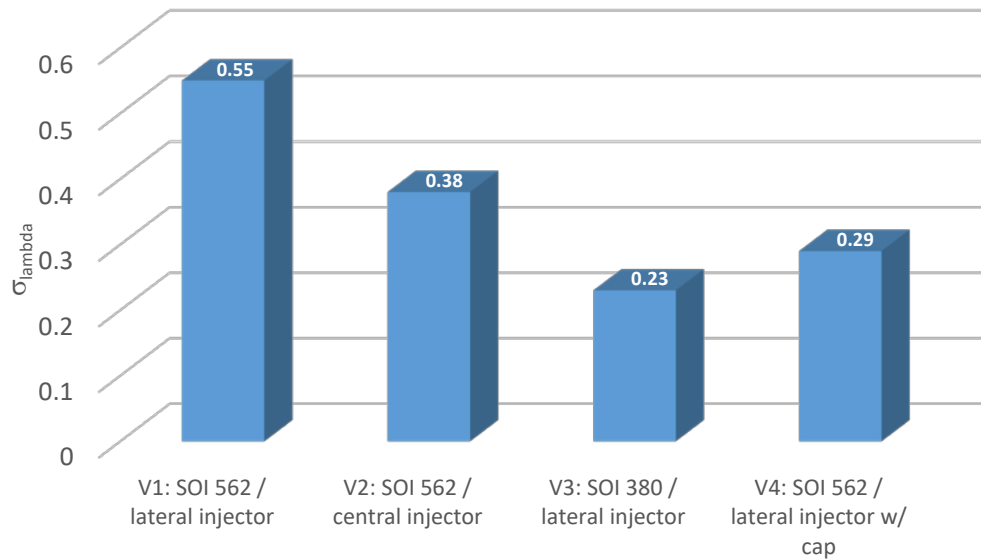


**Figure 37:** Quantitative comparison of the mixture homogenization achieved at 720°C

On the basis of the initial results presented here for the investigation and optimization of mixture formation with low-pressure direct injection, it remains to be stated that even with the fundamentally advantageous properties of hydrogen over other gases, in particular the high diffusion coefficient, the known problems of gas-in-gas mixture formation remain. If the full potential of direct injection is to be exploited in terms of avoiding irregular combustion and high charge pressures with injection pressures of less than 30 bar, and if nitrogen oxide emissions are to be kept to a minimum in line with the ideal assumption of perfect homogenization - as discussed in the previous chapters - both injector and overall combustion process optimization is necessary.

### Summary and development priorities H<sub>2</sub>-ICE

The investigations carried out by ICE with homogeneous, premixed H<sub>2</sub> combustion processes show a maximum efficiency of 42.2 % for passenger cars and light commercial vehicles. Here, the supercharging unit in particular is decisive for the maximum lean burn potential and thus efficiency increase at the best point as well as reduction of NO<sub>x</sub> emissions. With the aim of maximizing efficiency, a two-stage VTG turbocharging concept with an optimized shift strategy was used for passenger cars and light commercial vehicles. The WG-ATL investigated offers a cost-oriented alternative for hybrid applications. Here, the ICE without valve train variability achieves a maximum efficiency of 41.4 % with lowest NO<sub>x</sub> emissions of below 120 ppm, or below 10 ppm in most of the map. Comparison of intake manifold and direct injection (SOI with intake valve closed) shows significantly higher lean potential with DI at lower intake manifold pressure. Furthermore, the displacement effect of PFI can be completely eliminated with DI, allowing higher power densities or a lean air ratio with identical power density. In addition, with a late DI injection, the high-pressure efficiency can be improved by reducing the compression work by up to 1.2 %. However, this requires correspondingly high injection pressures, and homogenization of the mixture is a critical development focus. Consideration of cooled EGR at high loads yielded efficiency benefits of up to 1 and 1.5 % for both low-pressure and high-pressure EGR. Here, the EGR valve in interaction with the gas dynamics pose a development challenge. Miller valve strokes exacerbate the problem of boost pressure requirements as shown in combination with EGR

in the studies. However, these allow efficiency advantages to be achieved by reducing throttle losses, especially in the low intake manifold load.

For heavy-duty vehicles, e.g., in engine class 12-13L, one can imagine better efficiencies with homogeneous premixed H<sub>2</sub> process up to 44 %. This can be increased by further measures, as shown below.

Further optimization measures on the homogeneous premixed H<sub>2</sub>-ICE as well as the introduction of additional technologies provide an outlook for further potential to increase efficiency in the short term towards a brake efficiency of 45 %. The following technology packages are worth mentioning here:

- **Increase of the lean burn potential** at the homogeneous premixed H<sub>2</sub> combustion process via further optimization of the charging unit (high loads) as well as design of the ignition system for leanest mixtures (shift of the ignition limit towards higher combustion air ratios at low loads);
- **Increase of compression ratio with dedicated combustion chamber design** (stroke/bore or surface/volume ratio as well as firestone design) with late fuel injection to minimize preignition and knock tendency;
- **Adaptation of intake port characteristics** taking into account the significant influence of direct fuel injection on charge motion and turbulent kinetic energy in the cylinder, together with optimization of mixture preparation
- **Active component temperature management with phase-change cooling** to significantly reduce the tendency to knock and increase the exhaust gas enthalpy, in particular via active control of the exhaust manifold temperature (including supersaturation of the cooling medium), possibly including a waste heat recovery system;
- **Friction reduction** through targeted engine design for the peak pressures and pressure gradients specific to the combustion process;
- **Heavily cooled external EGR** to lower intake manifold and high-pressure process temperatures and thus reduce wall heat losses and NO<sub>x</sub> raw emissions
- **Water injection** to reduce raw NO<sub>x</sub> emissions and further increase efficiency thanks to lower knocking tendency with the aid of targeted exhaust gas cooling for water recovery. The transient NO<sub>x</sub> peaks with lambda undershoot can thus be reduced. This technology may be of particular interest for heavy commercial vehicles and large engines.

In addition to the above-mentioned measures to increase the efficiency of the homogeneous premixed H<sub>2</sub> VCM, further developed inhomogeneous combustion processes (stratified / diffusive combustion, **Table 4**) offer potential. High-pressure injection (200-300 bar) can be used to inject the hydrogen during combustion, and diffusive combustion can be used to avoid all the problems of pre-inflammation, knocking, etc. This offers good potential for increasing efficiency and power density. This is where the challenge lies in the development of injection components. The need for high pressures reduces the range with a CGH<sub>2</sub> tank system if no compressor associated with parasitic losses is on-board.

Depending on the application and the technical basis, peak efficiencies of up to approx. 50 % can be achieved with a hydrogen ICE in heavy-duty commercial vehicle applications. However, the associated, not inconsiderable increase in component costs and development effort must be taken into account here. Against this background, the premixed low-pressure DI combustion process represents the most balanced compromise between target conflict resolution (efficiency / power density / raw emissions / time to market and costs, **Figure 23**.

	PFI-SI	Low Pressure DI-SI	High Pressure DI-SI	High Pressure DI-Diffusive
Brake Efficiency	👎	👉	👍	👍
Power Density	👎	👍	👍	👍
NO <sub>x</sub> Formation (Part   Full Load)	👍   👉	👍   👎	👉   👉	👉   👉
Combustion Anomalies & Combustion Stability	👎	👉	👉	👍
Tank Capacity Utilization	👍	👍	👉	👎
Costs	👍	👉	👎	👎
Controllability	👉	👉	👉	👉

**Table 4:** Evaluation of different H<sub>2</sub> combustion processes

## Exhaust gas aftertreatment concepts to achieve future emission regulations for H<sub>2</sub>-ICEs

### Passenger cars and light commercial vehicles

The concept discussion on possible exhaust aftertreatment systems is conducted for passenger cars, light trucks and heavy trucks. **Figure 38** shows the driving cycles considered for emission control of passenger cars and light commercial vehicles.

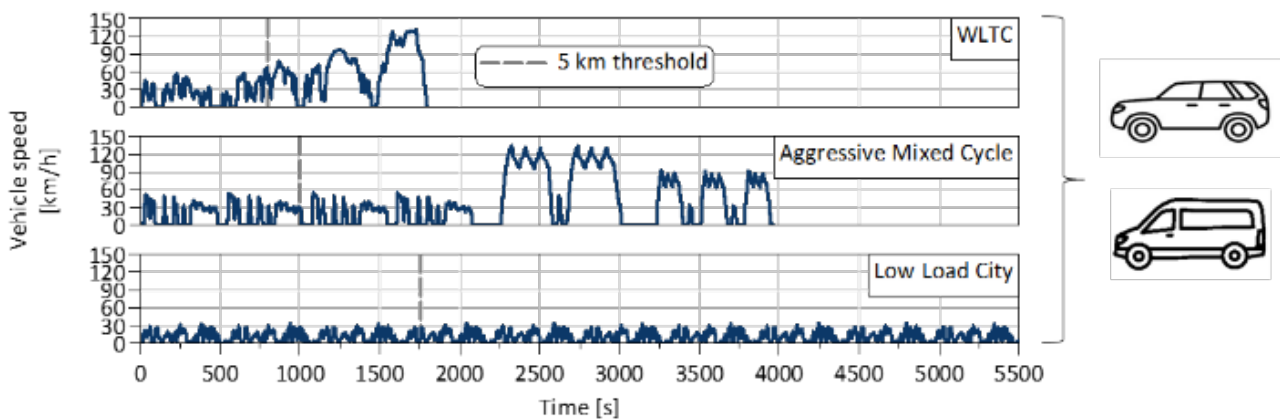


**Figure 38:** Test cycles for the PC and LCV EAT investigations

In addition to the WLTC, an aggressively driven RDE cycle with an urban, highway and interurban part (Aggressive Mixed Cycle - AMC) and a very low-load urban driving cycle (Low Load City - LLC) are considered. Emissions in the WLTC, AMC and LLC are also evaluated after a driving distance of 5 km.

**Figure 39** shows qualitatively the course of typical NO<sub>x</sub> tailpipe results of "Pre RDE" and "EU6d" vehicles in a plot over the average driving speed of the RDE cycles. From the higher NO<sub>x</sub> values at the edges of the "Cf bathtub curve", i.e. for particularly low and particularly high driving speeds, one can see the challenge of the currently discussed EU7 emission legislation with a Cf = 1.0 for all possible RDE driving profiles.

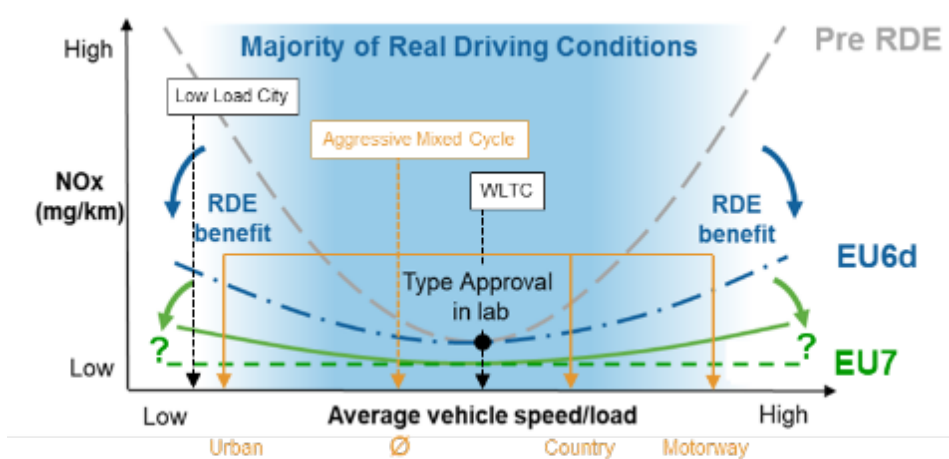


**Figure 39:** Typical behavior of the achievable conformity factor in RDE cycles

Due to the lean combustion process and NO<sub>x</sub> raw emissions, which cannot be avoided completely especially in transient operation, a DeNO<sub>x</sub> exhaust aftertreatment (EAT) based on SCR systems is considered for the H<sub>2</sub>-ICE. For the passenger car and the light commercial vehicle, a current diesel EAT system from the reference engine of the light commercial vehicle is used as a starting point.

As a basis for considering suitable EAT systems, **Figure 40** shows a map comparison for engine-out NO<sub>x</sub> emissions and exhaust gas temperature T<sub>3</sub> between the diesel reference engine (left - 2.0l R4, 1-stage VTG, 140 kW) and the H<sub>2</sub>-ICE designed for the light commercial vehicle (right - 2.0l R4 2-stage VTG 130 kW).

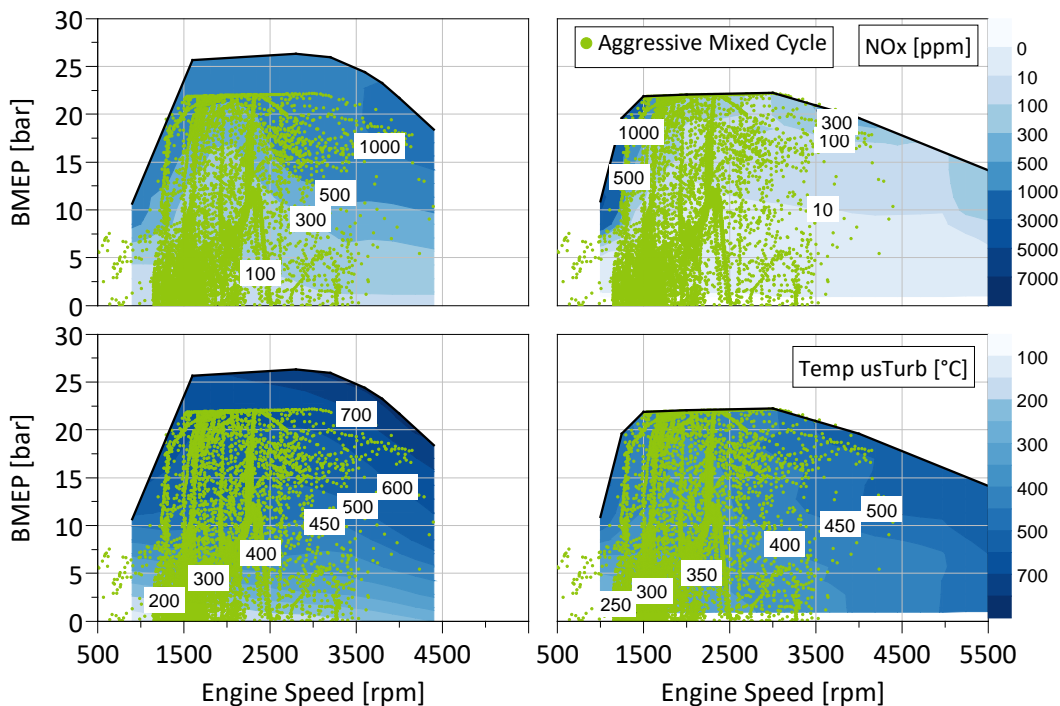


**Figure 40:** NO<sub>x</sub> and T<sub>3</sub> engine map (left diesel, right 130 kW H<sub>2</sub>-ICE)

The maps also show the scatter plot of the engine operating points in the aggressive mixed cycle as it occurs in the light commercial vehicle driven by the H<sub>2</sub>-ICE and an adapted transmission.

It can be seen that the map of the H<sub>2</sub>-ICE covers a wider engine speed range, but lower mean effective pressures (higher combustion speed, but load limitation by pre-ignition and knock). The NO<sub>x</sub> raw emission is lower with the H<sub>2</sub>-ICE than with the reference engine, particularly in the upper load range, due to the homogeneous lean combustion process. Due to the comparatively high excess charge, the exhaust gas temperature in the full-load range is also significantly lower for the H<sub>2</sub>-ICE ( $\Delta T_3 > 200$  °C). Accordingly, consideration can be given to omitting an underfloor SCR system.

It is also noticeable that the exhaust gas temperature of the H<sub>2</sub>-ICE in the low load range is higher than that of the reference diesel engine. This is due to the variability used in the valve train, which allows unnecessary excess charge to be avoided at low engine loads with minimal charge exchange losses. Accordingly, a lower effort can be assumed for EAT thermal management in low load and for short and cold-started RDE cycles.

**Figure 41** shows the results obtained in the EAT simulation for NO<sub>x</sub> reduction in the three driving cycles AMC, WLTC and LLC. The bar charts on the left show the evaluation after the entire cycle length, while the bar charts on the right contain the evaluation after 5 km driving distance.

The upper part of the figure shows the results for the reference EAT system carried-over from diesel powered light commercial vehicle (DOC-SCRf-SCR). It can be seen that, due to the favorable map behavior mentioned above with regard to NO<sub>x</sub> and T<sub>3</sub>, NO<sub>x</sub> tailpipe values below the current EU6 limit can be achieved with the basic EAT system in the WLTC and LLC after a driving distance of 5 km (NO<sub>x</sub> ≤ 80 mg/km). With the AMC, on the other hand, the EU6 limit is exceeded quite significantly due to the aggressive accelerations directly after engine start (NO<sub>x</sub> = 133 mg/km).

The lower part of the figure shows the benefit of an innovative EAT system for further reducing NO<sub>x</sub> tailpipe emissions. The oxidation catalyst of the basic system is replaced by a relatively large passive NO<sub>x</sub> adsorber (PNA) and a downstream electric heating disc. This measure makes it possible to store a large proportion of the NO<sub>x</sub> emitted at the start of the cycle on the PNA until the SCRf catalyst close to the engine has reached its light-off temperature. The electric heating disc helps to bring the close-coupled SCRf catalyst up to or above the light-off temperature in good time before the NO<sub>x</sub> desorption temperature in the PNA is attained. In the demanding AMC cycle, this measure achieves a reduction in NO<sub>x</sub> tailpipe emissions after 5 km from 133 mg/km to 49 mg/km.

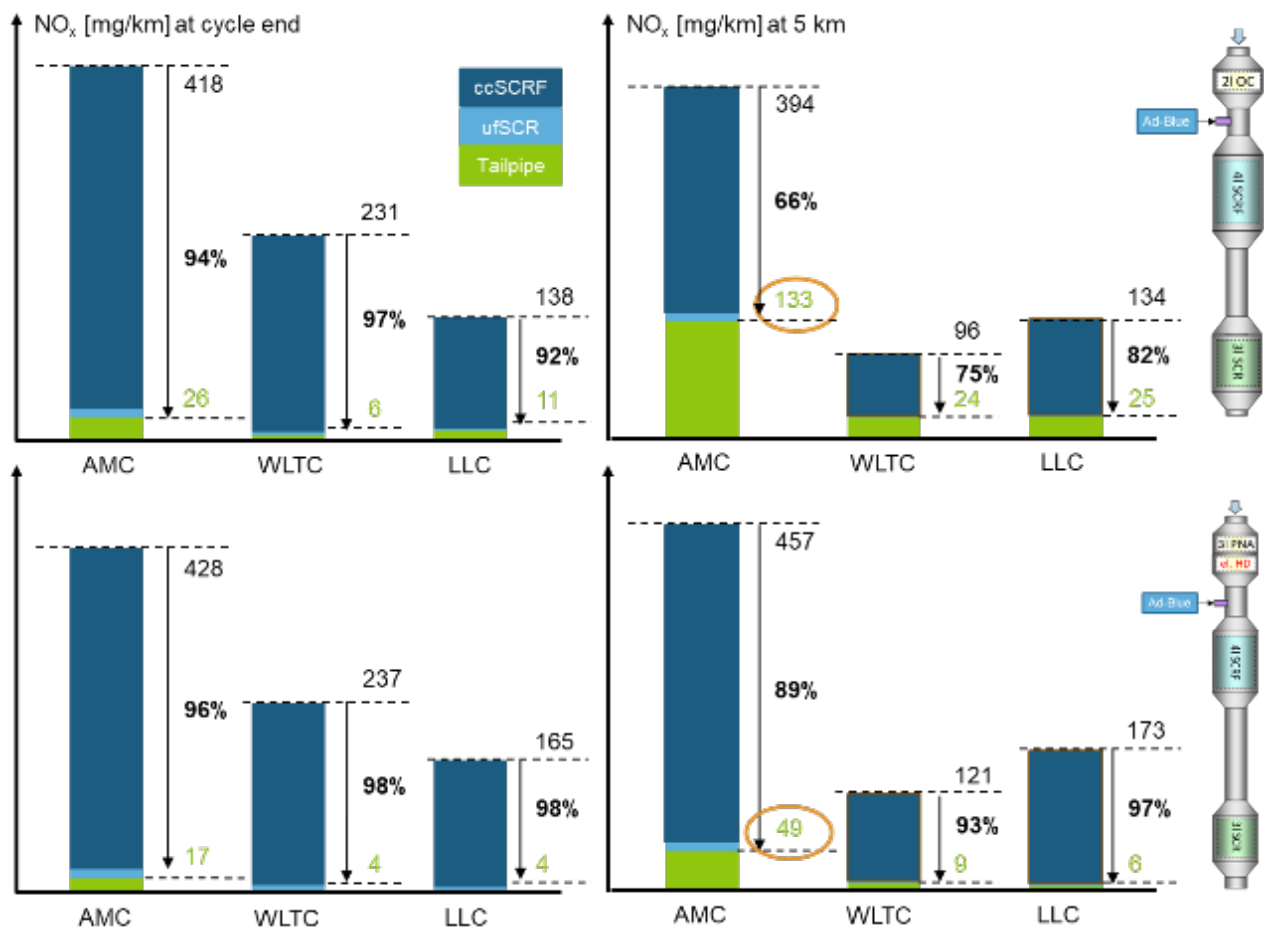


**Figure 41:** Tailpipe emission results of LCV valid for full WLTC cycle and after 5 km

The **Figure 42** shows a comparison of the time plots of NO<sub>x</sub> conversion in the AMC for the basic EAT system and the innovative EAT system. It can be seen very clearly how the light-off time of the close-coupled SCRf can be advanced significantly with the aid of the electric heating disc (advance from approx. 600s to approx. 250s). In this context, the intensive operation of the electric heating disc within the first 5 km driving distance leads to an H<sub>2</sub> consumption increase of 6 %. The lower three diagrams show the time plot of NO<sub>x</sub> storage and desorption in the PNA and the NO<sub>x</sub> conversion via the close-coupled SCRf. It can be seen that the NO<sub>x</sub> desorption from the PNA occurs after approx. 300s and thus temporally after the SCR light-off. This represents a successful "handshake" between PNA and SCRf.

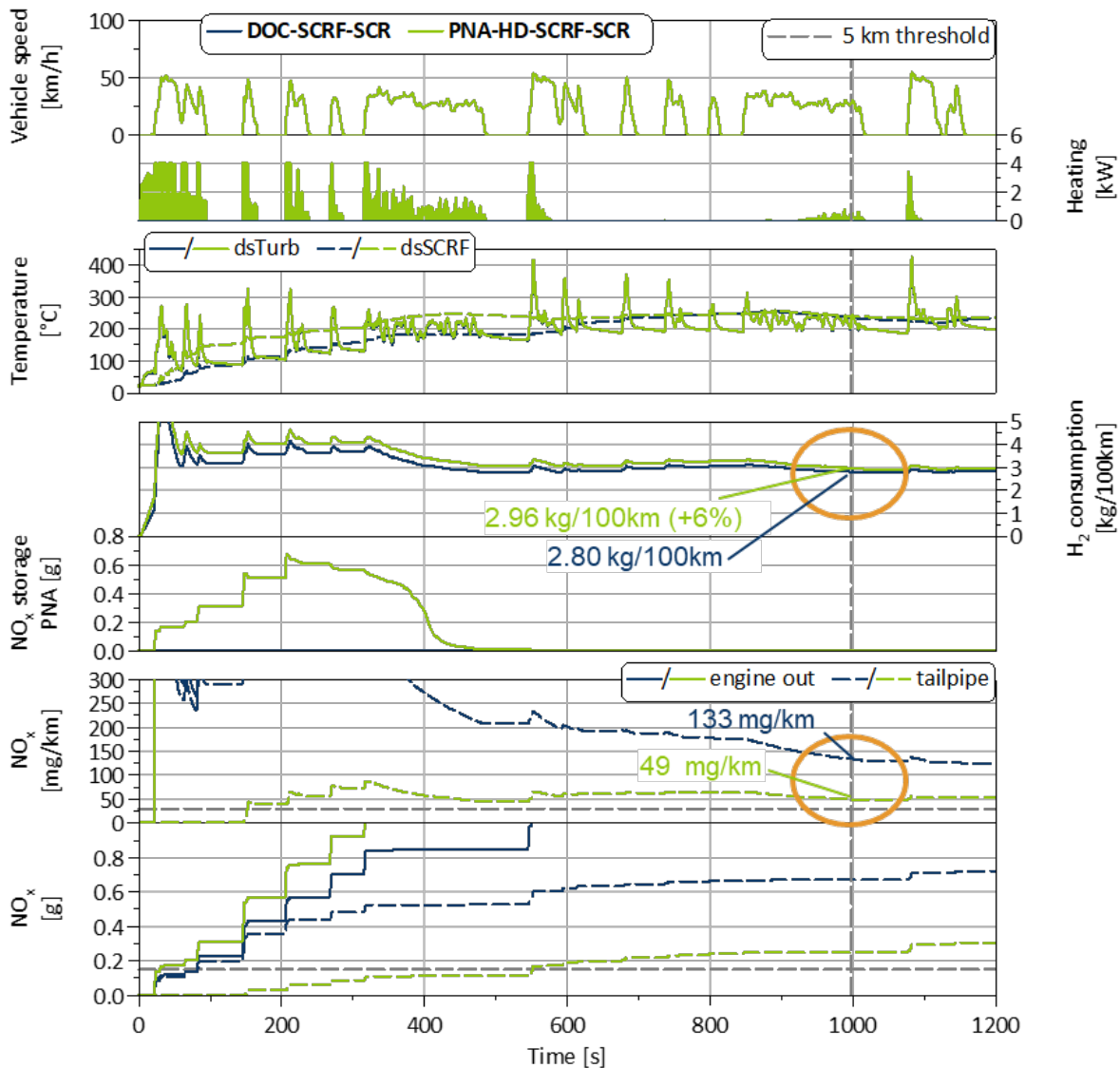


Figure 42: NO<sub>x</sub> emissions for AMC cycle with basic and innovative EAT system

### Heavy-duty vehicles

For the heavy-duty vehicle, the FTP cycle is investigated for emission control. Figure 43 shows the standardized specifications for engine speed and engine torque.

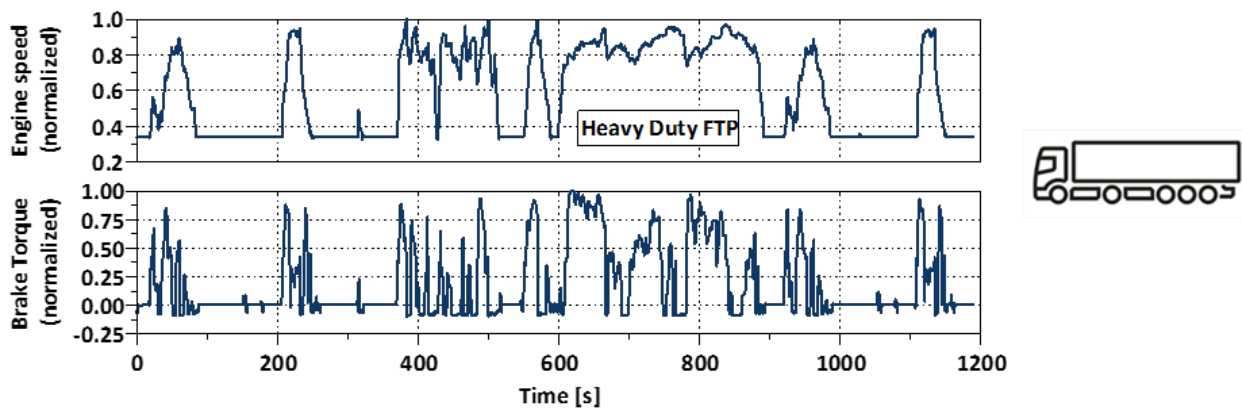
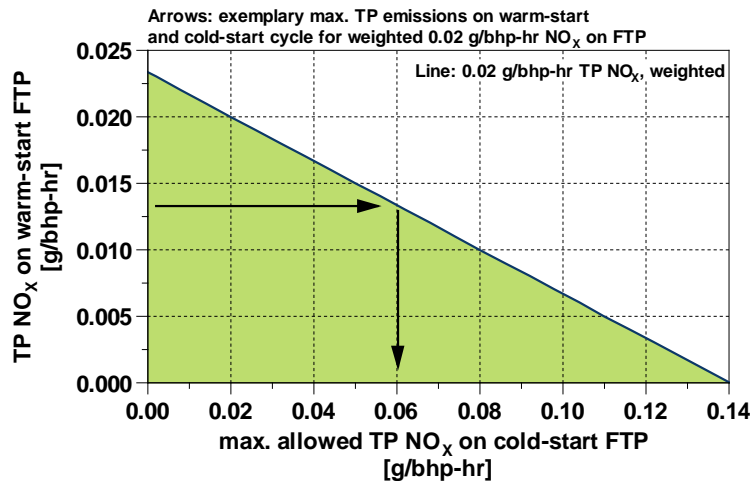


Figure 43: Test cycle for HD truck EAT investigations

For the FTP emission cycle, the NO<sub>x</sub> limits are now defined as 0.05 g/bhp-hr from 2024, and 0.02 g/bhp-hr from 2027. **Figure 44** shows the breakdown of NO<sub>x</sub> target values possible under the legislation for hot and cold-started FTP cycles in the case of an overall NO<sub>x</sub> target of 0.02 g/bhp-hr. Since higher SCR conversion rates can be assumed for warm-started cycles, a target value of 0.06 g/bhp-hr (0.08 g/kWh) was set for the cold-started FTP cycle. This results in 0.013 g/bhp-hr as the target value for the warm-started FTP cycle.



**Figure 44:** NO<sub>x</sub> targets for warm and cold started FTP cycles for CARB 2027.

Previous studies on compliance with future regulations [16] [17] [18] [19] have shown that the cold cycles pose the maximum challenge to the engine and exhaust aftertreatment and are therefore the most suitable for concept evaluation. Moreover, a fast warm-up of the exhaust gas aftertreatment (EAT) by increasing the exhaust enthalpy is crucial for meeting the emissions to achieve the required low NO<sub>x</sub> emissions.

**Figure 45** shows a simulated engine-out NO<sub>x</sub> trace in the cold started FTP cycle. It can be seen that very high NO<sub>x</sub> peaks can occur in transient operation. Depending on the control strategy, NO<sub>x</sub> peaks of 5000 to 8000 ppm are possible here. Highlighted is the start of the cycle to motivate that a fast warm-up behavior is crucial to comply with the legislative requirements. The selected target of 0.08 g/kWh is already exceeded after 400 s, assuming that the EAT system cannot yet convert any nitrogen oxides. The height of the NO<sub>x</sub> peaks, the average engine-out NO<sub>x</sub> emission level and the exhaust gas temperature downstream of the turbine can be optimized by engine calibration measures. The response behavior of the turbocharger and the air path control have a strong influence in this context.

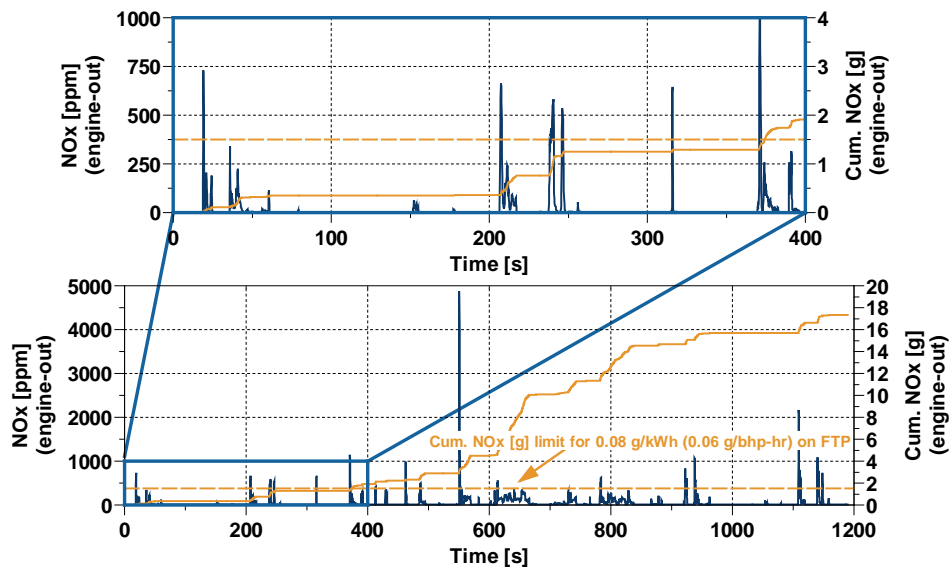


**Figure 45: Engine-out NO<sub>x</sub>-Trace in cold FTP for HD truck application**

**Figure 46** shows the results of a coupled engine and EAT simulation in GT-Power for an SCR-based EAT system without an oxidation catalyst, but with an NH<sub>3</sub> slip catalyst (Ammonia Oxidation Catalyst - AMOX) downstream of the SCR. In the simulation study, the particulate filter was assumed to be downstream of the assembly of SCR and AMOX, so that its heat capacity would not adversely affect the heating behavior of the SCR catalyst. The figure shows the result of iterative calibration loops with respect to NO<sub>x</sub> tailpipe emissions and BSFC:

- Starting from the basic calibration ("Calib#1"), the ignition timing (IT) was delayed in phases with reduced lambda and thus increased NO<sub>x</sub> emissions.
- The range of the IT variation was carried out with 4°C<sub>A</sub>, 6°C<sub>A</sub> and 8°C<sub>A</sub> for the variants "Calib#2", "Calib#3" and "Calib#4".
- In order to achieve a further reduction in engine-out NO<sub>x</sub> emissions and to reduce the demands on the EAT system, the late adjustment of the IT was applied in the initial phase of the cold-started cycle regardless of the lambda value in "Calib#5", "Calib#6" and "Calib#7".
- It can be seen that the NO<sub>x</sub> peaks also affect the NO<sub>x</sub> tailpipe emission at later stages of the cycle even when the EAT system is operating in a favorable temperature range.

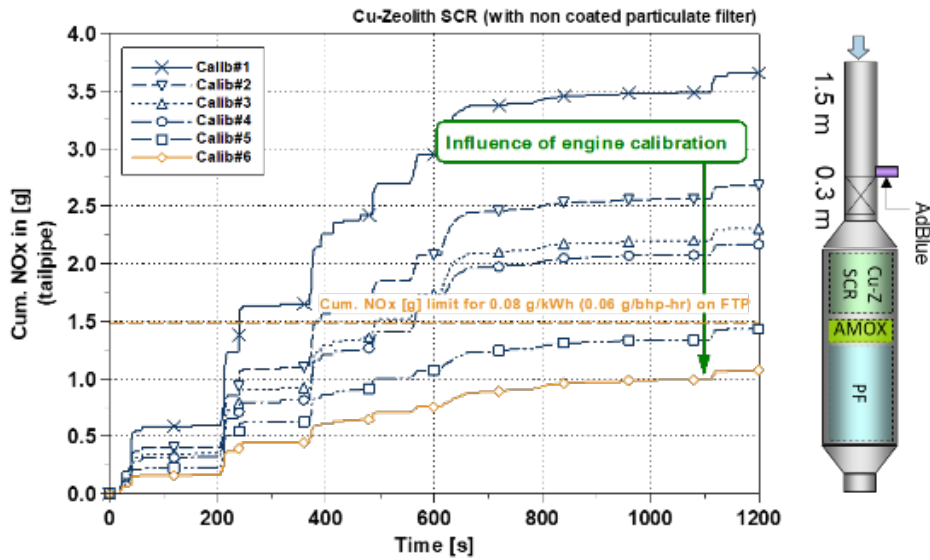


**Figure 46:** Optimized tailpipe NO<sub>x</sub>-emissions in cold FTP for HD Trucks (simulation)

In order to test the necessity of using a particulate filter as part of the EAT system for H<sub>2</sub>-ICE, measurements were carried out on a heavy duty single-cylinder engine with H<sub>2</sub> intake manifold injection. **Figure 47** shows exemplary results at the operating point  $n_M = 1100 \text{ min}^{-1}$  / IMEP = 8 bar. The indicated mean pressure was kept constant during the test and the air to fuel ratio was varied from 1.8 to 3.4.

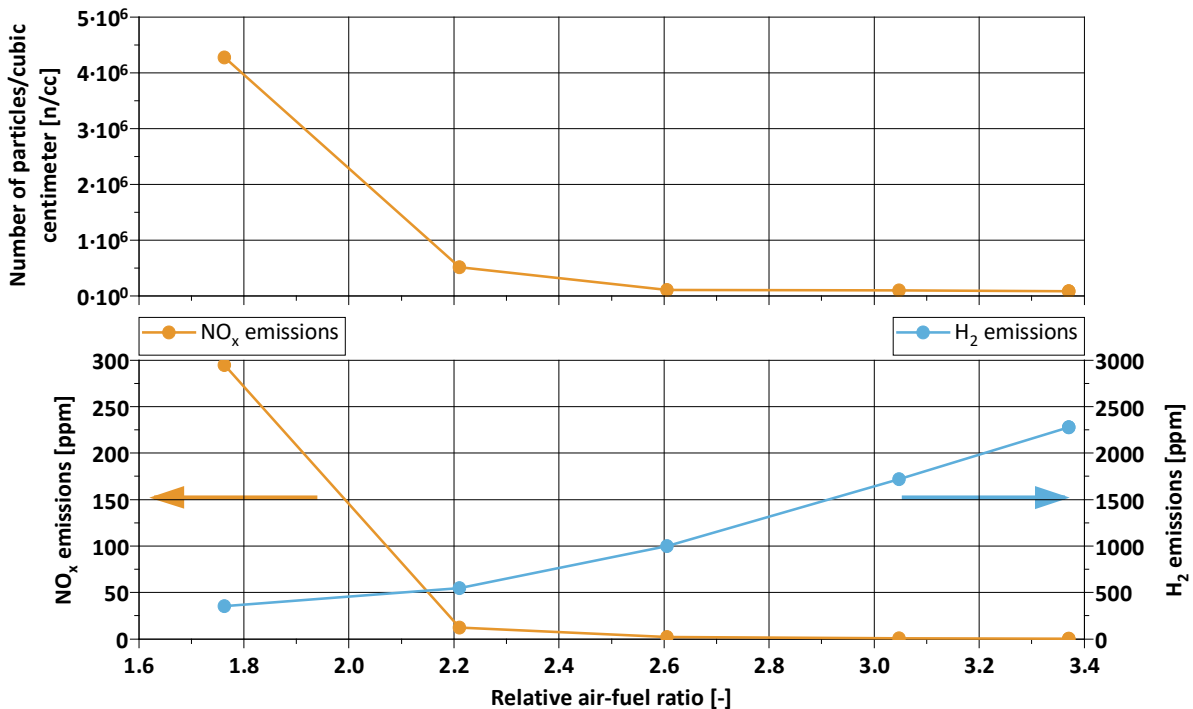


**Figure 47:** Particle number, NO<sub>x</sub> and H<sub>2</sub> emissions vs. air to fuel ratio

The measurement data for the particulate emissions was generated on the basis of a Cambustion DMS500 measurement system. There are basically three sources of particulate emissions in the exhaust gas: the lubricating oil, impurities in the hydrogen and impurities in the charge air. Impurities in the hydrogen can be excluded, since high-purity hydrogen was used on the single-cylinder test rig. The intake air was also measured separately with the

particle measuring device and only very small particulate numbers were measured in the intake air. From this, it is concluded that the combustion of lubricating oil is the main cause of particulate emissions from H<sub>2</sub>-ICEs.

Due to space limitations, not all EAT studies could be shown and explained in the preceding text. However, the main findings of the studies can be summarized as follows:

- The tailpipe NO<sub>x</sub> trajectories produced at H<sub>2</sub>-ICE exhibit a characteristic "steppiness" that is due to transient NO<sub>x</sub> peaks and high raw NO<sub>x</sub> emission levels in the low-end torque region.
  - Engine sizing and full-load calibration of the air to fuel ratio are very crucial for the technological effort in the EAT system.
  - Technologies that allow phlegmatization of the ICE (hybrid), or else transient support of the charging system (eCompressor or eTC), suggest an even greater emission reduction potential for H<sub>2</sub>-ICEs than for conventional gasoline or diesel engines. For heavy-duty vehicles, hybridization is of course not as relevant due to cost reasons.
- Despite the non-existent (or extremely low) CO and HC emission from H<sub>2</sub>-ICEs, an oxidation catalyst can be part of the EAT system, depending on the application (passenger car or commercial vehicle). The reason for this is the strong influence of the NO to NO<sub>2</sub> ratio on the SCR reaction, especially in the exhaust gas temperature range relevant for the H<sub>2</sub>-ICE. The advantage of an EAT architecture without an oxidation catalyst is accelerated heating of the SCR system close to the engine.
- Due to the lower exhaust gas temperature level for H<sub>2</sub>-ICE with lean combustion even at full load, a second SCR and thus a second dosing point can be skipped. The SCR close to the engine must be designed to be correspondingly large.
- A particulate filter should be planned to avoid any tailpipe particulate emissions and associated discussions. However, due to the significantly lower particulate emissions, the filter size can be significantly reduced. Due to the different required dimensions of the SCR and the particulate filter, no integrated component is suitable (i.e. no SDPF). This allows the thermal inertia of the SCR to be reduced.
- In addition to the FTP cycle, compliance in low load cycles is also required for heavy-duty trucks. This can be achieved by adapting the engine's operating strategy in combination with other EAT technologies. For example, dedicated H<sub>2</sub>-deNO<sub>x</sub> catalysts can make a valuable contribution at very low exhaust temperatures.

## Hydrogen storage systems

### Overview hydrogen storage systems

Hydrogen as a fuel in vehicles can be stored in different forms, gaseous under high pressure, cryogenically (liquid or supercritical under pressure) and by chemical or adsorptive bonds to solids or liquids. In addition to storage under high pressure (CGH<sub>2</sub>), which is already ready for series production today, current developments are focusing in particular on cryogenic storage (LH<sub>2</sub>, CcH<sub>2</sub>), which can most likely reach series production readiness for vehicle applications in the near future. Other material-based storage technologies have attractive storage densities in some cases, but most of the technology is not yet ready for series production and a major disadvantage is high heat generation during filling, which means that rapid refueling, which is important for road vehicles and work machines, can only be realized with considerable effort. Optimal solutions would essentially be to store hydrogen at the lowest possible pressures and at ambient temperature, with simultaneously high volumetric and gravimetric density and low costs. There are some research approaches for this, but

their further development into a solution superior to CGH<sub>2</sub>, LH<sub>2</sub> or CcH<sub>2</sub> is at least open. The advantages and disadvantages described below are therefore limited to gaseous and cryogenic storage methods.

### **CGH<sub>2</sub> (Compressed Gaseous Hydrogen)**

The storage of H<sub>2</sub> gas under high pressure from 350 up to 700bar at ambient temperature is the most widely used technology. To enable sufficiently lightweight storage for mobile use, the cost-intensive use of carbon fiber is currently unavoidable. The decision for the pressure level is determined not only by the costs, but also by the package requirements and the complexity of the refueling infrastructure:

- The manufacturing costs in relation to the storage capacity increase slightly and progressively due to the compressibility at high pressures.
- For passenger cars and heavy-duty trucks, range and package requirements mean that higher pressure levels are needed.
- Costs of the refueling infrastructure increase with the required storage pressure due to the increasing compression energy, increase in the number of pressure stages as well as due to the pre-cooling requirement for fast refueling.

The energy expended to produce hydrogen to a high pressure range of 700bar, based on the calorific value of the hydrogen, is about 1/2 - 1/3 compared to the liquefaction energy for LH<sub>2</sub>. Gas storage systems of 350bar maximum pressure have the further advantage that the gas does not have to be strongly pre-cooled during the refueling process in order to achieve an acceptable refueling speed.

In order to achieve structurally favorable membrane stress conditions for the pressure vessel design, the geometric shaping is generally limited to spherical or cylindrical shapes and the utilization of installation spaces is somewhat restricted as a result, **Figure 48**. In principle, cylindrical vessels are more advantageous from the point of view of installation space than spherical vessels, for example in a package consisting of quite slim cylinders for utilizing the volume behind the driver's cab of trucks.

Another advantage of pressure vessels is that the hydrogen is already available in gaseous form under high pressure. This means that injection pressures of up to 30 bar can be maintained for a long time in internal combustion engines without having to expend energy on compression.

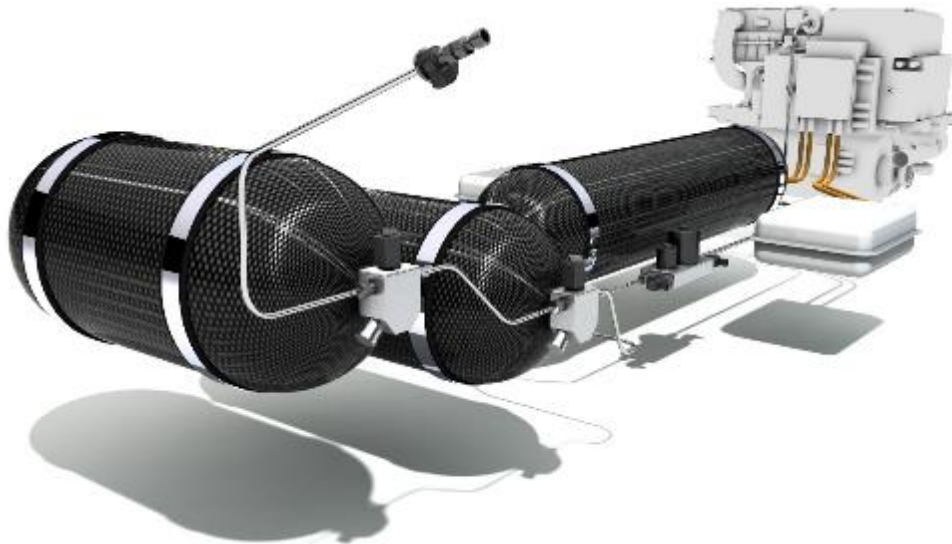


**Figure 48:** Exemplary CGH<sub>2</sub> storage system for passenger car applications

### **LH<sub>2</sub> (Liquid Hydrogen)**

LH<sub>2</sub> is stored in liquid form at a cryogenic temperature of approx. -253°C, with an internal pressure of approx. 3 bar. This requires storage tanks with high vacuum insulation, which limits unavoidable heat ingress from the warmer environment to a minimum. The residual heat ingress leads to an evaporation of the liquid hydrogen combined with the pressure increase. To limit the pressure, hydrogen must be released (boil-off), i.e. hydrogen is lost as fuel in this case. The main advantages of LH<sub>2</sub> compared to CGH<sub>2</sub> are the lower storage costs due to the saving of carbon fiber and the higher volumetric and gravimetric density. Furthermore, slightly different geometries from the pure cylinder shape to package-optimized shapes are basically possible with LH<sub>2</sub> due to the low pressures. Regardless of the tank size, a certain wall thickness is required for high-vacuum insulation, so larger tanks are always more advantageous in terms of volume utilization due to the surface-to-volume ratio.

### **CcH<sub>2</sub> (Cryo Compressed Hydrogen)**

CcH<sub>2</sub> is in principle a combination of CGH<sub>2</sub> and LH<sub>2</sub>. The hydrogen is stored supercritically, for example, up to approx. 350bar and -253°C. The storage is highly vacuum insulated and pressure resistant, which extends the time to unavoidable release of hydrogen (blow-off). CcH<sub>2</sub> thus combines some of the advantages of LH<sub>2</sub> and CGH<sub>2</sub>, but the combination of the vacuum insulation and pressure resistance results in increased costs compared to LH<sub>2</sub> storage tanks, as well as a limitation to spherical/cylindrical tank geometries. In addition, as with LH<sub>2</sub>, larger vessel pressure volumes are more advantageous due to the smaller surface area to volume ratio to minimize heat ingress.

### **Selection of the most advantageous storage system**

Thus, cryogenic and compressed gas stored hydrogen are currently competing, **Table 5**. A key factor regarding the choice of storage system is the vehicle it shall be used in. Cryogenic storage systems with their boil-off or blow-off losses have an unfavorable effect on vehicles with long parking periods, whereas CGH<sub>2</sub> storage systems have only very small and negligible permeation losses. On the other hand, cryogenic systems offer a significantly higher volumetric and gravimetric density, which is particularly favorable for vehicles with

high H<sub>2</sub> consumption or high range requirements. For example, pressurized storage systems would therefore be more favorable for passenger cars and light commercial vehicles, while cryogenic systems would be more advantageous for heavy trucks and heavily utilized work machines. In addition to the pure consideration of the vehicle tank system, the required or existing refueling infrastructure and the price of hydrogen at the refueling station are also decisive factors, see also Chapter: *Techno-economic comparison of H<sub>2</sub> supply pathways*.

**Table 5:** Main parameters for Hydrogen storage systems

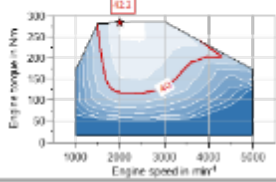
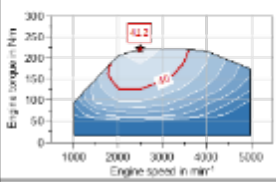
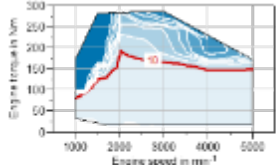
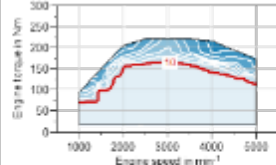
	Unit	CGH <sub>2</sub> 35 MPa	CGH <sub>2</sub> 50 MPa	CGH <sub>2</sub> 70 MPa	LH <sub>2</sub> / Cch <sub>2</sub>
<b>Volumetric Capacity</b> [mass H <sub>2</sub> /Volume]	kg H <sub>2</sub> / m <sup>3</sup> Sys	15-19	18-22	20-25	50-65
<b>Gravimetric Capacity</b> [mass H <sub>2</sub> /mass]	kg H <sub>2</sub> / kg Sys	4-6 %	4-6 %	3-5 %	8-12 %
<b>Estimated Production Cost</b> [Storage Cost/kg H <sub>2</sub> ]	€ Sys/ kg H <sub>2</sub>	400-500	420-520	450-550	180-300

### **Potential analysis of hybridized H<sub>2</sub>-ICE powertrains**

In the case of H<sub>2</sub> ICE, the fundamental question arises as to whether hybridization makes sense. In the case of conventional ICE based on the combustion of fossil fuels, this serves to reduce CO<sub>2</sub> emissions during driving, whereas the corresponding necessity is eliminated here due to carbon-free combustion. However, there are still reasons to reduce fuel consumption in H<sub>2</sub> ICE. In nature, hydrogen is only present in bound form and must be converted into molecular H<sub>2</sub> in an energy-intensive process. A reduction in H<sub>2</sub> consumption during driving therefore leads to a reduction in primary energy use and CO<sub>2</sub> emissions associated with hydrogen production. Electrification of the powertrain also offers the opportunity to make the H<sub>2</sub>-ICE much less technically complex, thus reducing production costs. While the hybrid powertrain offers better driving performance compared to the conventional one, the ICE itself can be phlegmatized. This offers advantages in terms of pollutant emissions.

In the hybridized environment, a different H<sub>2</sub>-ICE is used in the passenger car than in the conventional environment. A comparison of the two ICE's can be found in the **Table 6**. The engine adapted for the hybrid drive could not be realized in a conventional drive from the point of view of driving performance.

**Table 6:** Comparison of H<sub>2</sub>-ICE's for conventional and hybridized powertrain for PC

Parameter	Unit	Engine type	
		Conventional	Hybrid
Engine efficiency map	%		
Engine out NO <sub>x</sub> -emission	ppm		
Rated power	kW (min <sup>-1</sup> )	90 (3,000)	90 (4,000)
Max. torque	Nm (min <sup>-1</sup> )	280 (1,500)	220 (2,500)
Compression ratio	-	12	
Stroke / bore	mm / mm	92.8 / 82.5	
Injection system	-	H <sub>2</sub> -DI	
Inlet / outlet valve variabilities	°CA	Cam timing / cam timing	None / none
Turbocharging system	-	2-stage VTG system	1-stage wastegate turbocharger
Combustion		Lean H <sub>2</sub>	

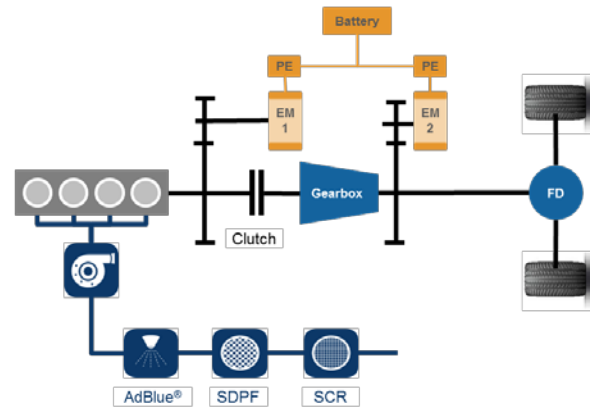
In this work, the conventional powertrain is compared with the hybridized powertrain using a longitudinal dynamics simulation (map-based) with respect to H<sub>2</sub> consumption and NO<sub>x</sub> emission in the WLTC and another highly dynamic cycle. The functional relationship between the dynamics of the engine torque build-up or the dynamics of the working gas mixture control and the NO<sub>x</sub> emission is considered in the model. The maximum H<sub>2</sub> savings potential in the hybrid powertrain is defined with a hybrid strategy designed purely for fuel reduction. The classic standard ECMS combined with an optimizer to find the best equivalence factor is used.

In the second step, the operating strategy is defined as an adaptive ECMS. Battery state of charge and exhaust gas temperature are weighted in the cost function to enable a hybrid strategy optimized for exhaust gas temperature and emissions in addition to consumption optimization. This is additionally combined with a rule-based heating strategy at the start of the cycle. Here, the combustion engine is dragged to 1500 rpm over 10 s with the aid of EMG 1 and held. The engine is then started. The operating point at 50 Nm is maintained until the light-off temperature in the SCR system is reached. After this, the engine switches to efficiency mode, where SOC (State of Charge) of battery and exhaust gas temperature are kept within the defined optimum range (reference gas temperature at SCR inlet = 230 °C, reference SOC = 67 %). The start-up strategy of the combustion engine at the beginning of the cycle with the aid of the electric motor to heat up the exhaust system is state of the art [20]. In addition to the passenger car results for both optimization strategies, corresponding results for a light commercial vehicle are also discussed at the end.

The specifications of the passenger cars used in the simulation and the corresponding conventional and hybrid powertrains can be found in the **Table 7**.

**Table 7:** Vehicle and powertrain specification PC

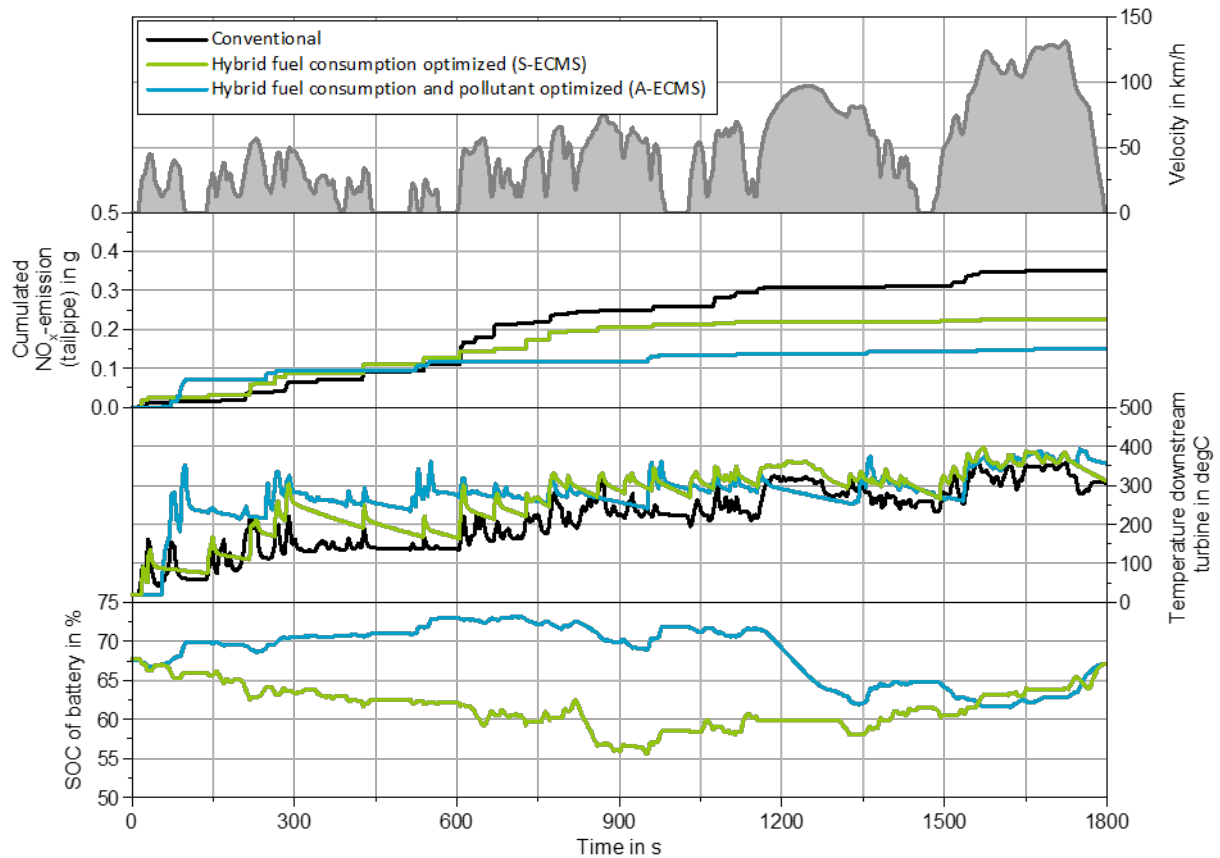
Component	Vehicle/powertrain specification	
	Conventional	Hybrid
Powertrain definition	Conventional	Hybrid
$c_w \cdot A$	0.943 m <sup>2</sup>	
Curb weight	1,690 kg	1,776 kg
Gearbox	6-stage automatic	6-stage
Hybrid topology	-	Serial-parallel
E-machine 1 (EM1)	-	60 kW (peak) 150 Nm (peak) 12,000 min <sup>-1</sup>
E-machine 2 (EM2)	-	100 kW (peak) 250 Nm (peak) 17,000 min <sup>-1</sup>
High voltage battery capacity	-	2.5 kWh (gross)



The **Figure 49** shows the time-resolved curves for speed, cumulative NO<sub>x</sub> emissions, exhaust gas temperature after the turbine and the state of charge of the hybrid vehicle's battery in the WLTC for the three powertrain concepts investigated. Already the hybrid vehicle with the purely consumption-optimized operating strategy shows a significantly reduced NO<sub>x</sub> emission. This can be explained by the significantly higher raw emission of the base engine in the range of low engine speeds and high engine loads, **Table 6**.

Operation in this critical range can be avoided by electrification in the hybridized engine. In the hybrid vehicle with the pure consumption-optimized strategy, the ICE is electrically supported far into the extra-urban part of the cycle or the vehicle is operated purely electrically. This is reflected in the falling state of charge of the battery. Through brake recuperation and load point shift of ICE in the high-speed range is a balanced state of charge reached at the end of the cycle. From the point of view of reducing pollutant emissions, this is not the optimum behavior. The exhaust gas temperature remains below the level required for NO<sub>x</sub> emission conversion for a long time in the cycle.

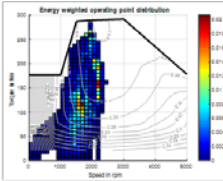
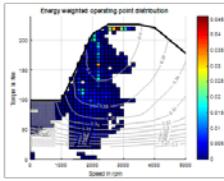
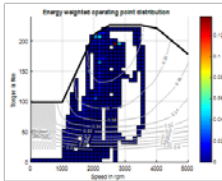
The goal of the consumption-optimized and pollutant emission-optimized strategy is to operate the exhaust after-treatment system in a more advantageous temperature range and thus reduce NO<sub>x</sub> emission. Unlike the consumption-optimized hybrid strategy, the battery is charged early in the cycle. The operating points in the engine map are shifted to higher loads and the exhaust gas temperature increases.



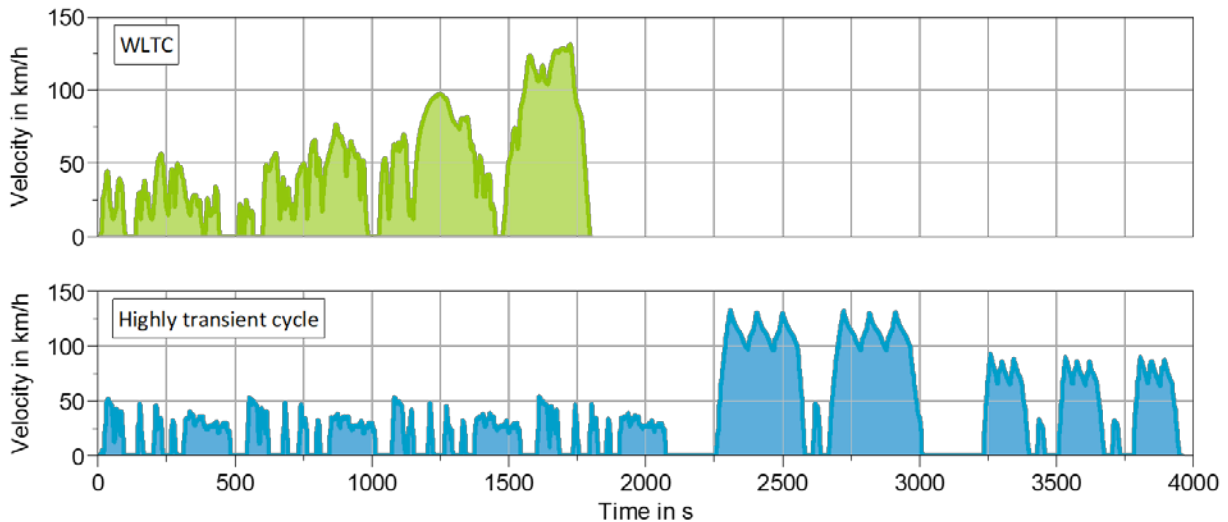
**Figure 49:** Time-resolved profiles for PC application within WLTC

This is associated with slight losses in terms of consumption reduction potential compared with the purely consumption-optimized strategy, **Table 8**. However, this vehicle concept is the only one to comply with the planned NO<sub>x</sub> target value of 30 mg/km for the year of 2025 (possible scenario of EU7 emission standard), even after just five kilometers [21].

**Table 8:** Operating point distribution ICE, fuel consumption and NO<sub>x</sub>-emission for the PC application within WLTC

Parameter	Unit	Conventional powertrain	Hybrid powertrain (fuel consumption optimized)	Hybrid powertrain (fuel consumption and pollutant optimized)
Energy weighted operation point distribution	-			
Mean engine efficiency	%	36.3	39.0	37.5
H <sub>2</sub> consumption cycle	kg/100 km	1.57	1.30	1.36
NO <sub>x</sub> -emission 5 km (tailpipe)	mg/km	47	38	24
NO <sub>x</sub> -emission cycle (tailpipe)	mg/km	15	10	6

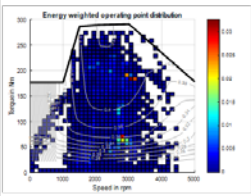
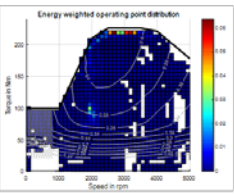
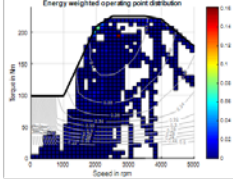
The simulations in the aggressive cycle illustrate this problem, **Table 8**



**Figure 50:** Velocity profile of the highly dynamic/aggressive cycle in comparison with WLTC

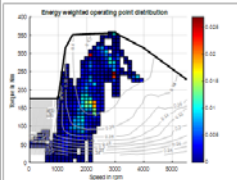
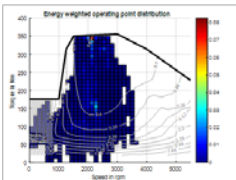
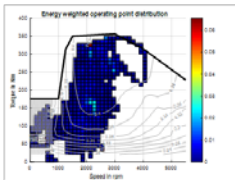
The basic engine in its current design with the exhaust gas aftertreatment shown in **Table 7** is not able to meet the emission target. Hybridization thus enables a reduction in fuel consumption in passenger cars while at the same time complying with the NO<sub>x</sub> target values when using a less complex ICE, **Table 9**.

**Table 9:** Operating point distribution ICE, fuel consumption and NO<sub>x</sub>-emission for the PC application within highly aggressive cycle

Parameter	Unit	Conventional powertrain	Hybrid powertrain (fuel consumption optimized)	Hybrid powertrain (fuel consumption and pollutant optimized)
Energy weighted operation point distribution	-			
Mean engine efficiency	%	37.5	39.2	38.0
H <sub>2</sub> consumption cycle	kg/100 km	1.76	1.50	1.56
NO <sub>x</sub> -emission 5 km (tailpipe)	mg/km	95	71	24
NO <sub>x</sub> -emission cycle (tailpipe)	mg/km	28	13	7

Finally, this chapter will discuss the fuel consumption and pollutant emission results of a light commercial vehicle in the WLTC. Unlike the passenger car, the H<sub>2</sub>-ICE does not differ between conventional and hybridized powertrains. The engine has a rated power of 130 kW. It also does not use a series-parallel hybrid topology, but a P2 architecture with a 7-speed automatic transmission. The battery is the same as that of the passenger car. The same traction motor is also used. The light commercial vehicle has a cw\*A value of 2.1 m<sup>2</sup>. With an unladen weight of 2551 kg, the hybrid version has a mass that is 66 kg higher than the vehicle with the conventional powertrain.

**Table 10:** Operating point distribution ICE, fuel consumption and NO<sub>x</sub>-emission for the LCV application within WLTC

Parameter	Unit	Conventional powertrain	Hybrid powertrain (fuel consumption optimized)	Hybrid powertrain (fuel consumption and pollutant optimized)
Energy weighted operation point distribution	-			
Mean engine efficiency	%	36.7	40.6	40.5
H <sub>2</sub> consumption cycle	kg/100 km	2.97	2.38	2.41
NO <sub>x</sub> -emission 5 km (tailpipe)	mg/km	116	103	33
NO <sub>x</sub> -emission cycle (tailpipe)	mg/km	26	26	9

Here, too, it can be seen that the pollutant- and consumption-optimized strategy delivers the best results with regard to NO<sub>x</sub> emissions while at the same time saving fuel compared with the conventional powertrain.

In the heavy-duty commercial vehicle sector, the use of waste heat recovery and phase change cooling, as well as a mild hybrid, can leverage further efficiency potential of the H<sub>2</sub>-ICE.

In a long-haul application, the combination of both technologies can reduce fuel consumption in the VECTO long-haul cycle from 8.98 kg/100km to up to approx. 8.25 kg/100km. This corresponds to an improvement of up to approx. 8 %. This is offset by significant additional costs for the propulsion system, resulting in only a minimal improvement in the TCO rating (< 5 ct/km) and no fundamental change in the TCO ranking between H<sub>2</sub>-ICE, H<sub>2</sub>-FC and BEV. With simultaneous development and use of the technologies by means of a common parts concept to a highly efficient diesel engine, the additional costs can be reduced.

In the area of heavy regional delivery vehicles, a hybrid can play out further advantages due to the more favorable driving profile for recuperation and boosting. However, in this segment, a preference for BEV or H<sub>2</sub>-FC vehicles on the part of fleet operators is to be expected. This can be justified by expected entry restrictions for vehicles powered by internal combustion engines. To circumvent these, the hybrid would need to be able to run electrically without internal combustion engine assistance. Such an implementation is unlikely to be acceptable in terms of vehicle cost and reduction in payload by the vehicle operator. The hybrid also cannot exploit range advantages in this application; a BEV meets typical range requirements of regional delivery operations.

### **Demand analysis and development of the necessary H<sub>2</sub> infrastructure**

The aim of this chapter is to outline and evaluate supply scenarios for the various vehicle classes. In addition, the statements made above regarding costs and LCA are explained in more detail here.

To this end, the current status of the German H<sub>2</sub> infrastructure is first reflected before defining the key requirements and vision for the H<sub>2</sub> infrastructure in 2030. Finally, different supply chains are analyzed in terms of costs and CO<sub>2</sub> impact.

## Status of H<sub>2</sub> infrastructure 2021

To illustrate the enormity of the task of implementing a suitable infrastructure, here is a brief recap of the current status.

As of March 2021, 143 publicly accessible H<sub>2</sub> refueling stations were operated in Europe, and another 43 were under construction. The vast majority of these refueling stations (> 100) are located in Germany.

To the authors' knowledge, fewer than ten of these 100 filling stations are suitable for commercial vehicles (in Frankfurt, Wuppertal and Hamburg, among others), although this statement refers exclusively to refueling at 350 bar and so-called type 3 tanks (primarily for local public transport buses).

Furthermore, to the authors' knowledge, there is no fueling station in productive use (public access or private) that supports 700-bar fast refueling for commercial vehicles in accordance with SAE J2601:2020. Accordingly, more than 90 % of operational refueling stations are currently for passenger cars only.

## H<sub>2</sub> infrastructure in 2030: requirements and vision

The following chapter outlines the picture of the H<sub>2</sub> infrastructure on which the analysis in this paper is based. First, the Germany-wide H<sub>2</sub> demand is estimated, before options for its provision are discussed. Finally, the actual filling station network is described.

### H<sub>2</sub> demand for road transport

In this study, the total hydrogen demand generated by German road transport in 2030 is estimated to be about 4 - 12 TWh (TtW, or 120,000 - 360,000 tons). This includes the estimate of 4 TWh TtW [22] with only about 6000 commercial vehicles (> 3.5 t, very high mileage) as a lower limit, and on the other hand sees the forecast of 9.6 TWh TtW for Germany (49,000 vehicles in the stock [23]) as reasonable, but ambitious. Another study forecasts the demand for Europe, restricted to certain applications of heavy commercial vehicles, at 113,000 vehicles and 28 TWh TtW. [24].

It is assumed here - similar to other studies - that the above-mentioned demand mainly arises from the commercial vehicle segment. This means that a significant proportion could potentially also be covered by LH<sub>2</sub>. Since the technology is still being developed, a forecast is particularly difficult here; however, it can be assumed that at least 0.5 TWh of LH<sub>2</sub> will be required for long-distance and other special applications in 2030, which corresponds to approx. 190 million vehicle kilometers with heavy commercial vehicles.

This demand in road transport is accompanied by a dramatic increase in overall demand (in other sectors as well). Thus, forecasts [22] predict a Germany-wide total demand for CO<sub>2</sub>-neutral hydrogen of 63 TWh for 2030, and the hydrogen strategy of the German government even assumes 90 to 110 TWh [22].

### Production and supply

Various production processes can be considered for the production of hydrogen. At present, by far the largest proportion of hydrogen is produced by steam or autothermal reforming (SMR or ATR) of fossil natural gas (grey hydrogen). If CO<sub>2</sub> is captured during this process (CCS), it is referred to as blue hydrogen. It should be noted however, that this definition is not clear-cut because the amount of CO<sub>2</sub> captured varies greatly depending on the plant

configuration. For example, some configurations (especially those that have been tested for a long time) capture less than 60 % of the CO<sub>2</sub> produced [25]. The energy input is almost exclusively in the form of natural gas; consequently, the cost is also highly dependent on the price of this resource.

Water electrolysis is considered to be the alternative with the potentially lowest CO<sub>2</sub> impact. Here, water is split into hydrogen and oxygen using large amounts of electrical energy (green hydrogen). The CO<sub>2</sub> footprint and cost of this technology therefore scale very significantly with electricity mix and electricity price. In countries with high availability of renewable energies, cost parity with blue or even grey hydrogen can therefore be achieved within the next decade, even without regulatory intervention.

In the future, hydrogen production via methane pyrolysis will also play a role (turquoise hydrogen). In this process, methane is split into gaseous hydrogen and solid carbon, which can either serve as a raw material (not to be burned) or at least be stored very easily. Several (still relatively immature) technology approaches exist here, but only one configuration (plasma reactor using renewable electricity) has the potential to meet the requirements in terms of cost and CO<sub>2</sub> emissions [26].

The question that now needs to be answered is how the demand forecast for 2030 will be met. The future legal framework conditions in the EU will have a decisive influence on this. It is conceivable that the existing SMR plants will be upgraded for the production of blue hydrogen by retrofitting CCS. Whether additional SMR plants are built, however, is likely to depend primarily on the available CO<sub>2</sub> storage capacity. Since this is relatively low in Germany, only a small amount of additional capacity is expected. A demand of 12 TWh/a for road transport could be met even with the German government's target of 5 GW electrolysis capacity by 2030. [27] with domestically produced green hydrogen. Turquoise hydrogen will probably play only a minor role in the transport sector by 2030.

Thus, to satisfy the total demand, imports are likely to be necessary. This is consistent with the German National Hydrogen Strategy, which foresees imports of at least 23 TWh for 2030 (90 TWh consumption, 55 TWh production by SMR as of 2020, 12 TWh production by electrolysis) [27]. This is especially true for the LH<sub>2</sub> demand: Due to the high energy demand and the comparatively high electricity costs, the liquefaction of hydrogen in Germany does not make economic sense. It can therefore be assumed that all LH<sub>2</sub> demand will be covered by imports, especially since the liquid form of hydrogen is the most suitable form for transport by ship.

In the case of imports, the question generally arises as to the type of transport:

From nearby (potential) export countries, gaseous hydrogen can be imported in significant quantities by rededicating natural gas pipelines. This is especially true for the Scandinavian countries, Turkey and certain North African countries.

For more distant export countries, such as Chile, Argentina, but also certain West African countries, Iceland or (in extreme cases) Australia, transport by ship in cryogenic, liquid form is an option [28]. This is also the only practicable option for importing LH<sub>2</sub>. Ideally, the boil-off losses would be used directly for the propulsion of the ship.

It is also technically possible to chemically bind the hydrogen - for example in so-called liquid organic hydrogen carriers (LOHC) or as ammonia - and then transport it in liquid form, either by ship or by pipeline. However, the processes for binding and dissolving the hydrogen are so energy-intensive that this is only worthwhile if the carrier itself is the basic material for the further process (e.g. ammonia for fertilizer production). [29]. It therefore seems unlikely that such carriers will be used to transport hydrogen as a fuel.

The authors see three principal options for domestic distribution in 2030:

1. gaseous by trailer delivery (up to 1100 kg per delivery at 500 bar),
2. in gaseous form via the gas network (possibly converted, pure hydrogen pipelines) or
3. liquid / cryogenic by trailer delivery (up to approx. 4000 kg per delivery)

It can be assumed that relevant capacities in the gas network will already be available for hydrogen transport in 2030. [30] focused on transport pipelines and with regional priorities. In addition, it is currently not foreseeable that the distribution networks will even come close to the coverage of today's natural gas network. Therefore, presumably only a few filling stations will be able to supply themselves directly by pipeline; rather, mixed forms will probably develop for gaseous supply, so that the trailer will only have to overcome the proverbial "last mile".

This option does not exist for the supply of LH<sub>2</sub>; here it can be assumed that the service stations are supplied by trailer directly from the liquefaction plant or the import terminal.

### **Type and density of the service station network**

To enable the smoothest possible market launch of H<sub>2</sub> vehicles, a quantitatively and qualitatively satisfactory refueling station network is a necessary prerequisite.

There are very different statements regarding quantity:

[23] proposes only 70 strategically positioned service stations for 2030, serving just under 49,000 heavy-duty commercial vehicles. In such a scenario, there would be (on average) 695 trucks per service station, which would have to deliver more than 11,000 kg/d on a 365-day average, with the largest service stations having a nominal capacity of 30,000 kg/d. However, this would only cover the relevant long-distance routes. However, this would only cover the relevant long-distance routes.

[31] on the other hand, assumes a Europe-wide network of 3700 filling stations for approx. 45,000 commercial vehicles in 2030, each of which would then deliver an average of around 500 kg per working day. However, it can be assumed that this size and capacity utilization cannot be operated to cover costs, especially in the case of liquid deliveries.

For the present study, an average value is assumed: For the lower limit of the forecasted demand (4 TWh / 120,000 tons), about 400 filling stations should be sufficient to achieve sufficient coverage and utilization at the same time (H<sub>2</sub> delivery on weekday average: about 1500 kg/d or refueling of 20 - 30 commercial vehicles). For the increased demand (12 TWh / 360,000 tons), a (not proportionally) increasing number of approx. 800 filling stations is expected, which would then have to provide 2,250 kg/d on average. Individual filling stations would then certainly be confronted with load peaks of up to approx. 6,000 kg/d, which would still be roughly within the range outlined by [32] outlined above.

These quantities inevitably mean considerable traffic for H<sub>2</sub> delivery if the filling stations are not supplied directly from the pipeline. A filling station with a hydrogen output of 2,250 kg/d would have to be approached by a trailer four to five times a day in the case of gaseous supply; in the case of liquid supply, it would still have to be approached every two days at the latest.

With such volumes, it is also inevitable that refueling operations can be carried out reliably and quickly one after the other (quality). This means that, compared with the current state of the art, the failure rates of filling stations must be drastically reduced and the necessary intervals between refueling operations greatly accelerated.

In the case of hydrogen stored in gaseous form, this inevitably leads to significantly larger buffer storage tanks, fast-running, possibly redundant compressors and very powerful pre-cooling systems, which significantly increases the space requirement, investment and operating costs.

Here, liquid-supplied filling stations have clear advantages due to their principle: On the one hand, the required storage tanks are significantly cheaper; on the other hand, the hydrogen can be refueled directly in a cryogenic state relatively easily (LH<sub>2</sub>) or pressurized by a cryopump with significantly higher efficiency and then preheated (GH<sub>2</sub>). Even if the hydrogen is only supplied in gaseous form, a liquid supply makes sense, especially for large plants: The buffer storage can be significantly smaller; maintenance-prone (booster) compressors and cooling units (and thus electrical power consumption in the triple-digit kW range) are completely eliminated. Corresponding (GH<sub>2</sub>) filling stations are already in productive use.

### Techno-economic comparison of H<sub>2</sub> supply pathways

For the cost and life-cycle analysis in the powertrain comparison study in the beginning of this paper different options for manufacturing, long-range transportation, distribution, and refueling are combined and compared, although not all combinations are reasonable. An overview is provided in **Table 11**.

For grey, blue and turquoise hydrogen, only regional production is considered, which can also include neighboring German countries. Exclusively for green hydrogen, an import scenario was also considered, in which the hydrogen is transported either in gaseous form (by pipeline) or in liquid form (by ship). Liquefaction in Germany is not considered because of the foreseeable high costs. Distribution (for the gaseous variants) takes place by trailer, by gas network or as a combined solution, in which case the trailer only has to cover the distance from the transport pipeline to the filling station. The filling stations are set up according to their supply. For this calculation, differences in storage quantity and type, configuration of compressors and energy consumption (compressor and cooling) are considered. More details on the assumptions can be found in the appendix.

**Table 11:** Analyzed H<sub>2</sub> supply chain elements

Production	Long-distance transport (for MENA import)	Distribution	Dispensing
SMR (grey H <sub>2</sub> )	Pipeline	GH <sub>2</sub> Truck	GH <sub>2</sub> (Truck)
SMR + CCS (blue H <sub>2</sub> )	LH <sub>2</sub> shipping	GH <sub>2</sub> Grid + Truck	GH <sub>2</sub> (Grid)
Electrolysis, DE		GH <sub>2</sub> Grid (direct)	LH <sub>2</sub> → GH <sub>2</sub>
Electrolysis, MENA		LH <sub>2</sub> Truck	LH <sub>2</sub> → LH <sub>2</sub>
Methane pyrolysis		GH <sub>2</sub> Grid + Truck	GH <sub>2</sub> (Grid)

The results of the cost calculation is shown in **Figure 51**. The following key statements can be derived from these results:

1. The production of grey hydrogen by SMR is the cheapest under the given assumptions (but of course not CO<sub>2</sub>-reduced).
2. Production in MENA foreign countries using electrolysis (green) is cheaper than domestic production using SMR + CCS (blue) and significantly cheaper than electrolysis in Germany.

3. Green hydrogen produced in Germany by electrolysis has a cost disadvantage due to the relatively high energy costs. This scenario therefore only becomes interesting if production can take place at favorable locations (e.g. coastal areas) and, above all, the distances to the filling stations are very short. However, this does not mean that small decentralized electrolyzers for onsite supply are advantageous across the board, because these small plants are significantly more expensive than the centralized electrolysis plants considered here.
4. SMR + CCS and methane pyrolysis are practically equivalent in terms of costs under the assumptions made. However, this strongly depends on the boundary conditions, namely the costs for electricity, natural gas, CO<sub>2</sub> disposal and the selling price for solid carbon (was assumed as a moderate additional source of revenue). If, for example, significant costs for CO<sub>2</sub> disposal are incurred here and/or the selling price of carbon can be increased, methane pyrolysis becomes more advantageous.
5. Long-distance transport by pipeline (as GH<sub>2</sub>) is cheaper than by ship (as LH<sub>2</sub>).
6. The majority of LH<sub>2</sub> import costs (totaling 1.73 €/kg) are for depreciation and operating costs of the liquefaction plant and import terminals; only 0.48 €/kg are liquefaction energy costs (not shown separately). Thus, technological advances are unlikely to result in significant cost reductions here. The transport by ship, on the other hand, is hardly significant at 0.12 €/kg for an assumed transport distance of 3,000 km; imports from more distant countries are therefore also conceivable.
7. For the quantities considered, it is cheaper to supply the hydrogen as LH<sub>2</sub> liquid than to deliver it directly to the filling station via the gas distribution network. This is mainly due to the high investment costs of the network and the not inconsiderable energy input for recompression within the network. For much larger consumers, the statement is reversed; dedicated pipelines to supply steel mills or chemical parks thus have a definite justification.
8. If GH<sub>2</sub> has to be transported by trailer only a few kilometers, the costs increase further. Supplying large commercial vehicle refueling stations with GH<sub>2</sub> trailers over long distances represents a significant cost factor and is not economical (therefore not shown).
9. The influence of the filling station configuration on the costs is noteworthy: While GH<sub>2</sub> filling stations supplied by trailer are comparatively expensive, filling stations supplied directly by the gas network are somewhat less expensive because the low-pressure storage tanks are not required. However, expensive compression and cooling units remain, as well as a correspondingly high energy requirement. The liquid-supplied filling station is significantly less expensive (if sufficiently utilized); it makes little difference whether GH<sub>2</sub> or LH<sub>2</sub> is delivered.

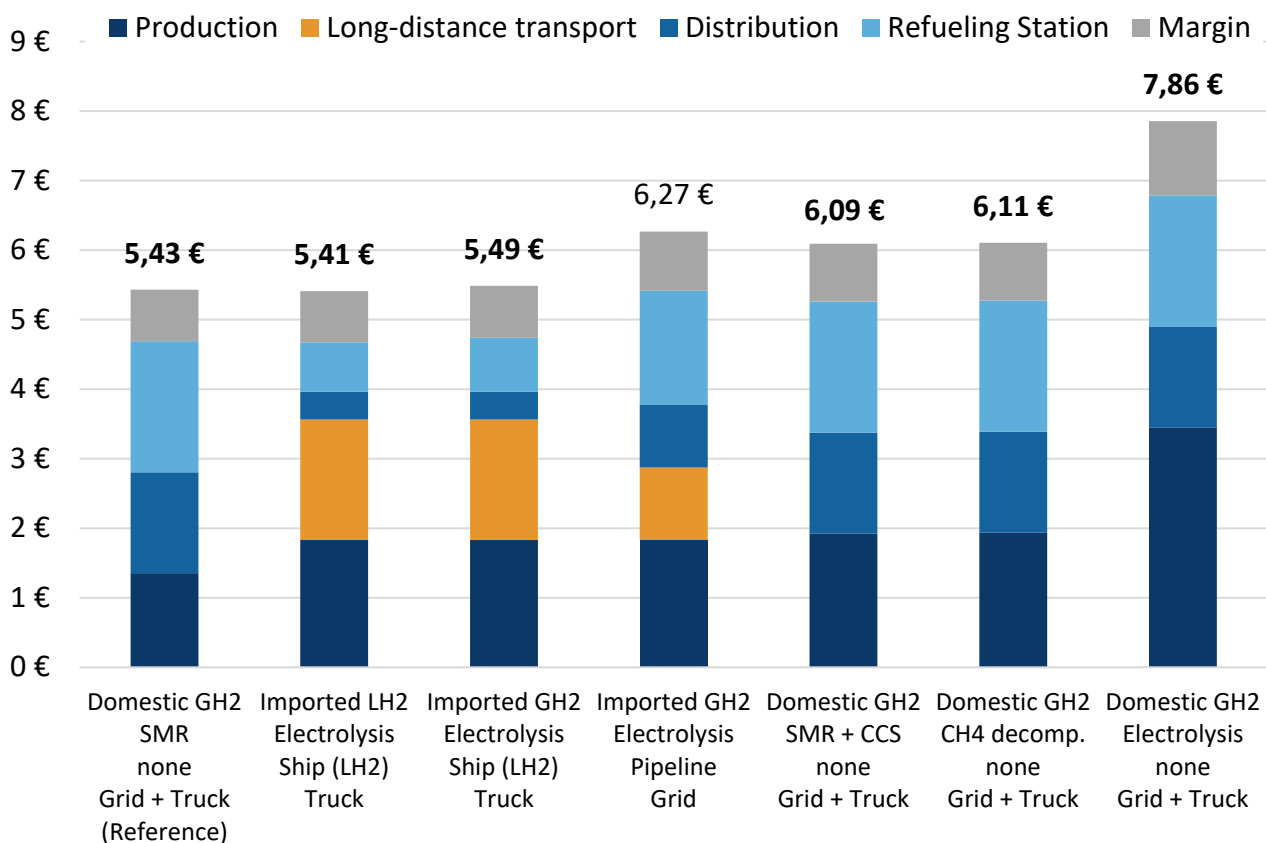


**Figure 51:** Retail prices for hydrogen per kilo in 2030 according to different supply scenarios (values in bold are used in the comparison study chapter).

The results of the LCA calculation are shown in the **Figure 52**, where the left column shows the results for the electricity mix for 2030 (220 g CO<sub>2</sub>e/kWh) and the right column the figures for pure renewable electricity. The allocation of energy consumption for compression and liquefaction is not completely clear-cut: In this diagram, only compression for road transport is listed separately; any compression work at the filling station or for grid transport is included in the respective categories.

The following core statements can be derived:

1. The production of hydrogen by electrolysis from (partly) fossil-derived electricity is - as expected - ecologically nonsensical.
2. The CO<sub>2</sub> emissions of hydrogen produced by SMR are - as expected - independent of the electricity mix.
3. Turquoise hydrogen (methane pyrolysis) is comparable to blue hydrogen (SMR + CCS) not only in terms of cost, but also in terms of CO<sub>2</sub> emissions. Production with non-renewable electricity is quite conceivable - unlike electrolysis.
4. Transport by ship (excl. liquefaction) is significantly more energy efficient than by long-distance pipeline (not shown separately). This always leads to an advantage for LH<sub>2</sub> import. If the energy consumption for regular recompression in the pipeline is covered by fossil electricity, this is reflected in significant additional emissions.

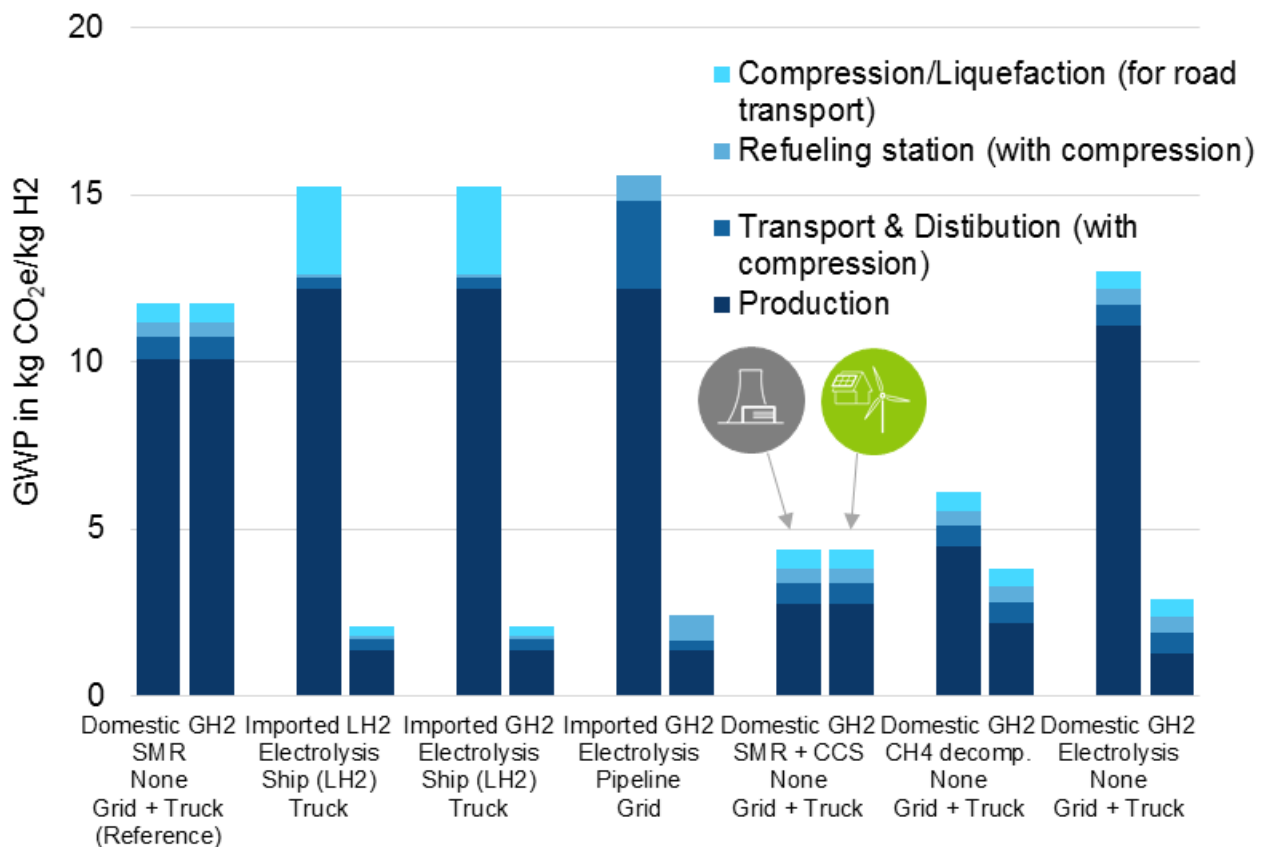


**Figure 52:** Global warming potential for different supply scenarios.

Analyzing **Figure 52** more in detail, several viable paths exist to achieve acceptable CO<sub>2</sub> emissions:

In the case of blue (SMR + CCS) and green (import) hydrogen, environmental and economic attractiveness coincide, with LH<sub>2</sub> import preferred over GH<sub>2</sub> import. Green hydrogen produced in Germany by electrolysis is comparatively expensive, but has among the lowest CO<sub>2</sub> emissions and is a possibility in certain special cases. For methane pyrolysis, there is in no case a unique selling point under the assumptions made; turquoise hydrogen is therefore always comparable with blue. However, this strongly depends on the costs for CO<sub>2</sub> disposal and the prices that can be achieved with carbon; a final statement is difficult. However, it can be assumed that methane pyrolysis (as a plasma reactor with renewable electricity) will increasingly replace production by steam reforming, but only on a large scale after 2030.

Furthermore, should CO<sub>2</sub> disposal become a significant cost factor, it can be assumed that the production of blue hydrogen by means of SMR + CCS will take place in the immediate vicinity of CO<sub>2</sub> storage sites in the future (i.e. abroad); such a scenario was not considered here.

### **Summary of the study findings**

How do hydrogen powertrains compare with battery-electric powertrains and fossil-fuel based internal combustion engine powertrains from the perspective of specific CO<sub>2</sub> intensities and their costs from the user's point of view? This study examines this question in detail.

For this purpose, the results of a techno-economic analysis of different powertrains operated with different energy carriers in three different vehicle categories, namely the heavy passenger car, the light commercial vehicle and the heavy commercial vehicle, are presented and discussed. For all investigated vehicle categories the travelling range requirement is defined for a possible long-distance use. In each of the aforementioned vehicle categories, the following powertrains are considered:

1. Diesel ICE powered by fossil Diesel fuel.
2. Battery-electric propulsion system operated with different electricity mixes
3. Fuel cell system powered by hydrogen from various electricity mixes
4. Internal combustion engine powered by hydrogen from various electricity mixes

For each of the powertrains described, an optimization of the system configuration was carried out in the respective vehicle with a focus on energy consumption in the related cycle. Detailed technology variations in hardware and software approaches have been carried out in order to find the most beneficial operating strategy and hardware configuration. The year 2030 was defined as the technical status for the techno-economical assessment. In this respect, and in order to consider a technological evaluation the present study also discusses the further technical development potential of hydrogen-based powertrains, i.e. the fuel cell and the hydrogen combustion engine. The 2030 technical development status was then used for the technology evaluation in the techno-economical assessment. It should be emphasized that some technical approaches, such as the hybridization of hydrogen combustion engines in light commercial vehicles or the outlook for exhaust gas heat recuperation in H<sub>2</sub>-ICE powertrains in heavy commercial vehicles, are only presented and discussed in terms of their basic potential but has not been considered in the techno-economical study for the 2030 powertrain package.

In this study the following techno-economic aspects are evaluated and discussed in 2030 for each propulsion system in each of the vehicles mentioned:

1. TtW energy consumption in kWh
2. WtW-CO<sub>2</sub> equivalent for green, turquoise, blue, grey H<sub>2</sub> and fully renewable H<sub>2</sub> produced and imported from MENA countries and for the BEV electricity according to national electricity mix forecast 2030 and fully renewable electricity produced in Germany.
3. CtG-CO<sub>2</sub> equivalent for above mentioned H<sub>2</sub> production pathways.
4. Manufacturing costs of propulsion system and storage/tank in 2030.
5. TCO also for 2030 at a lifetime of 4 years and 160 Tkm for passenger cars, 4 years and 400 Tkm for light commercial vehicles and 5 years and 600 Tkm for heavy commercial vehicles.

The main result of the study is that there is not “the” one technical solution superior to all other powertrains. Hydrogen-based propulsion systems show a clear disadvantage in TtW energy consumption compared to battery electric powertrains, mainly due to their poorer system efficiencies. In this respect, a hasty conclusion could be, that only the BEV drive should be used. However, as soon as fuel production is included in the assessment, i.e. a WtW consideration is made, this picture can be reversed and the CO<sub>2</sub> overall intensity can be lower for hydrogen powertrains over the battery electric powertrain. That of course strongly depends on the hydrogen production pathway, and it must be considered, that the CO<sub>2</sub> intensity of nationally produced electricity is based in this comparison on forecasts that predict a value of 220 g CO<sub>2</sub>eq/kWh of produced electricity in 2030. As soon as only

nationally produced, renewable electricity is available, the BEV also wins in this WtW balancing.

The study also shows that, in order to rapidly reduce the CO<sub>2</sub> contribution of the transport sector, not only one technical solution should be pursued. Depending on the application various technical approaches must remain in focus, as there is an ideal drive system for each application with its specific requirements:

1. In a pure consideration of TtW CO<sub>2</sub> emissions, the BEV has an advantage over all other drive systems due to its high system efficiency.
2. In a WtW consideration, depending on the production method of the hydrogen, the hydrogen-powered combustion engine powertrains as well as the fuel cell can have an advantage over the battery-electric powertrain in passenger cars and light commercial vehicles. This applies to the use of blue and turquoise hydrogen as well as a comparison to BEV's with use of the German electricity mix predicted for 2030. For the heavy duty vehicle, this only applies to the FC.
3. If both, hydrogen and electricity will be produced completely regeneratively, the hydrogen powertrains and the battery-electric drivetrain are largely equal in terms of CO<sub>2</sub> equivalents in a CtG balance; with very slight fluctuations from vehicle concept to vehicle concept, for which the battery size is the decisive influencing parameter.
4. Depending on the production route of the hydrogen, both the FC system powertrain and the hydrogen internal combustion engine represent a highly attractive solution compared to the BEV in terms of TCO. It must be emphasized here, that the study does not take into account any monetary regulatory aspects that are not yet known, i.e. could still change the picture in the future.
5. A direct comparison between FC and H<sub>2</sub> ICE shows an identical cost burden according to TCO for the passenger car.
6. From a TCO perspective, the light commercial vehicle even shows a slight advantage for the H<sub>2</sub>-ICE compared to the FC system, since the efficiency advantage of the FC compared to the H<sub>2</sub>-ICE is significantly reduced in this vehicle concept. This is due to the operating regime of the vehicle, which allows the ICE to operate increasingly in higher load ranges, resulting in a higher average cycle efficiency for the ICE than is the case in the passenger car.
7. For the heavy-duty commercial vehicle, the picture is slightly different, which is entirely due to the higher specific mileage and the different operating scenario. In 2025, the hydrogen ICE has a clear advantage over the FC as well as the battery electric powertrain from a TCO point of view, but this changes in favor of the FC and the approximately equal BEV powertrain by 2030.
8. In terms of achievable TtW-CO<sub>2</sub> values, the heavy-duty vehicle shows an advantage for FC over H<sub>2</sub> ICE, both in 2025 and in 2030. This is mainly due to the absolute efficiency advantage of the fuel cell.

Further technical conclusions from the extensive considerations in this study can be summarized as follows:

1. An efficiency increase potential of approx. 15-20% to approx. 65% system efficiency is still expected for the fuel cell system by 2030, based on the status in 2021, through detailed optimizations in the stack and the overall system.
2. A higher efficiency can also be achieved by increasing the fuel cell system power above the target value (oversizing) by dividing the required total power among several stacks with then a smaller power to be delivered or by selecting a larger system in general. This is justified by the fact that the operating regime will then be shifted to more favorable

operating ranges with higher FC stack efficiencies. Additionally, the lower tank volume requirement results in lower weight and.

3. For the H<sub>2</sub>-ICE, the current development work shows the potential to increase the peak efficiency in the engine map by approx. 10 % - 15 % until 2030. The combustion system process to be applied is decisive here.
  - The 15 % increase in efficiency can only be achieved with the transition from premixed to diffusive combustion, which is being worked on.
  - With premixed process control, a maximum of approx. 44 % - 46 % in effective peak efficiency of the internal combustion engine appears to be a realistic target.
4. Without direct H<sub>2</sub> injection a similar efficiency level as with direct injection will be possible, but at lower specific power levels, as the volume displacement of intake air by the hydrogen is a limiting factor.
  - Premixed combustion processes should use low-pressure direct injection in the range of 30-50 bar due to faster technical feasibility and from an overall system perspective.
  - Diffusive combustion processes require higher injection pressures of 200-300 bar, making the system significantly more complex and most likely to be applied to heavy-duty commercial vehicles.
5. Hydrogen combustion engines can, with an appropriately designed exhaust aftertreatment system, undercut very challenging exhaust emission limits, which are far below today's EURO6d limits, even with lean-burn operation implemented throughout the engine map.
6. In hydrogen storage, there are two main competing systems for use in vehicles: high-pressure storage between 350 bar and 700 bar at ambient temperature and cryogenic storage at approximately ambient pressure.
7. Based on the advantages and disadvantages, compressed gas storage appears to be the target for passenger cars and light commercial vehicles, and cryogenic or even the mixed form cryogenic-compressed may be advantageous for vehicles with extremely high range requirements, such as heavy commercial vehicles.
8. Hybridization of the H<sub>2</sub> internal combustion engine, which has received little attention to date, brings many advantages. On the one hand, it can significantly close the efficiency gap with the fuel cell, and on the other hand, hybridization enables the adaptation of the combustion engine map. This makes it possible to exclude critical operating ranges within the engine map, such as very low speeds and high loads, and thus to exploit further efficiency advantages of the H<sub>2</sub>-ICE.
9. The study comes to the conclusion that for a sufficient hydrogen supply in the first step, a filling station network of approx. 400 filling stations, sensibly distributed, is sufficient to enable heavy-duty traffic.
10. Hydrogen produced domestically (here: Germany) with electrolysis leads to by far the highest prices per kilogram of hydrogen, due to the high energy costs for producing the H<sub>2</sub>. Blue and turquoise hydrogen are about 10 % - 15 % lower in price, but the final price depends mainly on the CO<sub>2</sub> prices for disposal or the profit as raw material. The cheapest hydrogen comes from grey production, whereas imported hydrogen from green production (e.g. from MENA countries) is also on this level in terms of price.

All the above partial results allow the following main conclusions:

1. In passenger cars, hydrogen powertrain may well be an alternative to battery electric powertrains, at least in the medium term, until a sufficient amount of nationally generated fully renewable electricity is available.

2. For the fuel cell, it is even possible to speak of a long-term alternative in the passenger car sector. In this case, however, blue and turquoise hydrogen or imported green hydrogen must be available and used.
3. Hybridized H<sub>2</sub> ICE powertrains represent a real alternative to battery-electric mobility and the fuel cell for light commercial vehicles in the medium and long term, both from a CO<sub>2</sub> equivalent and TCO point of view.
4. In heavy-duty commercial vehicles for long-haul application, hydrogen powertrains represent a rapid measure for achieving a CO<sub>2</sub>-free mobility, especially in the short and medium term. From a TCO point of view, the H<sub>2</sub>-ICE can be seen as a short-term solution with an advantage over the FC. From 2030 on, the FC will also have an advantage in terms of TCO. In the regional delivery sector, the BEV will prevail. For special applications with increased power density requirements, highly efficient diesel (e-fuel) or H<sub>2</sub>-ICE powertrains will also play a role in the long term.
5. If the focus is purely on the TtW efficiency of the powertrain, the FC is basically at an advantage over the H<sub>2</sub> ICE in all applications.

The potentials of the powertrains show that there are different ways to achieve a low CO<sub>2</sub> road transport. As shown in the study, the hydrogen combustion engine, the fuel cell system and also the battery electric drive still have a number of conceivable improvements. With respect to 2030, it is difficult to predict the chronological order in which the innovation leaps in the individual powertrains will be achieved. From today's perspective, it is therefore recommended to create an environment in which hydrogen powertrains and battery-electric powertrains can be used by customers. In such an environment, the risk of having chosen the wrong powertrains solution for achieving the CO<sub>2</sub> targets is minimized.

## **Appendix A**

All important boundary conditions, assumptions and interim results of the presented study are included in the appendix. This can be requested at any time under the following e-mail address: marc.sens@iav.de.

## **Acknowledgements**

The present study is so comprehensive that it could only be produced through the collaboration of many domain-specific specialists. The people involved go far beyond the authors mentioned. In this respect, the authors mentioned would like to express their sincere thanks to all colleagues involved. In particular, the colleagues Dr. Adalbert Wolany, Dr. Alexander Fandakov, Alexander Forell, Alexander Poppitz, Dr. Ralf Troeger, Dr. Jens Kitte, Marcel Pannwitz, Torsten Tietze, Oliver Waetzig, Dr. Ingmar Hartung, Richard Trott, Matthias Roths Schuh, Dr. Reza Rezaei, Tom George, Stefan Jung, Thaddäus Delebinski, Michael Riess should be mentioned here.

## **List of abbreviations**

A-ECMS	Advanced Equivalent Consumption Minimization Strategy
AMC	Aggressive Mixed Cycle
ATR	Auto Thermal Reformation
BDC	Bottom Dead Center
BMEP	Break Mean Effective Pressure
CA	Crank Angle
CcH <sub>2</sub>	Cryogen Compressed Hydrogen
CCS	Carbon Capture and Storage

CGH <sub>2</sub>	Compressed Gaseous Hydrogen
Cf	Conformity Factor
CH <sub>4</sub>	Methane
CO <sub>2</sub>	Carbon dioxide
CR	Compression Ratio
CtG	Cradle to Grave
ct/km	cent per Kilometer
Cum.	Cumulative
DE	Deutschland
DI	Direct Injection
DOC	Diesel Oxidation Catalyst
eTC	Electrically assisted Turbo Charger
EAT	Exhaust After Treatment
EGR	Exhaust Gas Recirculation
EOI	End of Injection
EU	Europe
EU7	EURO7
EVC	Exhaust Valve Closing
FC	Fuel Cell
FTP	Federal Test Procedure
g	Gramm
g/bhp-hr	Gramm per Brake Horse Power Hour
GH <sub>2</sub>	Gaseous Hydrogen
g/kWh	Gramm per Kilo Watt Hour
GW	Giga Watt
GWP	Global Warming Potential
H <sub>2</sub>	Hydrogen
HD	Heavy Duty
HP-EGR	High Pressure Exhaust Gas Recirculation
ICE	Internal Combustion Engine
IVC	Intake Valve Closing
IVO	Intake Valve Opening
K	Kelvin
kg	Kilogram
kg/d	Kilogram per Day
kw	Kilo Watt
LCA	Life Cycle Assessment
LCV	Light Commercial Vehicle
LDV	Light Duty Vehicle
LET	Low End Torque
LH <sub>2</sub>	Liquified Hydrogen
LLC	Low Load City Cycle
LOHC	Liquid Organic Hydrogen Carrier
LP-EGR	Low Pressure Exhaust Gas Recirculation
m <sup>3</sup>	Cubic Meter
MENA	Middle East North Africa
NH <sub>3</sub>	Ammonia
NO <sub>x</sub>	Nitrogen Oxide
PC	Passenger Car
PF	Particulate Filter

PFI	Port Fuel Injection
PMEP	Pump Mean Effective Pressure
PNA	Passive NO <sub>x</sub> Adsorber
ppm	Parts Per Million
RDE	Real Driving Emissions
rpm	Revolution per Minute
s	Seconds
SCR	Selective Catalytic Reduction Filter
SCRf	Selective Catalytic Reduction
SDPF	Selective Catalytic Reduction in Diesel Particulate Filter
S-ECMS	Standard Equivalent Consumption Minimization Strategy
SI	Spark Ignited
SMR	Steam Methane Reforming
SOI	Start of Injection
SUV	Sports Utility Vehicle
TC	Turbocharger
TCO	Total Cost of Ownership
TDC	Top Dead Center
TtW	Tank to Wheel
TWh	Terra Watt Hour
TWh/a	Terra Watt Hour per Annum
VTG	Variable Turbine Geometry
WLTC	World Harmonized Light Duty Test Cycle
WOT	Wide Open Throttle
WtW	Well to Wheel

## **Bibliography**

- [1] Umweltbundesamt, „Wege in eine ressourcenschonende Treibhausgasneutralität - RESCUE,“ Dessau-Roßlau, 2019.
- [2] W. Wukisiewitsch, C. Danzer und T. Semper, „Systematische Entwicklung nachhaltiger Antriebe für das Jahr 2030 und darüber hinaus,“ *MTZ*, 02 2020.
- [3] C. Danzer, M. Kratzsch, M. Vallon und T. Günther, „Fleet Powertrain 2025 - CO<sub>2</sub>- and cost-optimized modular powertrains,“ *MTZ Worldwide*, 02 2018.
- [4] Backofen, Dennis; IAV GmbH, „Innovatives Brennstoffzellensystem für den Einsatz im Mittelklasse PKW,“ *ATZ live - Der Antrieb von morgen*, 2021.
- [5] Bilz, Sebastian; Rothschuh, Matthias; Schütte, Katharina; Wascheck, Ralf; IAV GmbH, „Model-Based Efficiency Improvement of Automotive Fuel Cell Systems,“ *Simulation and Testing for Vehicle Technology*, 18 May 2016.
- [6] U.S. Department of Energy - Fuel Cell Technologies Office, „Multi-Year Research, Development, and Demonstration Plan,“ 2017.
- [7] Soongil Kweon, Jong Jin Park; Dr.-Ing. Sae Hoon Kim; Hyundai Motor Company, „The Hydrogen-powered Bus and Truck from Hyundai Motor Company,“ in *Internationales Wiener Motorensymposium*, 2020.
- [8] K. Schütte, „Out of space - Anschluss unter dieser Nummer,“ *Automotion - Das IAV-Kundenmagazin*, Nr. 01/2021, pp. 26-29, 2021.

- [9] Takahiko Hasegawa, Hiroyuki Imanishi, Mitsuhiro Nada, Yoshihiro Ikogi, Toyota Motor Corporation, „Development of the Fuel Cell System in the Mirai FCV,“ *SAE Technical Paper 2016-01-1185*, 2016.
- [10] Palavinskas, Christian; Berger, Ulrich; Sahlbach, Frank; Backofen, Dennis; Wascheck, Ralf; IAV GmbH, „Development of a physicochemical model for the platinum degradation in fuel cells,“ *ECFC: Low-Temp. FUEL CELLS, ELECTROLYSERS & H2 Processing*, July 2019.
- [11] R. Rezaei, M. Riess, Q. Li, P. Rolke, A. Wohlrab, C. Hayduk und C. Bertram, „Decarbonization of commercial vehicles with hydrogen combustion: from concept to start of production and beyond,“ *2nd World Congress on Internal Combustion Engines*, 2021.
- [12] R. Rezaei, C. Hayduk, A. Fandakov, M. Riess, M. Sens und T. Delebinski, „Numerical and Experimental Investigations of Hydrogen Combustion for Heavy-Duty Applications,“ *SAE World Congress Technical paper 2021-01-0522*, 2021.
- [13] R. Rezaei, M. Mennig, C. Hayduk, C. Bertram, C. Hahn und S. Kureti, „Holistic engine and exhaust after-treatment system development for hydrogen combustion concepts,“ *18th FAD Conference Challenge – Exhaust aftertreatment, Radebeul*, 2020.
- [14] R. Rezaei, C. Hayduk, M. Sens, A. Fandakov und C. Bertram, „Model-based Development Methodology for HD Hydrogen Combustion System Optimization,“ *ATZ Experten-Forum Powertrain 2020 „Ladungswechsel und Emissionierung*, 2020.
- [15] R. Rezaei, C. Hayduk, M. Sens, A. Fandakov und C. Bertram, „Hydrogen Combustion – a Puzzle Piece of Future Sustainable Transportation!,“ *SIA Powertrain & Energy, France*, 2020.
- [16] H. Rauch, D. Kovács, R. Rezaei, V. Strots, S. Kah und A. Wille, „Two-Stage SCR System for Commercial Vehicle Applications,“ in *7th International MinNOx Conference*, Berlin, 2018.
- [17] D. Kovacs, H. Rauch, R. Rezaei und Y. Huang, „Modeling Heavy-Duty Engine Thermal Management Technologies to Meet Future Cold Start Requirements,“ *SAE Technical Paper 2019-01-0731*, 2019.
- [18] H. Rauch, R. Rezaei, M. Weber und D. Kovács, „Holistic Development of Future Low NOx Emission Concepts for Heavy-Duty Applications,“ *SAE Technical Paper 2018-01-1700*, 2018.
- [19] D. Kovacs, M. Mennig, R. Rezaei und C. Bertram, „Holistic Engine and EAT Development of Low NOX and CO2 Concepts for HD Diesel Engine Applications,“ *SAE Technical Paper 2020-01-2092*, 2020.
- [20] Kawaguchi, Bungo; Umemoto, Kazuhiro; Misawa, Seitaro; Kawai, Tagashi; Hirooka, Shigemasa; TOYOTA MOTOR CORPORATION, „ICE Challenges toward Zero Emissions: Future Technology Harmonization in Electrified Powertrain System,“ *SAE Technical Paper 2019-01-2217*, 2019.
- [21] S. Hausberger, G. Mellios und Z. Samaras, „Preliminary findings on possible Euro 7 emission limits for LD and HD vehicles,“ *AGVES, AGVES online Meeting*, 2020.
- [22] Prognos, Öko-Institut, Wuppertal-Institut, „Klimaneutrales Deutschland. Studie im Auftrag von Agora Energiewende, Agora Verkehrswende und Stiftung Klimaneutralität,“ 2020.
- [23] P. Rose, M. Wietschel und T. Gnann, „Wie könnte ein Tankstellenaufbau für Brennstoffzellen-Lkw in Deutschland aussehen?,“ *Fraunhofer ISI*, 2020.

- [24] Roland Berger, „Fuel Cells Hydrogen Trucks: Heavy-Duty's High Performance Green Solution,“ 2020.
- [25] C. Antonini, K. Treyer, A. Streb, M. van der Spek, C. Bauer und M. Mazzotti, „Hydrogen production from natural gas and biomethane with carbon capture and storage - A techno-environmental analysis,“ *Sustainable Energy & Fuels*, Nr. 4, p. 2967, 2020.
- [26] S. Timmerberg, M. Kaltschmitt und M. Finkbeiner, „Hydrogen and hydrogen-derived fuels through methane decomposition of natural gas - GHG emissions and costs,“ *Energy Conversion and Management: X*, Nr. 7, 2020.
- [27] D. Bundesregierung, „Die Nationale Wasserstoffstrategie,“ Bundesministerium für Wirtschaft und Energie, 2020.
- [28] Kawasaki Heavy Industries Ltd., „World's First Liquefied Hydrogen Carrier SUIISO FRONTIER Launches Building an International Hydrogen Energy Supply Chain Aimed at Carbon-free Society,“ 11 12 2019. [Online]. Available: [https://global.kawasaki.com/en/corp/newsroom/news/detail/?f=20191211\\_3487](https://global.kawasaki.com/en/corp/newsroom/news/detail/?f=20191211_3487). [Zugriff am 11 03 2021].
- [29] International Energy Agency, „The Future of Hydrogen, Report prepared by the IEA for the G20, Japan,“ 2019.
- [30] Enagás, Energinet, Fluxys Belgium, Gasunie, GRTgaz, NET4GAS, OGE, ONTRAS, Snam, Swedegas, Teréga, „European Hydrogen Backbone: How a dedicated hydrogen infrastructure can be created,“ 2020.
- [31] Fuel Cell and Hydrogen 2 Joint Undertaking, „Hydrogen Roadmap Europe - A sustainable pathway for the European energy transition,“ FCH 2 Ju, 2019.
- [32] T. Mayer, M. Semmel, M. Albert Guerrero Morales, K. M. Schmidt, A. Bauer und J. Wind, „Techno-economic evaluation of hydrogen refueling stations with liquid or gaseous stored hydrogen,“ *International Journal of Hydrogen Energy*, pp. 25809-25833, 2019.
- [33] Bilz, Sebastian; Roths Schuh, Matthias; Wascheck, Ralf; IAV GmbH, „Model-Based Powertrain Design for Fuel Cell Electric Vehicles,“ *HEV Hybrid und Elektrofahrzeuge 2017*, 2017.
- [34] M. Klell, H. Eichlseder und A. Trattner, Wasserstoff in der Fahrzeugtechnik, Wiesbaden: Springer Vieweg, 2018.
- [35] R. Rezaei, M. Sens, M. Riess und C. Bertram, „Potentials and challenges of hydrogen combustion system development as a sustainable fuel for commercial vehicles,“ *ATZ Engine Conference, Baden-Baden*, 2021.